ISSN 1881-7815 Online ISSN 1881-7823

BST BioScience Trends

Volume 14, Number 1
February, 2020

IRCA BSSA

IACMHR

www.biosciencetrends.com

BST
BioScience Trends

ISSN: 1881-7815
Online ISSN: 1881-7823
CODEN: BTIRCZ
Issues/Year: 6
Language: English
Publisher: IACMHR Co., Ltd.

BioScience Trends is one of a series of peer-reviewed journals of the International Research and Cooperation Association for Bio & Socio-Sciences Advancement (IRCA-BSSA) Group and is published bimonthly by the International Advancement Center for Medicine & Health Research Co., Ltd. (IACMHR Co., Ltd.) and supported by the IRCA-BSSA and Shandong University China-Japan Cooperation Center for Drug Discovery & Screening (SDU-DDSC).

BioScience Trends devotes to publishing the latest and most exciting advances in scientific research. Articles cover fields of life science such as biochemistry, molecular biology, clinical research, public health, medical care system, and social science in order to encourage cooperation and exchange among scientists and clinical researchers.

BioScience Trends publishes Original Articles, Brief Reports, Reviews, Policy Forum articles, Case Reports, News, and Letters on all aspects of the field of life science. All contributions should seek to promote international collaboration.

Editorial Board

Editorial Office

Pearl City Koishikawa 603,
2-4-5 Kasuga, Bunkyo-ku, Tokyo 112-0003, Japan
Tel: +81-3-5840-8764 Fax: +81-3-5840-8765
E-mail: office@biosciencetrends.com

BioScience Trends

Editorial and Head Office

Pearl City Koishikawa 603, 2-4-5 Kasuga, Bunkyo-ku,
Tokyo 112-0003, Japan

Tel: +81-3-5840-8764, Fax: +81-3-5840-8765
E-mail: office@biosciencetrends.com
URL: www.biosciencetrends.com

Editorial Board Members

CONTENTS

Volume 14, Number 1, 2020

Editorial

Policy Forum

Original Article

Brief Report

Communication

Letter

Editorial

DOI: 10.5582/bst.2020.01056

COVID-19: Real-time dissemination of scientific information to fight a public health emergency of international concern

Peipei Song[1], Takashi Karako[2,3,*]

[1] Institute for Global Health Policy Research, Bureau of International Health Cooperation, National Center for Global Health and Medicine, Tokyo, Japan;
[2] International Health Care Center, National Center for Global Health and Medicine, Tokyo, Japan;
[3] Department of Surgery, the University of Tokyo Hospital, Tokyo, Japan.

SUMMARY Rapidly sharing scientific information is an effective way to reduce public panic about COVID-19, and doing so is the key to providing real-time guidance to epidemiologists working to contain the outbreak, clinicians managing patients, and modelers helping to understand future developments and the possible effectiveness of various interventions. This issue has rapidly reviewed and published articles describing COVID-19, including the drug treatment options for SARS-CoV-2, its clinical characteristics, and therapies involving a combination of Chinese and Western medicine, the efficacy of chloroquine phosphate in the treatment of COVID-19 associated pneumonia according to clinical studies, and reflections on the system of reserve medical supplies for public health emergencies. As an academic journal, we will continue to quickly and transparently share data with frontline healthcare workers who need to know the epidemiological and clinical features of COVID-19.

Keywords 2019-nCoV, SARS-CoV-2, COVID-19, sharing data

A novel coronavirus, formerly designated 2019-nCoV and now taxonomically termed SARS-CoV-2, emerged in Wuhan, China at the end of 2019 and rapidly spread through many countries in Asia and elsewhere worldwide. This incident was labeled a public health emergency of international concern (PHEIC) on Jan. 30, 2020 (*1*). This is the 6th time WHO has declared a PHEIC since the International Health Regulations (IHR) came into effect in 2005.

The clinical condition caused by SARS-CoV-2 has been designated COVID-19 by the WHO. As of Feb. 23, 2020, WHO reported a total of 77,042 confirmed cases and 2,445 deaths in China and 1,769 confirmed cases and 17 deaths in 28 other countries (*2*). The rapid increase in infections and deaths caused anxiety, panic, stigma, mistrust, and rumor-mongering among public.

Rapidly sharing scientific information is an effective way to reduce public panic, and it is the key to providing real-time guidance to epidemiologists working to contain the outbreak, clinicians managing patients, and modelers helping to understand future developments and the possible effectiveness of various interventions.

This information includes routes of transmission and transmissibility, the natural history of infection in humans, the populations at risk, the successful clinical practices that are being used to manage patients, the laboratory information needed to diagnose patients, and the genetic sequence information used to assess viral stability.

Scientists from numerous countries have published and analyzed the genome of the pathogen responsible, SARS-CoV-2 (*3-5*). On Jan. 2020, a study that analyzed data on the first 425 confirmed cases in Wuhan, China provided evidence of human-to-human transmission among close contacts and suggested that measures to prevent or reduce transmission be implemented in populations at risk (*6*). Two studies published in Jan. 2020 described the epidemiological and clinical features of laboratory-confirmed COVID-19 in 41 and 99 patients, respectively, in Wuhan (*7,8*). On Feb. 9, 2020, a study involving 1,099 laboratory-confirmed cases at 552 hospitals was published online to provide an up-to-date delineation of the epidemiological and clinical characteristics of COVID-19 throughout mainland China (*9*). The study's findings encourage a shift in focus to identifying and managing patients at an earlier stage, before disease progression. In addition to confirmed cases from China, several reports identified clusters of locally transmitted cases in other countries, adding to the understanding of this disease.

To prompt real-time sharing of scientific information, many international academic journals have rapidly reviewed and published articles on COVID-19. Several coronavirus websites have also been created to assemble and disclose articles on this disease, such as the NEJM Coronavirus page, the Lancet COVID-19 Resource Centre, and the Cell Press Coronavirus Resource Hub. In order to overcome the language barrier, many articles have also been translated into Chinese to directly benefit frontline health professionals and policy makers in China as well as to reduce public panic; epidemiological information and scientific articles in Chinese have also been widely cited and rapidly reported in English. Broad dissemination in both Chinese and English will accomplish the goal of promptly communicating crucial findings to the international scientific community.

We still have a lot to learn about SARS-CoV-2 and the disease it causes, COVID-19. The real-time dissemination of scientific information is needed most during this period of uncertainty. Academic journals are responsible for facilitating the rapid dissemination of reliable information including transparent methods of identifying cases, sharing data, unfettered communication, and peer-reviewed research.

Since its inception in 2007, our journal – *BioScience Trends* – has highlighted the research on and dissemination of information regarding public health emergencies, leading us to publish articles on topics such as SARS, Ebola, MERS, avian influenza A H5N1, H1N1, and H7N9.

In this issue, we rapidly reviewed and published articles describing COVID-19, including the drug treatment options for SARS-CoV-2, its clinical characteristics, and therapies involving a combination of Chinese and Western medicine, the efficacy of chloroquine phosphate in the treatment of COVID-19 associated pneumonia according to clinical studies, and the reflections on the system of reserve medical supplies for public health emergencies.

As an academic journal, we will continue to quickly and transparently share data with frontline healthcare workers who need to know the epidemiological and clinical features of COVID-19.

References

1. World Health Organization Europe. 2019-nCoV outbreak is an emergency of international concern. *https://www.euro.who.int/en/health-topics/health-emergencies/international-health-regulations/news/news/2020/2/2019-ncov-outbreak-is-an-emergency-of-international-concern* (accessed February 22, 2020)
2. World Health Organization. Coronavirus disease 2019 (COVID-19) Situation Report – 33. *https://www.who.int/docs/default-source/coronaviruse/situation-reports/20200222-sitrep-33-covid-19.pdf?sfvrsn=c9585c8f_2* (accessed February 23, 2020)
3. Wu F, Zhao S, Yu B, *et al*. A new coronavirus associated with human respiratory disease in China. Nature. 2020; doi: 10.1038/s41586-020-2008-3.
4. Zhou P, Yang XL, Wang XG, *et al*. A pneumonia outbreak associated with a new coronavirus of probable bat origin. Nature. 2020; doi: 10.1038/s41586-020-2012-7.
5. Gorbalenya AE, Baker SC, Baric RS, *et al*. Severe acute respiratory syndrome-related coronavirus: the species and its viruses – A statement of the Coronavirus Study Group. bioRxiv preprint. Published online February 11, 2020; doi: *https://doi.org/10.1101/2020.02.07.937862*.
6. Li Q, Guan X, Wu P. Early transmission dynamics in Wuhan, China, of novel coronavirus-infected pneumonia. N Engl J Med. 2020; doi: 10.1056/NEJMoa2001316.
7. Huang C, Wang Y, Li X, *et al*. Clinical features of patients infected with 2019 novel coronavirus in Wuhan, China. Lancet. 2020; 395:497-506.
8. Chen N, Zhou M, Dong X, Qu J, Gong F, Han Y, Qiu Y, Wang J, Liu Y, Wei Y, Xia J, Yu T, Zhang X, Zhang L. Epidemiological and clinical characteristics of 99 cases of 2019 novel coronavirus pneumonia in Wuhan, China: A descriptive study. Lancet. 2020; 395:507-513.
9. Guan WJ, Ni ZY, Hu Y, *et al*. Clinical characteristics of 2019 novel coronavirus infection in China. medRxiv preprint. Published online February 9, 2020; doi: *https://doi.org/10.1101/2020.02.06.20020974*.

Received February 23, 2020; Accepted February 24, 2020.

**Address correspondence to:*
Takashi Karako, International Health Care Center, National Center for Global Health and Medicine, Tokyo, 1-21-1 Toyama Shinjuku-ku, Tokyo 162-8655, Japan.
E-mail: politang-tky@umin.ac.jp

Released online in J-STAGE as advance publication February 25, 2020.

Policy Forum

DOI: 10.5582/bst.2020.01043

Challenges to the system of reserve medical supplies for public health emergencies: reflections on the outbreak of the severe acute respiratory syndrome coronavirus 2 (SARS-CoV-2) epidemic in China

Xu Wang, Xiaoxi Zhang, Jiangjiang He*

Department of Health Policy Research, Shanghai Health Development Research Center (Shanghai Medical Information Center), Shanghai, China.

SUMMARY On December 31, 2019, the Wuhan Municipal Health Commission announced an outbreak of severe acute respiratory syndrome coronavirus 2 (SARS-CoV-2), China is now at a critical period in the control of the epidemic. The Chinese Government has been taking a series of rapid, comprehensive, and effective prevention and control measures. As the pandemic has developed, a fact has become apparent: there is a serious dearth of emergency medical supplies, and especially an extreme shortage of personal protective equipment such as masks and medical protective clothing. This is one of the major factors affecting the progress of epidemic prevention and control. Although China has made great efforts to strengthen the ability to quickly respond to public health emergencies since the SARS outbreak in 2003 and it has clarified requirements for emergency supplies through legislation, the emergency reserve supplies program has not been effectively implemented, and there are also deficiencies in the types, quantity, and availability of emergency medical supplies. A sound system of emergency reserve supplies is crucial to the management of public health emergencies. Based on international experiences with pandemic control, the world should emphasize improving the system of emergency reserve medical supplies in the process of establishing and improving public health emergency response systems, and it should promote the establishment of international cooperative programs to jointly deal with public health emergencies of international concern in the future.

Keywords public health emergency, SARS-CoV-2, COVID-19, medical supplies

1. Introduction

After several cases were identified in Wuhan in Dec. 2019, severe acute respiratory syndrome coronavirus 2 (SARS-CoV-2) has gradually affected China as a country and even spread worldwide. Prior to Feb. 12, 2020, China had reported 59,804 confirmed cases of coronavirus disease 2019 (COVID-19), 1,367 deaths, and 5,911 recoveries (*1*). Compared to the SARS epidemic in 2003, this time China has apparently made great progress in combating a pandemic through its development of the capacity for biological detection and its greater transparency with regard to information (*2,3*). However, the situation also revealed that China still faces major problems in terms of public health emergencies.

2. Shortage of medical supplies during the SARS-CoV-2 epidemic in China

The key to a response to a public health emergency lies in abundant reserves and proper allocation of emergency medical supplies, for timely supplies are crucial to reducing deaths and increasing the rate of successful treatment (*4*). An epidemic caused by a new pathogen can often deal a blow to the health system, resulting in a shortage of supplies and medicines. For example, the United States was faced with an outbreak of H1N1 influenza in 2009; many hospitals suffered from a shortage of personal protective equipment (*5*). The SARS-CoV-2 outbreak coincided with Chinese New Year, so most of the manufacturers and distributors were on holiday; this further intensified the shortage of medical protective supplies in combating the epidemic. Hospitals across the country, and especially those in Wuhan where the situation is the most severe, have cited a vast shortage of medical supplies, and especially personal protective supplies such as medical protective clothing and N95 masks; the hospitals are urgently calling for societal support (*6*). This shows that China is still facing significant challenges and still needs to

enhance the reserve medical supplies program and to remedy the faults in the allocation, distribution, and utilization of supplies to deal with public health emergencies.

3. Policy requirements and status of the reserve medical supplies program in China

China's current reserve medical supplies program dates back to the 1970s (*7*). In order to ensure the effective supply of medical supplies required after disasters, epidemics, or emergencies, the State Council issued the "*Notice on Reforming and Enhancing the Management of Medical Reserves*" in 1997. After the SARS outbreak in 2003, the Chinese Government heavily emphasized emergency preparation and related legislation. The government issued the "*Regulations on Public Health Emergencies*," the "*National Emergency Plan for Public Health Emergencies*," the "*(Draft) Catalogue of health emergency personnel and equipment*," and other documents (Table 1). Moreover, the emergency reserve supplies program clearly stipulates that "*municipal governments and county governments in areas where emergencies are likely to occur should establish a program for emergency reserve supplies, necessities, and equipment*"(*8*).

Although policies on the emergency reserve medical supplies program have been continuously improved, they are often not fully implemented. The SARS-CoV-2 epidemic shows that the Government failed to heed its responsibility for effectively "*reserving medical supplies for the prevention and control of the pandemic*" (*9*). In 2010, all of the Centers for Disease Control and Prevention on the provincial level were evaluated for their capacity to respond to public health emergencies, and the results indicated that the readiness of emergency reserve supplies was only 37.5%, only 4.8% of all centers met standards, and the types and quantities of supplies were far from adequate (*10*). The first reason for this is because the mechanism for funding reserve medical supplies still has flaws; it lacks long-term and sustainable input (*11*). Second, a mechanism for managing emergency reserve supplies has yet to be created; there is a lack of integrated planning, timely storage, or rapid distribution. Third, the risks of an emergency and response capabilities vary with the level of economic and social development, necessitating the continuous updating of lists of emergency supplies. Since the issuance of the "*(Draft) Catalogue of health emergency personnel and equipment*" in 2008, however, no adjustments or updates have been made, resulting in substantial inability to meet current standards (*12*).

4. Main systems of reserve medical supplies around the world

With the frequent occurrence of public health emergencies across the world, some countries have established relatively mature medical stockpile systems to protect their populations from potential public health emergencies (*13*). In 2003, the United States created the Strategic National Stockpile (SNS) Program to maintain a stockpile of life-saving pharmaceuticals and medical supplies for use in a public health emergency. The SNS represents a real material asset in federal warehouses that can be quickly activated to meet the country's needs, enhancing the country's ability to respond effectively to public health emergencies. There are mainly three categories of SNS including 12-hour push packages, vendor managed inventory (VMI), and stockpile managed inventory (SMI). 12-hour push packages can be delivered to the collection reserve within 12 h of an emergency, and each emergency package contains sufficient medicines and medical supplies for hundreds of thousands of individuals to sustain treatment and prevention for several days. Vendor managed inventory (VMI) is managed inventory maintained by specific vendors or manufacturers that is stored at the supplier in the form of signed contracts and that can be delivered within 24 to 36 hours upon approval. Stockpile managed inventory (SMI) is directly managed and reserved by the SNS and includes physical reserves and ordered reserves. The US also has other forms of emergency supplies, such as chemical kits and family medical kits. In the event of an emergency, the SNS Program will deploy a team of advisors to coordinate and assist state and local authorities in receiving, managing, distributing, and recovering emergency medical supplies. The stockpile service advance group (SSAG) and technical advisory response unit (TARU) consist of experts in public health, emergency response, and logistics. In response to public health emergencies, Canada and Australia have also established the National Strategic Stockpile (NESS) (*14*) and National Medical Stockpile (NMS) (*15*) systems; these systems provide key reserves of essential medicines and equipment, such as personal protective equipment, antibiotics, and antivirals. The NESS and NMS are maintained in various strategic locations by federally leasing warehouses and by other means (Table 2).

5. How to enhance the reserve medical supplies system to deal with public health emergencies

Emerging pandemic have been increasing around the world over the past few years, and more than 40 emerging infectious diseases have been detected, such as SARS, H7N9 avian influenza, Ebola virus, and MERS. Epidemics of novel infectious diseases have emerged and rapidly spread globally in the context of economic globalization and increasingly frequent international exchanges, and these epidemics have a significant impact on economic development and

Table 1. China's policy documents related to the reserve medical supplies programs

Year	Title of policy documents (*ref.*)	Regulations
1997	Notice of the State Council on Reforming and Enhancing the Management of Medical Supplies (*21*). State Council., [1997] Reference No. *23.*	Reforms the current national system of medical supplies and pharmaceutical reserves, establishes a reserves program both at the central and local levels, and implements a dynamic reserve and paid redeployment program.
1999	Measures for National Management of Medical Supplies and Pharmaceutical Reserves (*22*). Pharmacy department, National Economic Trade Committee., [1999] Reference No. 544.	When major disasters, epidemics, or emergencies occur, or several provinces, autonomous regions, or municipalities directly under the central government are involved, the region's own medical reserves are used first. If those reserves are inadequate, the government can request medical reserves from neighboring regions or designated departments based on the paid redeployment program. If there are still unmet needs, the government can apply to access the central medical reserves.
2003	Regulations on Preparedness for and Responses to Emergent Public Health Hazards (*23*). Order of the State Council of the People's Republic of China (No.376).	Relevant departments of the State Council, governments at or above the county level, and their relevant departments should ensure reserves of supplies such as emergency facilities, equipment, medications, and medical equipment in accordance with the requirements of emergency plans.
2004	The 2004 Revised Law of the People's Republic of China on the Prevention and Treatment of Infectious Diseases (*24*). Order of the President of the People's Republic of China (No.17).	Governments at or above the county level are responsible for reserving medicines, medical equipment, and other supplies for the prevention and control of future outbreaks of infectious diseases.
2005	Master State Plan for a Rapid Response to Public Emergencies (*25*).	Establishes and improves the emergency supplies monitoring network, the early warning system, and the emergency supplies production, storage, allocation, and distribution system; improves emergency protocols and ensures the timely supply of emergency supplies and daily necessities; enhances the supervision and management of supply reserves, and provides timely supplements and updates.
2006	National Contingency Plan for Public Health Emergencies (*26*).	Governments at all levels must establish reserves of supplies and ensure the production capacity to handle public health emergencies. When a public health emergency occurs, reserve supplies should be allocated as needed to manage the emergency. Emergency reserves should be replenished in a timely manner after use.
2007	Law of the People's Republic of China on Emergency Response (*8*). Order of the President of the People's Republic of China (No.69).	The state should establish a sound emergency reserve supplies program and improve the program for the supervision, production, storage, allocation, and distribution of important emergency supplies. Municipal governments and county governments in areas where emergencies are likely to occur should establish a reserve program for emergency supplies, necessities, and equipment.
2008	(Draft) Catalogue of health emergency personnel and equipment (*27*). Office of Health Emergency Response, Ministry of Health., [2008] Reference No. 207.	Enhances the creation of health emergency response teams, implements standardized management of health emergency response teams, and continuously improves health emergency response capabilities.
2010	Guidance on Accelerating the Creation and Development of Public Health Emergency Systems (*28*). Office of Health Emergency Response, Ministry of Health., [2010] Reference No. 57.	Further improves the health emergency reserve supplies and allocation system. Improves the list of health emergency supplies, reasonably determines the type, quantity, and nature of the reserves; establishes procedures for effective use of emergency supplies in conjunction with relevant departments, and improves the mechanism of inter-regional, inter-departmental, and cross-military allocation of emergency supplies. Establishes and improves the emergency reserve supplies program for health institutions at all levels to facilitate the timely availability of emergency supplies.
2016	Notice of the National Health and Family Planning Commission on Issuance of Guiding Opinions on Enhancing the Standardization and Devising of Responses to Health-related Emergencies (*29*). Office of Health Emergency, Ministry of Health., [2016] Reference No. 68.	Improves supplies and technological reserves. Cooperates with industry and information technology departments to improve the emergency reserve supplies program, reasonably determines the material reserve catalogue, scale, and the extent of physical reserves, social reserves, and production capacity reserves; establishes and improves the supply rotation and allocation system and promotes the digitization of supply reserves records to improve the comprehensive coordination and ensured provision of emergency supplies.

human health. Improving the national public health emergency response system is crucial to the prevention and control of novel infectious diseases, and the emergency medical supplies is an indispensable element of public health emergency response (*16*).

In the future, China and many other countries should pay close attention to the reserve medical supplies program in the process of enhancing the public health emergency response system based on the lessons of the SARS-CoV-2 pandemic and the prevention and control of other epidemics. First, China should establish a public health emergency reserve medical supplies system and improve the nature of reserve medical supplies based on the types, needs, and validity of reserves (*17*), such as contracted reserves, physical reserves, financial reserves, and production capacity

Table 2. Major forms of emergency reserve medical supplies around the world

Country	Reserve form (*ref.*)	Details
United States	Strategic National Stockpile, SNS (*13,30*).	Office of the Assistant Secretary for Preparedness and Response (ASPR), HHS manages the SNS program The Stockpile includes 12-hour push packs (less than 5% of the SNS inventory) and managed inventories maintained by specific vendors or manufacturers, or the SNS. Supplies are managed through vendor managed inventory (VMI) and stockpile managed inventory (SMI). The plan is to deliver critical medical resources to the site of a national emergency when local public health resources would likely be or have already been overwhelmed by the magnitude of the medical emergency. The stockpile includes vaccines, antitoxins (*e.g.*, botulinum), airway equipment, and other medicines for emergency conditions.
Canada	Emergency Strategic Stockpile, NESS (*14*).	The Public Health Agency maintains the NESS to provide emergency supplies to provinces and territories when requested. A total of 11 federal warehouses are leased by the Public Health Agency: two main depots in the National Capital Region (Ottawa) and nine warehouses located across Canada. There are no federal warehouses located in the territories. The Public Health Agency has contracts in place for both custodians and security for all 11 federal warehouses. In the event of a local emergency that overwhelms available municipal resources, the municipality contacts the provincial/territorial emergency management authorities for additional resources. The NESS contains a variety of assets, including medical equipment and supplies (such as ventilators, personal protective equipment such as masks and gloves, *etc.*); pharmaceuticals (individual items such as antiviral agents, antibiotics, *etc.*); social service supplies (such as generators, cots, blankets, flashlights, *etc.*)
Australia	National Medical Stockpile, NMS (*15*).	The Health Emergency Management Branch (HEMB), Office of Health Protection, within the Department of Health and Ageing (DHA), is responsible for managing the NMS, including inventory management, planning and developing Memoranda of Understanding with states and territories for deployment of the stockpile. The NMS is kept in various strategic locations around Australia. All jurisdictions possess a pharmaceutical stockpile separate from the NMS and all jurisdictions maintain stockpiles of personal protective equipment (PPE) for responding to chemical, biological and radio-nuclear (CBRN) health disaster or pandemic influenza. Decisions to use the NMS are based on both internal and external expert clinical advice and on threat and risk assessment from the Australian National Security Agency. The NMS is a national strategic reserve of essential vaccines, antibiotics, antiviral drugs, chemical and radiological antidotes, and personal protective equipment. It also includes specialized medical supplies, such as the nation's stock of smallpox vaccine.

reserves. Second, standards for emergency medical supplies should be rationally devised and dynamically adjusted in accordance with changes in international and domestic circumstances. Third, programs for the planning, management, storage, deployment, distribution, emergency production, and urgent requisition of emergency supplies should be improved through legislation, and the roles and responsibilities of various departments and individuals in institutional arrangements should be clarified to ensure the effective implementation of those systems. Interagency agreements among the Ministry of Health, the Ministry of Defense, and logistics companies should be drafted to actively facilitate the transportation of medical supplies in response to a public health emergency without disruption or delay. The World Health Organization has pointed out that the world faces a chronic shortage of personal protective equipment such as respirators and masks because of the COVID-19 pandemic (*18*). To respond to public health emergencies during special periods, countries around the world should establish a system of international cooperation to jointly cope with major emerging emergencies and they should improve the global system for procurement and deployment of emergency supplies, with priority given to medical personnel.

China has set up a team to ensure medical supplies under the State Council that is responsible for the joint prevention and control of the SARS-CoV-2 epidemic. The production of key medical supplies such as medical protective clothing, medical goggles, medical masks, and disinfection supplies is organized by the Ministry of Industry and Information Technology, which is also responsible for coordinating and deploying urgently needed materials (*19*). On January 23, the Ministry of Industry and Information Technology of China expedited the delivery of 10,000 sets of protective clothing and 50,000 sets of gloves to Wuhan from the National Medicines Reserve, and it instituted six measures including the establishment of a national temporary production scheduling system for key enterprises and national temporary reserve supplies for epidemic prevention and control (*20*). Since the SARS-CoV-2 outbreak, China has also received medical masks, protective clothing, goggles, and other materials donated by South Korea, Japan, Britain, France, and other countries. With joint efforts of the international community, China should be able to deal with the epidemic at an early date and help to safeguard regional and global public health security.

References

1. National Health Commission of the People's Republic of China. Latest information of the prevalence of pneumonia caused by the severe acute respiratory syndrome coronavirus 2 as of 12 AM Feb 12. *http://www.nhc.gov.cn/xcs/yqtb/202002/26fb16805f024382bf*

f1de80c918368f.shtml (accessed February 13, 2020) (in Chinese)
2. State Council of the People's Republic of China. Secretary-General of the Shanghai Cooperation Organization praises China's efforts to combat novel coronavirus pneumonia. *http://www.gov.cn/xinwen/2020-01/31/content_5473474.htm* (accessed February 9, 2020) (in Chinese)
3. World Health Organization. WHO Director-General's statement on IHR Emergency Committee on Novel Coronavirus (2019-nCoV). *https://www.who.int/dg/speeches/detail/who-director-general-s-statement-on-ihr-emergency-committee-on-novel-coronavirus-(2019-ncov)* (accessed February 9, 2020).
4. Wang LZ. A system for allocation of emergency medical supplies and reserves primarily in large hospitals. Soft Science of Health. 2010; 24:402-403. (in Chinese)
5. Rebmann T, Wagner W. Infection preventionists' experience during the first months of the 2009 novel H1N1 influenza A pandemic. Am J Infect Control. 2009; 37:e5-e16.
6. National Health Commission of the People's Republic of China. Transcript of a press conference on February 4, 2020. *http://www.nhc.gov.cn/wjw/xwdt/202002/35990d56cfcb43f4a70d7f9703b113c0.shtml* (accessed February 4, 2020) (in Chinese)
7. Wang ZJ. Discussion on establishing a medical stockpile system for public health emergencies. Chinese Journal of Public Health Management. 2004; 6:502-503. (in Chinese)
8. The Central People's Government of the People's Republic of China. Law of the People's Republic of China on Emergency Response. *http://www.gov.cn/ziliao/flfg/2007-08/30/content_732593.htm* (accessed February 4, 2020) (in Chinese)
9. Legalweekly. Medical stockpile system needs to be urgently implemented. *http://www.legalweekly.cn/rwjs/17400.html* (accessed February 4, 2020) (in Chinese)
10. Wu D, Hu DD, Sun M, Li CY, Chang FS, Zhang JH, Li PP, Ning N, Hao M. CDC emergency response capacity and current state of public health emergency in China. Chinese Journal of Health Policy. 2014; 7:30-37. (in Chinese)
11. Guangming Daily. The transformation of and hidden concerns with China's disease prevention and control system. *http://epaper.gmw.cn/gmrb/html/2015-04/24/nw.D110000gmrb_20150424_1-05.htm* (accessed February 4, 2020) (in Chinese)
12. Sun M, Wu D, Shi JH, Li CY, Lv J, Su ZX, Ning N, Zhang JH, Xu P, Hao M. Policy changes related to the handling of public health emergencies in China: From 2003 to 2013. Chinese Journal of Health Policy. 2014; 7:24-29. (in Chinese)
13. U.S. Department of Health & Human Services. Strategic National Stockpile. *https://www.phe.gov/about/sns/Pages/default.aspx* (accessed February 4, 2020).
14. Government of Canada. National Emergency Strategic Stockpile. *https://www.canada.ca/en/public-health/services/emergency-preparedness-response/national-emergency-strategic-stockpile.html* (accessed February 4, 2020)
15. The Department of Health of Australian Government. National Medical Stockpile. *https://www1.health.gov.au/internet/main/publishing.nsf/Content/health-pubhlth-strateg-bio-factsht_stckpile.htm* (accessed February 4, 2020)
16. Jiang XC, Gao XQ, Li WY. Discussion on the model of an integrated emergency stockpile for public health emergencies. Jiangsu Health Care. 2013; 15:36-37. (in Chinese)
17. Wang LZ. Discussion on the mechanism of an emergency medical stockpile for public health emergencies in Guangzhou. Chinese Health Service Management. 2010; 27(3:177-177. (in Chinese)
18. World Health Organization. WHO Director-General's briefing to the Executive Board on outbreak of 2019 novel coronavirus. *https://www.who.int/dg/speeches/detail/who-director-general-s-briefing-to-the-executive-board-on-outbreak-of-2019-novel-coronavirus* (accessed February 9, 2020).
19. Ministry of Industry and Information Technology of People's Republic of China. Six departments report on the state of key medical supplies and living supplies for epidemic prevention and control. *http://www.miit.gov.cn/n1146290/n1146402/n7039597/c7662828/content.html* (accessed February 9, 2020) (in Chinese)
20. Ministry of Industry and Information Technology of People's Republic of China. Six measures of the Ministry of Industry and Information Technology to meet demands for the epidemic prevention and control stockpile. *http://www.miit.gov.cn/n1146290/n1146402/n7039597/c7644932/content.html* (accessed February 9, 2020) (in Chinese)
21. Law Yearbook of China. Notice of the State Council on Reforming and Enhancing the Management of the Pharmaceutical Stockpile. *http://www.pkulaw.cn/fulltext_form.aspx?Db=qikan&gid=1510046077* (accessed February4, 2020) (in Chinese)
22. The State Economic and Trade Commission. Provisions for a National Pharmaceutical Stockpile. *http://www.ccdi.gov.cn/fgk/law_display/3502* (accessed February 4, 2020) (in Chinese)
23. National Health Commission of the People's Republic of China. Regulations on Preparedness for and Responses to Emergent Public Health Hazards. *http://www.nhc.gov.cn/wjw/flfg/200804/c0aef6fa264048b3b0af617e445144bc.shtml* (accessed February 4, 2020) (in Chinese)
24. The Central People's Government of the People's Republic of China. The 2004 Revised Law of the People's Republic of China on the Prevention and Treatment of Infectious Diseases. *http://www.gov.cn/gongbao/content/2004/content_62975.htm* (accessed February 4, 2020) (in Chinese)
25. The Central People's Government of the People's Republic of China. Master State Plan for a Rapid Response to Public Emergencies. *http://www.gov.cn/yjgl/2006-01/08/content_21048.htm* (accessed February 4, 2020) (in Chinese)
26. The Central People's Government of the People's Republic of China. National Contingency Plan for Public Health Emergencies. *http://www.gov.cn/yjgl/2006-02/26/content_211654.htm* (accessed February 4, 2020) (in Chinese)
27. National Health Commission of the People's Republic of China. (Draft) Catalogue of health emergency personnel and equipment. *https://wenku.baidu.com/view/b8261d33f111f18583d05aa6.html* (accessed February 4, 2020) (in Chinese)
28. National Health Commission of the People's Republic

of China. Guidance on accelerating the creation and development of a public health emergency system. *http://www.cqvip.com/QK/70161X/20108/664581203.html* (accessed February 4, 2020) (in Chinese)
29. National Health Commission of the People's Republic of China. Issuance of Guiding Opinions on Enhancing the Standardization and Devising of Responses to Health-related Emergencies. *http://www.nhc.gov.cn/yjb/s7859/201612/3a3b5ce97fa940c58a64ff1892f4b3e1.shtml* (accessed February 4, 2020) (in Chinese)
30. Esbitt D. The Strategic National Stockpile: Roles and responsibilities of health care professionals for receiving the stockpile assets. Disaster Manag Response. 2003; 1:68-70.

Received February 1, 2020; Revised February 14, 2020; Accepted February 16, 2020.

**Address correspondence to:*
Jiangjiang He, Shanghai Health Development Research Center (Shanghai Medical Information Center), No.1477 Beijing (W) Road, Jing'an District, Shanghai 200040, China.
E-mail: hejiangjiang@shdrc.org

Released online in J-STAGE as advance publication February 17, 2020.

Original Article

DOI: 10.5582/bst.2020.01013

Electrocardiographic abnormalities among people with HIV in Shanghai, China

Fang Shen[1,2,§], Bowen Zhu[1,§], Yingying Ding[1], Meiyang Gao[1], Na He[1,3,*]

[1] Department of Epidemiology, School of Public Health, Fudan University, Shanghai, China;
[2] Department of Electrocardiography, Shanghai Public Health Clinical Center, Fudan University, Shanghai, China;
[3] Key Laboratory of Health Technology Assessment of Ministry of Health, Fudan University, Shanghai, China.

SUMMARY People living with HIV (PLWH) have an excess risk of cardiovascular diseases (CVD). Electrocardiographic (ECG) abnormalities are independently predictive of incident cardiovascular events in the general population. Our study aimed to evaluate the prevalence and correlates of ECG abnormalities among PLWH in Shanghai, China. We used a cross-sectional design to collect data from Shanghai Public Health Clinical Center, China. A total of 587 HIV-infected patients aged between 18 and 75 years were recruited between January 2015 and February 2016. The overall prevalence of any type of ECG abnormalities was 53.3%. The prevalence of sinus tachycardia, ST-T segment elevation and left ventricular hypertrophy was 23.0%, 18.1%, and 6.8%, respectively. Multivariable logistic regression analysis indicated that ST-T segment elevation was positively associated with higher baseline HIV viral load (≥ 4 $\log_{10}$ copies/mL), and sinus tachycardia was negatively associated with older age but positively associated with lower CD4 cell count, higher baseline HIV viral load (≥ 4 $\log_{10}$ copies/mL) and higher lactic dehydrogenase (LDH) level (≥133 mg/dL). Any coded ECG abnormality was positively associated with higher baseline HIV viral load (≥ 4 $\log_{10}$ copies/mL). ECG abnormalities including sinus tachycardia and ST-T segment elevation are prevalent among Chinese HIV patients, which are significantly associated with immunodeficiency and HIV viral load. Routine ECG screening may be an important part of HIV clinical care in China.

Keywords HIV, ECG, antiretroviral therapy, sinus tachycardia, ST-T segment elevation

1. Introduction

Wide access to highly effective combination antiretroviral therapy (ART) has ostensibly changed HIV infection status in many parts of the world from a fatal diagnosis to a chronic condition. However, extended life expectancy comes with long-term noninfectious comorbidities (NICMs), such as cardiovascular disease (CVD) (*1*). Prior studies have demonstrated that CVD is more common among the HIV-infected population than HIV-uninfected controls (*2,3*). This increased risk was partly explained by traditional risk factors of CVD such as smoking, diabetes, age, gender, as well as HIV infection itself, such as CD4 cell count and/or viral load, which is known to cause inflammation response by oxidative stress or coagulation disorders (*4-6*). However, the relative contributions of conventional cardiovascular risk factors, metabolic side effects of ART, and HIV infection itself on CVD risk are difficult to identify, as these factors frequently occur simultaneously (*7*).

Due to its wide availability, low cost and the accumulating evidence that electrocardiographic (ECG) abnormalities are predictive of incident cardiovascular events in the general population (*8*), the 12-lead electrocardiogram is a very useful non-invasive tool for evaluation of cardiac disorders and risks in clinical settings. Several typical ECG parameters, including resting heart rate and markers of abnormal cardiac depolarization/repolarization, have been previously reported to be associated with increased risk of sudden cardiovascular death (SCD) (*9,10*). Cardiovascular involvement in HIV/AIDS was recognized as part of the pandemic and a wide spectrum of cardiovascular abnormalities including corrected QT (QTc) prolongation, widened spatial QRS-T angle, ST-segment depressions, T-wave changes, and resting heart rate have been widely reported (*11-13*). Moreover, the association between age, obesity, alcohol consumption, lower CD4 cell count and LV diastolic dysfunction and ECG abnormalities were documented among HIV-positive patients (*14,15*).

The limited literature suggests that CVD risks (*e.g*. carotid intima-media thickness [cIMT], chronic kidney disease [CKD], hypertension, glycometabolism abnormities) are prevalent among HIV-infected patients in China (*16-18*), but data for ECG manifestations in this population are lacking. To fill this gap, we conducted a cross-sectional study to investigate the prevalence and correlates of ECG abnormalities among PLWH in Shanghai.

2. Materials and Methods

2.1. Study sample and data collection

All HIV-infected inpatients admitted to Shanghai Public Health Clinical Center routinely received a standardized comprehensive physical examination. For the present study, all HIV-infected inpatients aged between 18 and 75 years with ECG records during the study period from January 2015 to February 2016 were included in the final analysis. In brief, a structured anonymous questionnaire was developed to extract data from the hospital's electronic medical records (EMR) system, including demographic data such as gender, age and marital status, and blood biochemical data such as fasting glucose, triglyceride (TG; mmol/L), total cholesterol (TC; mmol/L) and lactic dehydrogenase (LDH; u/L), as well as HIV-related characteristics such as CD4 cell count, plasma HIV viral load, and ART regimens, *etc*. Hyperlipidemia was defined as TG ≥ 1.7mmol/L or TC ≥ 5.2 mmol/L, and high level of LDH was defined as LDH ≥ 245 u/L, according to recommendations by World Health Organization (WHO) and China national guidelines. The study was approved by the Institutional Review Board (IRB) of Fudan University, Shanghai, China.

2.2. ECG examination and categorization

Identical electrocardiographs [EDAN SE-1201 PC ECG system, EDAN Instruments, Inc.,China] were operating at 1000 samples per second with a frequency response of 0.05 Hz to 150 Hz., and standard 12-lead ECG was performed on all subjects in a supine position after 5 min rest using strictly standardized procedures. ECG examination was performed and initially read by an experienced cardiologist blinded to the patients' clinical history, and reconfirmed by a senior cardiologist. In brief, a resting ECG with a SE-12 Express machine was employed, with the participant in the left lateral decubitus position. ECG abnormalities including arrhythmia, abnormalities of the QRS complex, hypertrophy of the ventricles, atrial dilation, and abnormal repolarization were recorded. ECG abnormalities were categorized into ten groups: sinus tachycardia, ST-T segment elevation, left ventricular hypertrophy, atrioventricular conduction abnormalities, axis deviation, sinus bradycardia, atrial fibrillation/flutter, ventricular tachycardia/fibration, ischaemic ECG findings and others.

2.3. Statistical analyses

Sociodemographic and HIV-related characteristics of study participants were tabulated with frequencies and proportions for categorical variables. Number and proportion of participants with ECG manifestations were also tabulated. Univariate and multivariate logistic regression analyses with calculations of odd ratio (OR) and 95% confidence intervals (CI) were performed to evaluate correlates of ST-T segment elevation, sinus tachycardia and any coded ECG abnormality. Variables with $p < 0.10$ in univariate analysis were subject to multivariate regression analysis for adjustment of potential confounders. Age was categorized into four groups: 18-29, 30-44, 45-59, 60-75 years. Pearson χ^2 test and linear trend χ^2 test were performed to assess the distribution and trend of ECG manifestations across the age groups. A 2-sided P value < 0.05 was regarded as being statistically significant. All the statistical analyses were performed under SAS software Version 9.3. (IBM Company, New York, USA).

3. Results

3.1. Demographic and clinical characteristics

As shown in Table 1, the median age of the participants was 39.0 (IQR: 30.0-53.0) years. Among them, 90.1% were male, 41.2% were currently married, 27.3% were local registered residents, 29.3% were infected with HIV through homosexual behaviors whereas 55.7% through heterosexual behaviors.

As for the comorbidities, 36.1% were diagnosed with lung infection, 22.3% with tuberculosis, 5.3% with diabetes and 3.2% with kidney disease; 36.1% were tested with dyslipidemia (*i.e.*, TG ≥ 1.7mmol/L or TC ≥ 5.2 mmol/L) and 45.8% were with LDH above cutoff level (*i.e*., >245 u/L) (Table 1).

3.2. HIV-specific Characteristics

Over two-thirds (68.5%) of the participants had plasma HIV viral load ≥ 4 $\log_{10}$ copies/mL and 77.0% had CD4 cell count < 200 cells/μL. About 47.0% of the participants were on ART, of whom 72.5% had been on treatment for ≤ 2 years, 80.0% received a first-line regimen of "2 Nucleoside reverse transcriptase inhibitor (NRTI)+1 Non-nucleoside reverse transcriptase inhibitor (NNRTI) (*e.g*. Nevirapine [NVP]/Efavirenz [EFV])" and 18.5% received "2NRTI/NNRTI+Protease inhibitors (PI)" treatment. (Table 1).

3.2. Prevalence of abnormal ECG manifestations

The overall prevalence of any coded ECG abnormalities

Table 1. Characteristics of HIV-positive study participants ($N = 587$)

Characteristics	No. (proportion, %)
Age, years	
Median (IQR)	39.0 (30.0-53.0)
18-29	141 (24.0)
30-44	223 (38.0)
45-59	140 (23.8)
60-75	83 (14.2)
Male sex	529 (90.1)
Current married	242 (41.2)
Local residents	160 (27.3)
Route of HIV transmission	
Homosexual	172 (29.3)
Heterosexual	327 (55.7)
others	88 (15.0)
Comorbid condition	
Lung infection	212 (36.1)
Tuberculosis	131 (22.3)
Diabetes	31 (5.3)
Kidney disease	19 (3.2)
Plasma biochemical tests	
Dyslipidemia	212 (36.1)
LDH ≥ 245, U/L	269 (45.8)
HIV-specific characteristics	
Years since HIV diagnosis ≥ 3	96 (16.4)
CD4 cells < 200, cells/mL	452 (77.0)
Baseline Viral load ≥ 4, (log_{10} copies/mL)	402 (68.5)
On cART	276 (47.0)
2NRTI+1NNRTI (NVP/EFV)	221 (80.0)
2NRTI/NNRTI+PI	51 (18.5)
Other cART regimen*	4 (1.5)
Duration of cART ≤ 2 years	200 (72.5)
Duration of cART > 2 years	76 (27.5)

*Including PI only or 2NRTI+RAL. Dyslipidemia defined as TG ≥ 1.7mmol/L or TC ≥ 5.2 mmol/L. IQR, Interquartile range; LDH, Lactic dehydrogenase; cART, Combination antiretroviral therapy; NRTI: Nucleoside reverse transcriptase inhibitor; NNRTI: Non-nucleoside reverse transcriptase inhibitor; NVP: Nevirapine; EFV: Efavirenz; PI: Protease inhibitors; RAL: Raltegravir.

was 53.3%. The most common abnormal ECG manifestation was sinus tachycardia (23.0%) and ST-T segment elevation (18.1%) (Table 2). Other prevalent ECG abnormal manifestations included left ventricular hypertrophy (6.8%), atrioventricular conduction abnormalities (5.1%) and sinus bradycardia (4.8%) (Table 2). Figure 1 further presents the age-specific prevalence of abnormal ECG manifestations. Both the prevalence of ST-T segment elevation (Pfor linear trend < 0.001) and the prevalence of left ventricular hypertrophy (Pfor linear trend < 0.001) increased as age increased, whereas the prevalence of sinus tachycardia decreased as age increased (Pfor linear trend < 0.001) (Figure 1).

3.3. Correlates of ST-T segment elevation, sinus tachycardia and any coded ECG abnormalities

Table 2. Prevalence of ECG abnormalities among the study participants

ECG abnormalities	No. (proportion, %)
Any coded ECG abnormalities	312 (53.3)
Sinus tachycardia	136 (23.0)
ST-T segment elevation	106 (18.1)
Left ventricular hypertrophy	40 (6.8)
Atrioventricular conduction abnormalities	30 (5.1)
Axis deviation	30 (5.1)
Sinus bradycardia	28 (4.8)
Atrial fibrillation/flutter	18 (3.1)
Ventricular tachycardia/fibration	14 (2.4)
Ischaemic ECG findings	3 (0.5)
Others*	24 (4.1)

ECG: Electrocardiography; *: including low voltage of limb leads, junctional rhythm, right ventricular hypertrophy, sinus bigeminy, clockwise transposition and pacing rhythm.

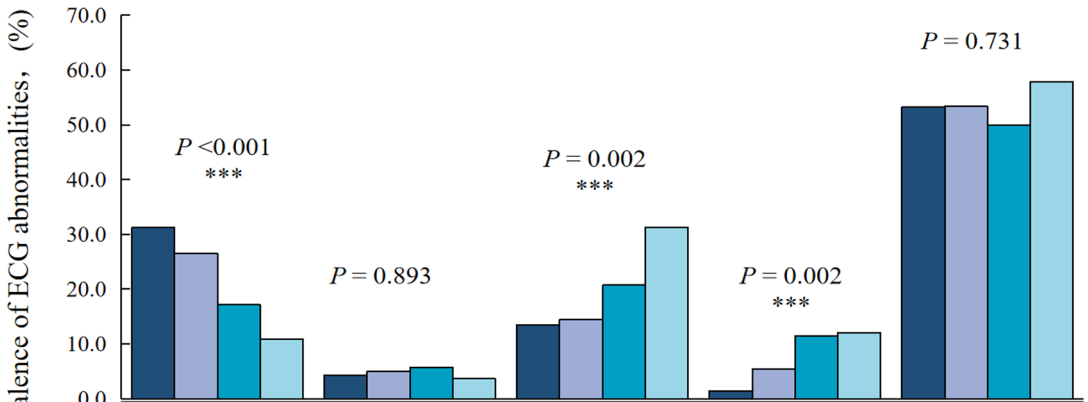

	Sinus tachycardia	Sinus bradycardia	ST-T segment elevation	Left ventricular hypertrophy	Any coded ECG abnormalities
18-29	31.2	4.3	13.5	1.4	53.2
30-44	26.5	4.9	14.4	5.4	53.4
45-59	17.1	5.7	20.7	11.4	50.0
60-75	10.8	3.6	31.3	12.0	57.8

Figure 1. Prevalence of electrocardiography (ECG) abnormalities among HIV-positive participants by age group (*** P for linear trend < 0.001).

Table 3. Univariate and multivariate logistic regression analyses of correlates with ST-T segment elevation, sinus tachycardia and any coded ECG abnormalities among HIV-positive participants, respectively

Items	ST-T segment elevation		Sinus tachycardia		Any coded ECG abnormalities	
	Univariate Models OR (95% CI)	Multivariable Modela OR (95% CI)	Univariate Models OR (95% CI)	Multivariable Modela OR (95% CI)	Univariate Models OR (95% CI)	Multivariable Modela OR (95% CI)
Age, years						
18–29	1.00	1.00	1.00	1.00	1.00	1.00
30-44	1.08 (0.58-1.98)	0.97 (0.49-1.92)	0.79 (0.50-1.26)	0.83 (0.48-1.44)	1.01 (0.66-1.54)	1.07 (0.69-1.64)
45-59	1.68 (0.89-3.16)	1.27 (0.58-2.79)	0.46 (0.26-0.80)**	0.43 (0.21-0.88)*	0.88 (0.55-1.41)	0.96 (0.60-1.55)
60-75	2.93 (1.50-5.72)**	2.25 (0.97-5.21)	0.27 (0.12-0.58)***	0.32 (0.13-0.78)*	1.21 (0.70-2.09)	1.39 (0.79-2.45)
Female sex	0.66 (0.35-1.26)	0.77 (0.38-1.54)	2.82 (1.19-6.73)*	2.26 (0.89-5.72)	1.24 (0.72-2.14)	1.23 (0.70-2.16)
Current married	0.56 (0.36-0.88)*	0.68 (0.38-1.20)	1.53 (1.04-2.25)*	0.89 (0.53-1.48)	1.07 (0.77-1.40)	
Local residents	1.64 (1.05-2.57)*	1.34 (0.82-2.21)	0.78 (0.50-1.21)		1.32 (0.91-1.90)	
Tuberculosis	1.32 (0.81-2.14)		1.35 (0.87-2.10)		1.02 (0.69-1.50)	
Kindey disease	2.16 (0.80-5.82)		0.88 (0.29-2.70)		1.53 (0.59-3.95)	
Diabetes	1.09 (0.44-2.74)		0.48 (0.16-1.39)		0.94 (0.45-1.93)	
Lung infection	1.04 (0.67-1.60)		1.97 (1.33-2.91)***	1.44 (0.92-2.27)	0.98 (0.70-1.37)	
Dyslipidemia	0.99 (0.64-1.53)		1.27 (0.86-1.89)		1.21 (0.86-1.69)	
LDH above cutoff	1.47 (0.94-2.31)	1.40 (0.88-2.25)	1.99 (1.30-3.05)**	1.61 (1.01-2.55)*	1.48 (1.06-2.07)*	1.37 (0.97-1.93)
Years since HIV diagnosis ≥ 3	0.48 (0.24-0.96)*	0.59 (0.28-1.24)	0.52 (0.28-0.94)*	0.84 (0.43-1.65)	1.16 (0.75-1.80)	
On ART	0.96 (0.63-1.47)		0.65 (0.44-0.97)*	0.94 (0.60-1.45)	0.95 (0.69-1.32)	
CD4 cells < 200, cells/mL	1.46 (0.85-2.49)		4.31 (2.25-8.26)***	2.69 (1.35-5.39)**	1.30 (0.88-1.91)	
Viral load at baseline ≥ 4, (log_{10} copies/mL)	2.25 (1.33-3.78)**	2.08 (1.19-3.63)*	3.35 (2.01-5.58)***	2.32 (1.29-4.18)**	2.04 (1.43-2.91)***	1.97 (1.38-2.83)***

ECG: Electrocardiography; LDH, Lactic dehydrogenase; cART, combination antiretroviral therapy; OR, odds ratio; CI, confidence interval. [a]: All listed variables with a *P* value of < 0.10 in univariate regression analysis were included in multivariable regression analysis. *$P < 0.05$; **$P < 0.010$; ***$P < 0.001$.

Table 3 presents results of three separate multivariable logistic regression analyses with adjustment of potential confounders to explore correlates of ST-T segment elevation, sinus tachycardia and any coded ECG abnormality, respectively. ST-T segment elevation was positively associated with higher baseline HIV viral load (≥ 4 log_{10} copies/mL), (aOR = 2.08, 95% CI: 1.19-3.63). Sinus tachycardia was negatively associated with older age (45-59 years: aOR = 0.43, 95% CI: 0.21-0.88; 60-75 years: aOR=0.32, 95% CI: 0.13-0.78) but positively associated with lower CD4 cell count (< 200 cells/mL) (aOR = 2.69, 95%CI: 1.35-5.39), higher baseline HIV viral load (≥ 4 log_{10} copies/mL) (aOR = 2.32, 95% CI: 1.29-4.18) and higher plasma LDH level (aOR = 1.61, 95%CI: 1.01-2.55). Any coded ECG abnormality was positively associated with higher baseline HIV viral load (≥ 4 log_{10} copies/mL) (aOR = 1.97, 95% CI: 1.38-2.83) (Table 3).

4. Discussion

ECG examination is a useful screening tool for CVDs, particularly in resource limited settings. This is particularly relevant for HIV patients who are expected to live much longer but with high probability of living with CVDs in the era of combination ART (*19*). Previous studies revealed that prolonged Q-T interval, a precursor to fatal cardiac arrhythmias, is the most prominent ECG manifestation among HIV patients (*20*). However, such data are not available for Chinese HIV patients who may also experience high prevalence of subclinical atherosclerosis (*21*). In the present study, we observed relatively high prevalence of sinus tachycardia and ST-T segment elevation in HIV-positive individuals, although the prevalence is slightly lower than that reported by studies in south-east Africa (*11*) and USA (*22,23*). Such differences reflect global diversities in a confluence of CVD risk factors that may or may not be directly associated with HIV among PLWH, such as environmental exposures, lifestyle, nutrition, coinfections, access to ART and healthcare continuum (*24-26*).

Notably, the prevalence of ECG abnormalities among HIV patients in this study is greater than that of the Chinese general population aged above 65 years *(27*). This suggests early onset of adverse cardiovascular affects by HIV infection, which are most likely associated with immune activation and inflammatory response but independent of classic CVD risk factors and could occur at younger ages (*21*). The increasing risks of sinus bradycardia, ST-T segment elevation and left ventricular hypertrophy among older patients underscore the importance of enhanced ECG monitoring and cardiovascular alerts for HIV-infected elders.

The prevalence of sinus tachycardia was higher than any other ECG abnormality among HIV patients in this study. This pattern has also been observed in other

studies (*11,28*). High heart rate has been observed as an independent risk factor for cardiovascular morbidity and mortality in the general population. In addition to negative association between older age and sinus tachycardia, which is well represented in the general population, lower CD4 cell count or more severe immunodeficiency and higher lactic dehydrogenase (LDH) level were positively associated with sinus tachycardia. Previous studies suggest that HIV infection with low CD4 cell count might further contribute to cardiovascular complications (*29*). The relationship between the CD4 cell count and cardiac complications may be mediated through the role of heightened inflammation and serum levels of inflammatory mediators, which likely occurred in patients with low CD4 cell count thereby predisposing them to sinus tachycardia (*30,31*). In advanced HIV disease, depletion of the CD4 cell count leads to the activation of CD8 killer T-cells which mediate persistent immune dysfunction and inflammation (*32,33*). On the other hand, LDH is associated with sinus tachycardia because it is a marker of common injuries and diseases such as myocardial infarction (MI) and heart failure and is released during tissue damage.

ST-T segment elevation on ECG is observed in HIV-infected patients in this study, which could be caused either by pericardial disease or dilated cardiomyopathy, that are known to occur frequently in HIV-positive individuals (*34-36*). Meanwhile, those who had higher levels of plasma HIV viral load had a greater risk of ST-T segment elevation and any coded ECG finding as well. Such associations were also observed in the VACS study (*37*). The HIV virus causes inflammatory reaction in the coronary vessels and myocardial cells, which is believed to promote endothelial dysfunction and atherosclerosis as well as early carotid artery atherosclerosis (*38,39*). In fact, HIV genomic sequences have been demonstrated in the coronary vessels of HIV-infected patients who died of acute myocardial infarction (*40*), reiterating that HIV infection is an independent risk for ECG abnormality by itself regardless of other traditional CVD risk factors. Nonetheless, the exact mechanism(s) need further investigation.

We did not observe any association of ART status or usage of antiretroviral drugs (ARV) with ECG abnormalities in this study, probably due to the low proportion of being treated and the short duration of ART for those treated. Untreated HIV patients had severe immunodeficiency and high HIV viral load, which were associated with high risk for CVD and ECG abnormalities. On the other hand, there is growing evidence that dyslipidemia and endothelial dysfunction are common side effects of ART particularly among patients receiving PIs (*41,42*). Longer duration of ART would also expose the patients to higher risk for CVD and higher likelihood of abnormal ECG manifestations. As the national ART program rapidly scales up and the availability of PIs increases in China, cardiovascular side effects and related ECG abnormalities are not ignorable and very likely to increase substantially.

This study had several limitations. First, only prevalence rather than incidence of ECG abnormalities could be investigated due to the cross-sectional nature of this study. Future longitudinal studies are needed to examine the incidence and causal mechanisms of CVDs and characteristic ECG manifestations. Second, this study was conducted in a municipal clinical center, which is the officially designated hospital for HIV care and treatment in Shanghai, China. Therefore, the study results may not be generalizable to other provinces. Multicenter studies are warranted in the near future. Third, no HIV-negative controls were enrolled for comparison in this study, further limiting our ability to draw a promising conclusion.

In summary, this exploratory study reveals high prevalence of typical ECG abnormalities including sinus tachycardia and ST-T segment elevation among the HIV-positive population in China, which could be employed as a useful screening tool for CVDs in Chinese HIV patients who are mostly living in rural areas and have limited access to comprehensive clinical care. The associations of ECG abnormalities with immunodeficiency and HIV viral load highlight the necessity of early and combined ART for prevention of cardiovascular comorbidities, which could also be adverse consequences of cART. This dilemma further underscores needs of careful monitoring and care continuum for CVDs in the era of combination ART scale up in China.

Acknowledgements

We thank all study participants without whom this research would not be possible. This work was supported by the Natural Science Foundation of China (Grant No. 81773485), the National Science and Technology Major Projects on Infectious Diseases of China (Grant No. 2018ZX10721102-004), and Shanghai Municipal Health Commission (Grant No. GWTD2015S05).

References

1. Guaraldi G, Orlando G, Zona S, Menozzi M, Carli F, Garlassi E, Berti A, Rossi E, Roverato A, Palella F. Premature age-related comorbidities among HIV-infected persons compared with the general population. Clin Infect Dis. 2011; 53:1120-1126.
2. Freiberg MS, Chang CC, Kuller LH, *et al*. HIV infection and the risk of acute myocardial infarction. JAMA Intern Med. 2013; 173:614-622.
3. Data Collection on Adverse Events of Anti-HIV drugs (D:A:D) Study Group, Smith C, Sabin CA, Lundgren JD, Thiebaut R, Weber R, Law M, Monforte Ad, Kirk O, Friis-Moller N, Phillips A, Reiss P, El Sadr W, Pradier C, Worm SW. Factors associated with specific causes of death amongst HIV-positive individuals in the D:A:D

study. AIDS. 2010; 24: 1537-1548.
4. Pasternak AO, de Bruin M, Jurriaans S, Bakker M, Berkhout B, Prins JM, Lukashov VV. Modest nonadherence to antiretroviral therapy promotes residual HIV-1 replication in the absence of virological rebound in plasma. J Infect Dis. 2012; 206:1443-1452.
5. Graham SM, Rajwans N, Jaoko W, Estambale BB, McClelland RS, Overbaugh J, Liles WC. Endothelial activation biomarkers increase after HIV-1 acquisition: plasma vascular cell adhesion molecule-1 predicts disease progression. AIDS. 2013; 27:1803-1813.
6. Mooney S, Tracy R, Osler T, Grace C. Elevated biomarkers of inflammation and coagulation in patients with HIV are associated with higher framingham and VACS risk index score. Plos One. 2015; 10(12):e0144312.
7. van Vonderen MG, Smulders YM, Stehouwer CD, Danner SA, Gundy CM, Vos F, Reiss P, Agtmael MA. Carotid intima-media thickness and arterial stiffness in HIV-infected patients: the role of HIV, antiretroviral therapy, and lipodystrophy. J Acquir Immune Defic Syndr. 2009; 50:153-161.
8. Nishi FA, Maia FO, Cruz DA. Assessing sensitivity and specificity of the Manchester Triage System in the evaluation of acute coronary syndrome in adult patients in emergency care: a systematic review protocol. JBI Database System Rev Implement Rep. 2015; 13:64-73.
9. Aro AL, Huikuri HV. Electrocardiographic predictors of sudden cardiac death from a large Finnish general population cohort. J Electrocardiol. 2013; 46:434-438.
10. Panikkath R, Reinier K, Uy-Evanado A, Teodorescu C, Hattenhauer J, Mariani R, Gunson K, Jui J, Chugh SS. Prolonged tpeak to tend interval on the resting electrocardiogram is associated with increased risk of sudden cardiac death. Circ Arrhythm Electrophysiol. 2011; 4:441-447.
11. Okoye IC, Anyabolu EN. Electrocardiographic abnormalities in treatment-naïve HIV subjects in south-east Nigeria. Cardiovasc J Afr. 2017; 28:315-318.
12. Gili S, Mancone M, Ballocca F, *et al*. Prevalence and predictors of long corrected QT interval in HIV-positive patients: a multicenter study. J Cardiovasc Med (Hagerstown). 2017; 18:539-544.
13. Njoku PO, Ejim EC, Anisiuba BC, Ike SO, Onwubere BJ. Electrocardiographic findings in a cross-sectional study of human immunodeficiency virus (HIV) patients in Enugu, south-east Nigeria. Cardiovasc J Afr. 2016; 27:252-257.
14. Mcintosh RC, Lobo JD, Hurwitz BE. Current assessment of heart rate variability and QTc interval length in HIV/AIDS. Curr Opin HIV AIDS. 2017; 12:528-533.
15. Isasti G, Pérez I, Moreno T, Cabrera F, Palacios R, Santos J. Echocardiographic abnormalities and associated factors in a cohort of asymptomatic HIV-infected patients. AIDS Res Hum Retroviruses. 2013; 29:20-24.
16. Guo F, Hsieh E, Lv W, Han Y, Xie J, Li Y, Song X, Li T. Cardiovascular disease risk among Chinese antiretroviral-naïve adults with advanced HIV disease. BMC Infect Dis. 2017; 17:287.
17. Cao Y, Gong M, Han Y, Xie J, Li X, Zhang L, Li Y, Song X, Zhu T, Li T. Prevalence and risk factors for chronic kidney disease among HIV-infected antiretroviral therapy-naïve patients in mainland China: a multicenter cross-sectional study. Nephrology (Carlton). 2013; 18:307-312.
18. Ding Y, Lin H, Liu X, Zhang Y, Wong FY, Sun YV, Marconi VC, He N. Hypertension in HIV-infected adults compared with similar but uninfected adults in China: body mass index-dependent effects of nadir CD4 count. AIDS Res Hum Retroviruses. 2017; 33:1117-1125.
19. Eyawo O, Brockman G, Goldsmith CH, Hull MW, Lear SA, Bennett M, Guillemi S, Franco-Villalobos C, Adam A, Mills EJ, Montaner JSG, Hogg RS. Risk of myocardial infarction among people living with HIV: an updated systematic review and meta-analysis. BMJ Open. 2019; 9:e025874.
20. Knudsen AD, Kofoed KF, Gelpi M, Sigvardsen PE, Mocroft A, Kühl JT, Fuchs A, Køber L, Nordestgaard BG, Benfield T, Graff C, Skov MW, Lundgren J, Nielsen SD; Copenhagen Comorbidity in HIV Infection (COCOMO) Study. Prevalence and risk factors of prolonged QT interval and electrocardiographic abnormalities in persons living with HIV. AIDS. 2019; 33:2205-2210.
21. Lin H, Ding Y, Ning C, Qiao X, Chen X, Chen X, Shen W, Liu X, Hong Y, He N. Age specific associations between HIV Infection and carotid artery intima media thickness in China: a cross-sectional evaluation of baseline data from the CHART Cohort. Lancet HIV. 2019; 6:e860-e868.
22. Patel N, Veve M, Kwon S, McNutt LA, Fish D, Miller CD. Frequency of electrocardiogram testing among HIV-infected patients at risk for medication-induced QTc prolongation. HIV Medicine. 2013; 14:463-471.
23. Gupta M, Miller CJ, Baker JV, Lazar J, Bogner JR, Calmy A, Soliman EZ, Neaton JD. NSIGHT SMART Study Group. Biomarkers and electrocardiographic evidence of myocardial ischemia in patients with human immunodeficiency virus infection. Am J Cardiol. 2013; 111:760-764.
24. Shahbaz S, Manicardi M, Guaraldi G, Raggi P. Cardiovascular disease in human immunodeficiency virus infected patients: a true or perceived risk? World J Cardiol. 2015; 7:633-644.
25. Vachiat A, McCutcheon K, Tsabedze N, Zachariah D, Manga P. HIV and ischemic heart disease. J Am Coll Cardiol. 2017; 69:73-82.
26. Kearns A, Gordon J, Burdo T H, Qin X. HIV-1-associated atherosclerosis. J Am Coll Cardiol. 2017; 69:3084-3098.
27. SL Liu, HY Wei, LL Yang, CQ Wen. ECG analysis of 2951 elderly community health examination. Shanghai Medical Journal. 2013; 34:55-57.
28. Ntsekhe M, Hakim J. Impact of human immunodeficiency virus infection on cardiovascular disease in Africa. Circulation. 2005; 112:3602-3607.
29. Charitakis E Barmano N, Walfridsson U, Walfridsson H. Factors predicting arrhythmia-related symptoms and health-related quality of life in patients referred for radio frequency ablation of atrial fibrillation: an observational study (the SMURF Study). JACC Clin Electrophysiol. 2017; 3:494-502.
30. Meier A, Bagchi A, Sidhu HK, Alter G, Suscovich TJ, Kavanagh DG, Streeck H, Brockman MA, LeGall S, Hellman J, Altfeld M. Upregulation of PD-L1 on monocytes and dendritic cells by HIV-1 derived TLR ligands. AIDS. 2008; 22:655-665.
31. Fernandez S, Lim A, French M. Immune activation and the pathogenesis of HIV disease: implications for therapy. J HIV Ther. 2009; 14:52-56.
32. Paiardini M, Müller-Trutwin M. HIV-associated chronic immune activation. Immunol Rev. 2013; 254:78-101.
33. Butt AA, Michaels S, Greer D, Clark R, Kissinger P, Martin DH. Serum LDH level as a clue to the diagnosis of histoplasmosis. AIDS Read. 2002; 12:317-321.

34. Deeks SG. HIV infection, inflammation, immunosenescence, and aging. Annu Rev Med. 2011; 62:141-155.
35. Becker AC, Sliwa K, Stewart S, Libhaber E, Essop AR, Zambakides CA, Essop MR. Acute coronary syndromes in treatment-naive black South Africans with human immunodeficiency virus infection. J Interv Cardiol. 2010; 23:70-77.
36. Bruner KM, Murray AJ, Pollack RA, Soliman MG, Laskey SB, Capoferri AA, Lai J, Strain MC, Lada SM, Hoh R, Ho YC, Richman DD, Deeks SG, Siliciano JD, Siliciano RF. Defective proviruses rapidly accumulate during acute HIV-1 infection. Nat Med. 2016; 22:1043-1049.
37. Salinas JL, Rentsch C, Marconi VC, Tate J, Budoff M, Butt AA, Freiberg MS, Gibert CL, Goetz MB, Leaf D, Rodriguez-Barradas MC, Justice AC, Rimland D. Baseline, time-updated, and cumulative HIV care metrics for predicting acute myocardial infarction and all-Cause mortality. Clin Infect Dis. 2016; 63:1423-1430.
38. Hoffmann C, Jaeger H. Cardiology and AIDS-HAART and the consequences. Ann N Y Acad Sci. 2001; 946:130-144.
39. Hsu JC, Li Y, Marcus GM, Hsue PY, Scherzer R, Grunfeld C, Shlipak MG. Atrial fibrillation and atrial flutter in human immunodeficiency virus-infected persons: incidence, risk factors, and association with markers of HIV disease severity. J Am Coll Cardiol. 2013; 61:2288-2195.
40. Soliman EZ, Prineas RJ, Roediger MP, Duprez DA, Boccara F, Boesecke C, Stephan C, Hodder S, Stein JH, Lundgren JD, Neaton JD. Prevalence and prognostic significance of ECG abnormalities in HIV-infected patients: results from the Strategies for Management of Antiretroviral Therapy study. J Electrocardiol. 2011; 44:779-785.
41. Worm SW, Sabin C, Weber R, Reiss P, El-Sadr W, Dabis F, De Wit S, Law M, Monforte AD, Friis-Møller N, Kirk O, Fontas E, Weller I, Phillips A, Lundgren J. Risk of myocardial infarction in patients with HIV infection exposed to specific individual antiretroviral drugs from the 3 major drug classes: the data collection on adverse events of anti-HIV drugs (D:A:D) study. J Infect Dis. 2010; 201:318-330.
42. Estrada V, Portilla J. Dyslipidemia related to antiretroviral therapy. AIDS Rev. 2011;13:49-56.

Received January 15, 2020; Revised February 13, 2020; Accepted February 16, 2020.

[§]These authors contributed equally to this work.
*Address correspondence to:
Na He, Department of Epidemiology, School of Public Health, Fudan University, Shanghai 200032, China.
E-mail: nhe@fudan.edu.cn

Released online in J-STAGE as advance publication February 20, 2020.

Original Article

DOI: 10.5582/bst.2019.01350

Effects of different mark-up drug policies on drug-related expenditures in tertiary public hospitals: an interrupted time series study in Shanghai, China, 2015-2018

Xianji Wang[1,§], Fen Li[2,§], Xuemei Wang[3], Xinping Zhang[3], Chenxi Liu[3], Dan Wang[3], Haiyin Wang[2], Yingyao Chen[1,*]

[1] Key Lab of Health Technology Assessment, National Health Commission, School of Public Health, Fudan University, Shanghai, China;
[2] Shanghai Health Development Research Center, Shanghai, China;
[3] School of Medicine and Health Management, Tongji Medical College of Huazhong University of Science and Technology, Wuhan, Hubei, China.

SUMMARY Irrational use of drugs remains a major challenge especially in developing countries, which contributed to a heavy pharmaceutical expenditure burden. Price regulation has been taken to curb the growth of pharmaceutical expenditures in many countries. This study aimed to investigate the impact of different mark-up drug policies on drug-related expenditures in tertiary public hospitals in Shanghai, China. Data were drawn from the audited financial statement in 24 tertiary public hospitals in Shanghai from January 2015 to December 2018. Drug-related revenue data and per capita cost data pre- and post-intervention were included. Interrupted time series design was applied to assess the actual effects of Fixed Percent Mark-up Drug (FPM) policy and Zero Mark-up Drug (ZMD) policy respectively. Results showed that ZMD policy achieved better intervention effects on declining drug-related expenditures than FPM policy. Apart from a declining trend in drug proportion (coefficient = -0.0017, $p = 0.031$), no other significant changes were found during FPM implementation. However, ZMD policy was associated with a level decline in per capita outpatient drug cost (coefficient = -12.21, $p = 0.025$) and a trend decline in per capita inpatient drug cost (coefficient = -25.12, $p < 0.001$), as well as a level decrease (coefficient = -0.0256, $p = 0.001$) and a downward tendency (coefficient = -0.0018, $p < 0.001$) in drug proportion. ZMD policy was effective in regulating drug-related expenditures, while FPM policy was difficult to achieve expected results due to the existence of profit space. Further regulation should be strengthened in the future, especially on drug revenue and per capita drug cost.

Keywords Zero Mark-up Drug policy, Fixed Percent Mark-up Drug policy, drug revenue, per capita drug cost, drug proportion

1. Introduction

Irrational use of drugs remains a widespread concern worldwide, especially in developing countries, where around 60% of drugs prescribed and sold in public health institutions were inappropriate (*1,2*). It was reported that irrational use of drugs contributed to a heavy pharmaceutical expenditure burden and the costs resulted from harmful effects after taking drugs were up to 870 million USD per year in the UK (*3*). Pharmaceutical expenditure was assumed to account for 25%-70% of total healthcare expenditures in developing countries and approximately 10% in most developed countries (*4*). In OECD countries, the pharmaceutical expenditure was estimated to be approximately 800 billion USD, accounting for 17% of total healthcare expenditures, with the range of less than 10% in Denmark to more than 30% in Hungary (*5*). For Japan and South Korea, pharmaceutical expenditure constituted 20.6% and 25.1% of total healthcare expenditure respectively (*6,7*).

In China, government investment was replaced by pharmaceutical profits, which became the major income source for hospitals for a long time (*2*). The overall healthcare expenditure increased almost sevenfold from approximately 75 billion USD to 519 billion USD since 2000, among which pharmaceutical expenditure was estimated to account for 42.5% and tertiary public hospitals was much higher (*7*). As one of the most common problems of irrational drug

use, unnecessary drug use is serious in China (*8-10*). A close interest relationship between drug sales and prescriptions made unnecessary prescriptions and drug rebates prevail in the long term (*11*). Physicians in China tend to rely heavily on drug revenue due to the existence of profit margins on drugs (*12*). They have financial incentives to recommend patients drug therapies even when not appropriate, while patients are generally unable to judge whether the recommended drugs are suitable, which provides a shortcut for physicians to prescribe and profit from unnecessary medications (*13,14*).

To curb the increasing growth of pharmaceutical expenditures, price regulation was put forward in many countries by setting, agreeing and cutting prices of drugs, aimed at increasing accessibility and restraining exorbitant prices (*5,15-18*). Separation of prescribing and dispensing was one of the essential price regulation measures, which has originally been formed since the 12th century and followed and adopted by numerous countries (*19*). For instance, in Korea, separation of drug prescribing from dispensing was implemented with the goal of fundamentally changing the inefficient provision and consumption of drugs to contain pharmaceutical expenditure (*13*). This approach could also help to decrease irrational drug use with the fact that prescriptions from dispensing physicians was twice and 7 times more than those by non-dispensing physicians in Zimbabwe and Malaysia, respectively (*20,21*). Similar price regulation methods could also be seen in Spain, where a new system for fixing prices was adopted and a Ministerial Decree for selective reimbursement of drugs was introduced by government, to keep increasing pharmaceutical expenditures under control (*22*).

In China, declining mark-up on drugs was undertaken as part of a separation of healthcare and medicine policy, so as to decouple provider compensation from the prescription and sales. There are two typical mark-up drug policies, one is Fixed Percent Mark-up Drug (FPM) policy, which allows drugs to be sold on fixed mark-up percent based on the purchase price; the other is Zero Mark-up Drug (ZMD) policy, which requires all public hospitals to prescribe drugs at purchase price without including a mark-up (*23*). Previous studies mostly presented positive effects on healthcare expenditures shortly after implementing ZMD policy, but showed mixed results regarding long-term effects (*11,14,24*). Regarding FPM policy, hospitals were found to show more preference for expensive drugs, which led to increasing healthcare expenditures and high drug revenue proportion in both outpatient and inpatient healthcare revenue (*9,25*). Different from others, mark-up-cancellation policy in Shanghai, China was gradually executed by declining 5% of mark-up step by step, until all the mark-up was eventually cancelled. Specially, FPM policy with a mark-up decline from 15% to 10% was attempted to be executed initially, followed by the final implementation of ZMD policy. The focus of ZMD policy was completely decoupling provider compensation from the prescription and sales and thus eliminated physicians' incentive for prescribing expensive drugs and reducing excessive household spending on irrational drugs.

Previous practices mainly directly focused on one-time implementation of cancelling mark-up, but ignored the gradually executed process. Additionally, previous studies mainly focused on primary care settings and have reported varying and sometimes conflicting results which may result from different study designs, e.g. cross-sectional or before-after study designs (*14*). Few applied interrupted time series to simultaneously evaluate the actual effects of different mark-up drug policies, especially those represented by ZMD and FPM. A simultaneous comparison between the intervention effects brought by these two typical regulation measures (intervention with mark-up vs. intervention without mark-up) were deficient until now.

This study aimed to investigate the impact of ZMD policy and FPM policy on drug-related expenditures and provide a foundation for policy and practice improvements to avoid physicians' irrational prescriptions and improve patients' drug affordability. We sought to assess different regulation intensity on pharmaceutical expenditure, with specific attention towards identifying different intervention effects caused by ZMD policy and FPM policy respectively, so as to provide more evidence-based experience for international practice in tertiary public hospital settings.

2. Materials and Methods

2.1. Setting

This study was set in Shanghai municipality, which is located on the Yangtze River Delta in east China and covered a provincial coastal area of 6,340 km^2. There are 24.18 million inhabitants in Shanghai (2017). The per capita GDP in Shanghai was 18,756 USD (2017), which was more than twice the average national per capita GDP (8,836 USD) and exceeded the high-income country threshold (12,235 USD). The life expectancy in Shanghai is estimated to be 83.37 years, like those in high-income countries (*26-28*). Public hospitals are responsible for majority of healthcare provision and account for appropriately 95% of all outpatient visits, inpatient discharges and inpatient surgical procedures (*29*). Among public hospitals, primary healthcare institutions provide essential medical care services, mainly including outpatient care as well as public health services, such as health education, maternity care, planned immunization, *etc.* (*30*). Secondary and

tertiary public hospitals provide both outpatient and inpatient care, among which tertiary public hospitals serve as a medical service center within a region and provide nearly half of the outpatient care as well as 42.5% of inpatient services (*29,31*).

In this study, all municipal tertiary public hospitals in Shanghai were selected for analysis, excluding the hospitals affiliated with the National Health Commission of the People's Republic of China. A total of twenty-four tertiary public hospitals were analyzed, including 9 Comprehensive hospitals, 4 Chinese medicine hospitals, and 11 Specialized hospitals, which accounted for 48.0% of all tertiary public hospitals, and 13.1% of all public hospitals in Shanghai. The scale of these 24 hospitals is large, whose number of beds, outpatients and inpatients account for 22.4%, 22.2% and 37.5% of all public hospitals in Shanghai, respectively (Table 1).

2.2. Policy Intervention

From December, 2015 to February, 2017, gradual policy intervention aiming at reducing drug price were continuously implemented in Shanghai, by declining 5% of mark-up each time. The first formally intervention measure is declining the mark-up from 15% to 10% in December 10, 2015 in all public hospitals (except for Chinese Herbal Medicine), and the actual procurement price over 500 RMB should not exceed 50 RMB. The final powerful intervention was declining the drug mark-up to zero in February 1, 2017 in all public hospitals (except for Chinese Herbal Medicine), and being sold according to the actual procurement price, which represented ZMD policy was implemented.

From the first intervention to the final intervention, a significantly symbolic change was observed during the gradual intervention measures, that is a drug regulation policy of the FPM is experimentally and gradually replaced by ZMD from small-scale to full-scale. In this study, the first intervention measure of cancelling partial mark-up in December 10, 2015 and the final intervention of cancelling all mark-up in February 1, 2017 were selected into analysis, respectively representing the intervention with mark-up and without mark-up.

2.3. Data sources and outcome indicators

Data in this study were derived from the audited financial statement of each hospital. Monthly data of 24 tertiary public hospitals from January 2015 to December 2018 were collected, including drug-related revenue data and cost data.

Indicators concerning drug-related expenditures were designed and selected in this study, including drug revenue (total drug revenue, outpatient drug revenue and inpatient drug revenue), per capita outpatient drug cost, per capita inpatient drug cost, as well as the proportion of drug revenue in total healthcare revenue (drug proportion). The calculations of related indicators are as follows:

i) Drug revenue was obtained directly from the audited financial statement;

ii) Per capita outpatient drug cost = total outpatient drug revenue/total number of outpatients;

iii) Per capita inpatient drug cost = total inpatient drug revenue/total number of inpatients;

iv) Proportion of drug revenue in total healthcare revenue (%) = (pharmaceutical revenue /total healthcare revenue) *100%.

2.4. Statistical analysis

Interrupted time series (ITS) design was employed to assess the change of drug-related expenditures in 2015-2018 based on pre-intervention and post-intervention data collected monthly from 24 tertiary public hospitals, so as to evaluate the actual effects of intervention policy. ITS design has been regarded as the strongest, quasi-experimental methodology to analyze longitudinal effects, which can overcome the shortcomings of simple pre- and post-evaluation, and have an advantage of evaluating intervention effects simultaneously from the level change of observed indicators before and after intervention, and the trend change (slope change) (*32,33*).

Segmented regression model was used in an interrupted time series analysis to assess the impact of FBM policy and ZMD policy. The data were divided into two segments, that is before intervention and after intervention. Level and trend were used to define each segment of a time series. Specifically, the level is the

Table 1. General characteristics of healthcare institutions in this study

Category	Institutions (number)	Beds (number)	Outpatients (million)	Discharged patients (million)
Comprehensive hospitals	9	15,992	31.7385	0.9599
Chinese medicine hospitals	4	4,224	11.9284	0.2077
Specialized hospitals	11	7,464	12.0858	0.4262
Maternity hospitals	2	1,333	3.0572	0.1141
Children's hospitals	2	1,389	4.1806	0.0865
Other specialized hospitals	7	4,742	4.8480	0.2256
Total	24	27,680	55.7527	1.5938

value at the beginning of a segment and trend (slope) is the rate of change during a segment. Both changes in the level following intervention implementation and trend that occurred after intervention can be observed by applying a segmented regression model. The vast strength of this model is evaluating the level changes and trend (slope) changes associated with intervention on the basis of controlling for baseline level and trend (slope) (*33*).

Two intervention points were included in this study. One is FPM policy (intervention with mark-up) and the other is ZMD policy (intervention without mark-up). The fit level and slope change model:

$$Y_i = \beta_0 + \beta_1 X_1 + \beta_2 X_2 + \sum \beta_j X_j + \varepsilon_i$$

Y_i represents the outcome indicator during a time period which changes on a monthly basis between January 2015 until December 2018 for hospital; X_1 represents trend (slope), pre-intervention is X_1=0, post-intervention is X_1=1; X_2 is the intervention measure, pre-intervention is X_2=0, post-intervention is X_2=1; β_1 represents the trend change (slope change), β_2 represents the level change; $\sum \beta_j X_j$ represents covariates (influential factors outside of the intervention measure and time); ε_i represents error. Durbin-Watson test was used to check for serial autocorrelation of the error terms, and *p* values and coefficients were estimated by use of the least squares method (*33,34*).

3. Results

3.1. Overall change of drug-related expenditures between 2015 and 2018

Seeing from Table 2, the increase of 6.8%, 4.5% and 9.6% were still observed respectively in total drug revenue, outpatient drug revenue and inpatient drug revenue after implementing FPM policy in 2016. After implementing ZMD policy, a decline of 2.0% was observed in total drug revenue in 24 tertiary public hospitals in 2017 (compared with 2016), while an increase of 2.7% was found in total drug revenue in 2018 (compared with 2017). Besides, a decline of 2.5% was observed in 2017 (compared with 2016) in outpatient drug revenue while an increase of 5.4% was found in 2018 (compared with 2017), and a decline of 1.5% was observed in 2017 (compared with 2016) in inpatient drug revenue and a continuous decrease still existed in 2018.

There was no decline in per capita outpatient drug cost in 24 tertiary public hospitals after implementing FPM policy in 2016. After ZMD policy was implemented, a decrease of 4.6% was observed in 2017 (compared with 2016), but then increased in 2018. For per capita inpatient drug cost, a decline of 1.2% was found after implementing FPM policy in 2016 (compared with 2015). After implementing ZMD policy, a significant decrease of 9.0% was found in 2017 (compared with 2016), and a continuous decline was observed in 2018.

The initial drug proportion in 24 tertiary public hospitals was 37.5% in 2015. After implementing FPM policy, drug proportion in 2016 was 35.3% (declined by 2.2%). After ZMD policy was implemented, the proportion decreased by 4.1% in 2017 (compared with 2016), and a continuous decline was observed in 2018. It was obvious to see that ZMD policy achieved larger effects on declining drug proportion than FPM policy (Table 2).

3.2. Results of the segmented regression analysis

As shown in Table 3, it was observed that drug revenue decreased immediately after implementing FPM policy and an increasing trend change was found though there was no statistical significance (coefficient = -69.06, *p* = 0.993; coefficient = 754.95, *p* = 0.156, respectively), indicating that FPM policy made no significant changes on drug revenue. After implementing ZMD policy, an immediate decline change and an increasing trend change was observed in drug revenue (coefficient = -11,547.50, *p* = 0.062; coefficient = 586.30, *p* = 0.038, respectively).

It was observed that the per capita outpatient

Table 2. Drug revenue, per capita drug cost and drug proportion in 24 tertiary public hospitals between 2015-2018

Indicator	Drug-related expenditures				Relative Ratio with Fixed Base/proportion change		
	2015	2016	2017	2018	2016/2015	2017/2015	2018/2015
Drug revenue (million)							
Total	1,405,269	1,500,859	1,470,348	1,510,502	1.068	1.046	1.075
Outpatient	759,956	793,881	774,300	815,864	1.045	1.019	1.074
Inpatient	645,313	706,978	696,048	694,638	1.096	1.079	1.076
Per capita drug cost (RMB)							
Outpatient	151	151	144	146	1.001	0.951	0.968
Inpatient	5,308	5,243	4,770	4,358	0.988	0.899	0.821
Drug proportion (%)							
Comprehensive hospitals	37.3	35.3	31.0	28.6	-2.0	-6.3	-8.7
Chinese medicine hospitals	38.0	36.3	31.2	27.1	-1.7	-6.8	-10.9
Specialized hospitals	37.6	34.9	31.8	29.9	-2.7	-5.7	-7.7
Total	37.5	35.3	31.2	28.7	-2.1	-6.2	-8.8

drug cost and per capita inpatient drug cost increased immediately after FPM policy though there was no statistical significance (coefficient = 0.85, p = 0.905; coefficient = 73.63, p = 0.548, respectively). Meanwhile, an increasing trend was found in per capita outpatient drug cost and a declining trend was observed in per capita inpatient drug cost with no statistical significance (coefficient = 0.08, p = 0.867; coefficient = -12.18, p = 0.157, respectively). After implementing ZMD policy, per capita outpatient drug cost and per capita inpatient drug cost decreased immediately (coefficient = -12.21, p = 0.025; coefficient = -226.40, p = 0.112, respectively). Meanwhile, an increasing trend change and a declining trend change were observed in per capita outpatient drug cost and per capita inpatient drug cost (coefficient = 0.27, p = 0.268; coefficient= -25.12, p < 0.001, respectively).

A decline with no statistical significance was observed in drug proportion immediately after implementing FPM policy, and a downward trend was presented in the long run (coefficient = -0.0001, p = 0.992; coefficient = -0.0017, p = 0.031, respectively). The implementation of ZMD policy was associated with a significant level decline in the drug proportion (coefficient = -0.0256, p = 0.001), and continuously showed a significant downward trend (coefficient=-0.0018, p < 0.001) (Table 3).

4. Discussion

To the best of our knowledge, it was the first study that attempted to simultaneously explore the intervention effects caused by FPM policy and ZMD policy using an interrupted time series design in tertiary public hospital settings. There is little empirical evidence on the comparison of different mark-up policies on declining drug-related expenditures. Overall, the ZMD policy achieved better intervention effects compared with FPM policy.

This study demonstrated that FPM policy made no significant effects on drug-related expenditures (except for the decreasing trend on drug proportion), while ZMD policy significantly declined drug proportion, and the level of per capita outpatient drug cost as well as the trend of per capita inpatient drug cost. It was obvious to see that ZMD policy was more powerful and intensive than FPM policy, which may result from the more thorough separation of provider compensation from the prescription and sales. Due to the existence of mark-up, FPM policy still retained some profit space, which allowed physicians to seek avenues of earning profits. After eliminating all possible profit space on drugs, hospitals may shift attention to other high value medical consumables or clinical processes and seek

Table 3. Results of change in drug-related expenditures pre- and post- the first intervention and final intervention

Indicator	*Variable*	β	S.E.	T	p
Pre- and post- the first intervention					
drug revenue	(Intercept)	111,230.29	4,200.88	26.478	0.000***
	X_1	754.95	514.44	1.468	0.156
	X_2	-69.06	7,473.40	-0.009	0.993
per capita outpatient drug cost	(Intercept)	152.62	3.98	38.330	0.000***
	X_1	0.08	0.49	0.170	0.867
	X_2	0.85	7.08	0.120	0.905
per capita inpatient drug cost	(Intercept)	5,394.91	67.88	79.476	0.000***
	X_1	-12.18	8.31	-1.466	0.157
	X_2	73.63	120.76	0.610	0.548
Drug proportion	(Intercept)	0.3880	0.0061	63.660	0.000***
	X_1	-0.0017	0.0007	-2.310	0.031*
	X_2	-0.0001	0.0108	-0.010	0.992
Pre- and post- the final intervention					
drug revenue	(Intercept)	114,280.70	5,646.50	20.239	0.000***
	X_1	586.30	272.10	2.155	0.038*
	X_2	-11,547.50	5,989.30	-1.928	0.062
per capita outpatient drug cost	(Intercept)	147.01	4.91	29.963	0.000***
	X_1	0.27	0.24	1.127	0.268
	X_2	-12.21	5.20	-2.346	0.025*
per capita inpatient drug cost	(Intercept)	5,707.84	130.64	43.692	0.000***
	X_1	-25.12	6.29	-3.991	0.000***
	X_2	-226.40	138.57	-1.634	0.112
Drug proportion	(Intercept)	0.3884	0.0067	58.143	0.000***
	X_1	-0.0018	0.0003	-5.438	0.000***
	X_2	-0.0256	0.0071	-3.615	0.001**

*p < 0.05; **p < 0.01; ***p < 0.001. Durbin-Watson test all indicated no autocorrelation.The first intervention study period was between January 2015 to January 2017, where pre-intervention was from January 2015 to December 2015 and post-intervention was from January 2016 to January 2017.The final intervention study period was between January 2016 to December 2018, where pre-intervention was from January 2016 to January 2017 and post-intervention was from February 2017 to December 2018.

for other price adjustments to compensate for the loss of revenue (*35*). Judging from this, a comprehensive mark-up-cancellation approach was more likely to bring about better intervention results, which have also been previously demonstrated (*25*). A separation reform in Taiwan also effectively reduced drug expenditure and changed prescribing behavior, which is consistent with our findings (*36*).

However, the intervention effects of ZMD policy on drug revenue and per capita drug cost were limited, especially on the trend of drug revenue and per capita outpatient drug cost in the long run. Similar findings also existed in previous studies. He YZ *et al.* found that drug expenditure declined sharply after ZMD policy initially, but the effects of ZMD policy gradually disappeared and became even worse in the long run, except for inpatient drug expenditure (*11*). Lee *et al.* assessed the effects of separation reform on drug expenditures and found medication expenditures increased by 98.4% for peptic-ulcer medication, among which expensive drugs and branded drugs accounted for the majority of this increase, even when generic drugs were available (*37*). Similar phenomena also occurred in China, with the fact that physicians tend to prescribe branded drugs that may be more effective but expensive to ensure quick recovery of their patients. Besides, with the population ageing, the number of elderly patients is growing rapidly, who may require more medication therapies, thus drug revenue was difficult to decrease overall. In addition, with the more comprehensive population coverage and further improvement of the medical insurance system, patients with insurance are more likely to be prescribed more drugs than before, and inpatients tend to have more prescriptions than outpatients due to a higher medical reimbursement rate (*38,39*).

There are some limitations in this study. First, FPM policy (the first intervention with mark-up) and ZMD policy (the final intervention without mark-up) were selected to represent two typical types of intervention measures, while other possibly relevant intervention measures that occurred during the period were not included in analysis. Second, Segmented regression was used to respectively evaluate the effects of the first intervention and the final intervention, while an integrated regression simultaneously including the first and final intervention was not applied due to other possibly relevant interventions that may have also occurred during that period. Third, indicators related to rational drug use were not included for analysis because the data was not available.

In conclusion, this study represents a segmented regression analysis of different mark-up drug policy on drug-related expenditures. Overall, ZMD policy achieved better intervention effects than FPM policy, especially on declining drug proportion. However, expected intervention effects on drug revenue and per capita drug cost were limited and further regulation should be strengthened in the future.

Acknowledgements

We thank Associate Prof. Zhi-Jie Zhang, and postgraduate Jian Hu, Department of Epidemiology, School of Public Health, Fudan University, for their help in the statistical analysis of this article.

References

1. Ofori-Asenso R, Agyeman AA. Irrational use of medicines – A summary of key concepts. Pharmacy (Basel). 2016; 4,35.
2. Mao W, Vu H, Xie Z, Chen W, Tang S. Systematic review on irrational use of medicines in China and Vietnam. PLoS One. 2015; 10:e0117710.
3. Hitchen L. Adverse drug reactions result in 250,000 UK admissions a year. BMJ. 2006; 332:1109.
4. World Health Organization. Measuring medicine prices, availability, affordability and price components 2nd edition. 2008; *http://www.haiweb.org/medicineprices/manual/documents.html* (accessed September 1, 2019).
5. Ben-Aharon O, Shavit O, Magnezi R. Does drug price-regulation affect healthcare expenditures. Eur J Health Econ. 2017; 18:859-867.
6. OECD/WHO. Pharmaceutical expenditure, in OECD/WHO. Health at a Glance: Asia/Pacific 2012. Paris: OECD Publishing. *http://dx.doi.org/10.1787/9789264183902-32-en* (Accessed November 27, 2019)
7. Chen Y, Hu S, Dong P, Kornfeld Å, Jaros P, Yan J, Ma F, Toumi M. Drug pricing reform in China: analysis of piloted approaches and potential impact of the reform. J Mark Access Health Policy. 2016; 4:30458.
8. le Grand A, Hogerzeil HV, Haaijer-Ruskamp FM. Intervention research in rational use of drugs: A review. Health Policy Plan. 1999; 14:89-102.
9. Yu X, Li C, Shi Y, Yu M. Pharmaceutical supply chain in China: Current issues and implications for health system reform. Health Policy. 2010; 97:8-15.
10. Vijayakumar TM, Sathyavati D, Subhashini T, Grandhi S, Dhanaraju MD. Assessment of prescribing trends and rationality of drug prescribing. International Journal of Pharmacology. 2011; 7:140-143.
11. He Y, Dou G, Huang Q, Zhang X, Ye Y, Qian M, Ying X. Does the leading pharmaceutical reform in China really solve the issue of overly expensive healthcare services? Evidence from an empirical study. PLoS One. 2018; 13: e0190320.
12. Yip W, Mahal A. The health care systems of China and India: performance and future challenges. Health Aff (Millwood). 2008; 27:921-932.
13. Kwon S. Pharmaceutical reform and physician strikes in Korea: separation of drug prescribing and dispensing. Soc Sci Med. 2003; 57:529-538.
14. Yi H, Miller G, Zhang L, Li S, Rozelle S. Intended and unintended consequences of China's zero markup drug policy. Health Aff (Millwood). 2015; 34:1391-1398.
15. Grandfils N. Drug price setting and regulation in France. 2008; *http://www.irdes.fr/EspaceAnglais/Publications/WorkingPapers/DT16DrugPriceSettingRegulationFrance.pdf* (accessed October 20, 2019).

16. Rockoff H. Price controls. *http://www.econlib.org/library/Enc/PriceControls.html* (accessed November 1, 2019)
17. Ess SM, Schneeweiss S, Szucs TD. European healthcare policies for controlling drug expenditure. Pharmacoeconomics. 2003; 21:89-103.
18. Lee IH, Bloor K, Hewitt C, Maynard A. International experience in controlling pharmaceutical expenditure: influencing patients and providers and regulating industry – a systematic review. J Health Serv Res Policy. 2015; 20:52-59.
19. Tiong JJ, Mai CW, Gan PW, Johnson J, Mak VS. Separation of prescribing and dispensing in Malaysia: the history and challenges. Int J Pharm Pract. 2016; 24:302-305.
20. Teng CL, Nik-Sherina H, Ng CJ, Chia YC, Atiya AS. Antibiotic prescribing for childhood febrile illness by primary care doctors in Malaysia. J Paediatr Child Health. 2006; 42:612-617.
21. Trap B, Hansen EH, Hogerzeil HV. Prescription habits of dispensing and non-dispensing doctors in Zimbabwe. Health Policy Plan. 2002; 17:288-295.
22. Lopez Bastida J, Mossialos E. Pharmaceutical expenditure in Spain: cost and control. Int J Health Serv. 2000; 30:597-616.
23. Li X, Lu J, Hu S, Cheng KK, De Maeseneer J, Meng Q, Mossialos E, Xu DR, Yip W, Zhang H, Krumholz HM, Jiang L, Hu S. The primary health-care system in China. Lancet. 2017; 390: 2584-2594.
24. Yang C, Shen Q, Cai W, Zhu W, Li Z, Wu L, Fang Y. Impact of the zero-markup drug policy on hospitalization expenditure in western rural China: an interrupted time series analysis. Trop Med Int Health. 2017; 22:180-186.
25. Liu Y, Lin Z, Ru Y, Zhang M. Small-scale or full-scale? The zero mark-up drug policy in China. Journal of Interdisciplinary Mathematics. 2017; 20:1167-1178.
26. Shanghai Municipal Bureau of Health. Annual Report of the Health Status of Shanghai. 2017; *http://tjj.sh.gov.cn/tjnj/nj18.htm?d1=2018tjnj/C0201.htm* (accessed September 20, 2019)
27. National Bureau of Statistics. China Statistical Yearbook. 2008; *http://www.stats.gov.cn/tjsj/ndsj/2018/indexch.htm* (accessed September 20, 2019).
28. World Bank. New country classifications by income level: 2017-2018. 2017; *http://blogs.worldbank.org/opendata/new-country-classifications-income-level-2017-2018* (accessed July 1, 2019)
29. Lin H, Dyar OJ, Rosales-Klintz S, Zhang J, Tomson G, Hao M, Stålsby Lundborg C. Trends and patterns of antibiotic consumption in Shanghai municipality, China: a 6 year surveillance with sales records, 2009–14. J Antimicrob Chemother. 2016; 71:1723-1729.
30. Tang Y, Liu C, Zhang Z, Zhang X. Effects of prescription restrictive interventions on antibiotic procurement in primary care settings: a controlled interrupted time series study in China. Cost Eff Resour Alloc. 2018; 16:1.
31. Xu GC, Zheng J, Zhou ZJ, Zhou CK, Zhao Y. Comparative study of three commonly used methods for hospital efficiency analysis in Beijing tertiary public hospitals, China. Chin Med J (Engl). 2015; 128:3185-3190.
32. Bernal JL, Cummins S, Gasparrini A. Interrupted time series regression for the evaluation of public health interventions: a tutorial. Int J Epidemiol. 2017; 46:348-355.
33. Wagner AK, Soumerai SB, Zhang F, Ross-Degnan D. Segmented regression analysis of interrupted time series studies in medication use research. J Clin Pharm Ther. 2002; 27:299-309.
34. Durbin J, Watson GS. Testing for serial correlation in least square regression. I. Biometrika. 1950; 37:409-428.
35. Liu X, Xu J, Yuan B, Ma X, Fang H, Meng Q. Containing medical expenditure: lessons from reform of Beijing public hospitals. BMJ. 2019; 365:l2369.
36. Chou YJ, Yip WC, Lee CH, Huang N, Sun YP, Chang HJ. Impact of separating drug prescribing and dispensing on provider behaviour: Taiwan's experience. Health Policy Plan. 2003; 18:316-329.
37. Lee EK, Malone DC. Comparison of peptic-ulcer drug use and expenditures before and after the implementation of a government policy to separate prescribing and dispensing practices in South Korea. Clin Ther. 2003; 25:578-592.
38. Sun X, Jackson S, Carmichael GA, Sleigh AC. Prescribing behaviour of village doctors under China's New Cooperative Medical Scheme. Soc Sci Med. 2009; 68: 1775-1779.
39. Zhang H, Hu H, Wu C, Yu H, Dong H. Impact of China's public hospital reform on healthcare expenditures and utilization: a case study in ZJ Province. PLoS One. 2015; 10:e0143130.

Received December 30, 2019; Revised February 6, 2020; Accepted February 12, 2020

[§]These authors contributed equally to this work.

**Address correspondence to:*
Yingyao Chen, Key Lab of Health Technology Assessment, National Health Commission, School of Public Health, Fudan University, Shanghai 200032, China.
E-mail: yychen@shmu.edu.cn

Released online in J-STAGE as advance publication February 25, 2020.

Original Article

DOI: 10.5582/bst.2019.01230

Suppression of tumor growth and metastasis by ethanol extract of *Angelica dahurica Radix* in murine melanoma B16F10 cells

Hyun Hwangbo[1,2], Eun Ok Choi[1,2], Min Yeong Kim[1,2], Da Hye Kwon[1,2], Seon Yeong Ji[1,2], Hyesook Lee[1,2], Sang Hoon Hong[3], Gi-Young Kim[4], Hye Jin Hwang[5], Su Hyun Hong[1,2], Yung Hyun Choi[1,2,*]

[1] Anti-Aging Research Center, Dong-eui University, Busan, Korea;
[2] Department of Biochemistry, Dong-eui University College of Korean Medicine, Busan, Korea;
[3] Department of Internal Medicine, Dong-eui University College of Korean Medicine, Busan, Korea;
[4] Department of Marine Life Sciences, Jeju National University, Jeju, Korea;
[5] Department of Food and Nutrition, Dong-eui University, Busan, Korea.

SUMMARY The roots of *Angelica dahurica* have long been used as a traditional medicine in Korea to treat various diseases such as toothache and cold. In this study, we investigated the effect of ethanol extract from the roots of this plant on metastatic melanoma, a highly aggressive skin cancer, in B16F10 melanoma cells and B16F10 cell inoculated-C57BL/6 mice. Our results showed that the ethanol extracts of *Angelicae dahuricae Radix* (EEAD) suppressed cell growth and induced apoptotic cell death in B16F10 cells. EEAD also activated the mitochondria-mediated intrinsic apoptosis pathway, with decreased mitochondrial membrane potential, and increased production of intracellular reactive oxygen species and ration of Bax/Bcl-2 expression. Furthermore, EEAD reduced the migration, invasion, and colony formation of B16F10 cells through the reduced expression and activity of matrix metalloproteinase (MMP)-2 and -9. In addition, *in vivo* results demonstrated that oral administration of EEAD inhibited lactate dehydrogenase activity, hepatotoxicity, and nephrotoxicity without weight loss in B16F10 cell inoculated-mice. Importantly, EEAD was able to markedly suppress lung hypertrophy, the incidence of B16F10 cells lung metastasis, and the expression of tumor necrosis factor-alpha in lung tissue. Taken together, our findings suggest that EEAD may be useful for managing metastasis and growth of malignant cancers, including melanoma.

Keywords Angelica dahurica; B16F10 cells; apoptosis; invasion; lung metastasis

1. Introduction

Over the past several decades, the incidence and mortality rates of melanomas have increased rapidly, and the number of cases has increased more rapidly than other types of solid tumors. In particular, metastatic melanoma is the most aggressive tumor due to its unique ability to metastasize prematurely and resistance to conventional therapies (*1,2*). However, clinical management of patients with metastatic melanoma is limited to treatment, due to the absence of effective target chemotherapy and control protocols (*3,4*). Although various therapies have been developed for the treatment of patients with melanoma, chemotherapy is still the primary approach for blocking cancer metastasis. However, some limitations, such as adverse side effects, drug resistance, and limited efficacy, remain to be solved (*5,6*). Therefore, it is urgent to develop new therapeutic strategies that minimize these limitations and have high therapeutic efficacy. In this regard, interest in natural resources that have traditionally been used in the prevention and treatment of various diseases is increasing (*7*). In addition, some herbal extracts have been shown to induce apoptosis and inhibit the metastasis of cancer cells, which are important strategies for the control of proliferation in cancer cells, without showing toxicity to normal cells (*8,9*).

Angelica dahurica Radix, the roots of *Angelica dahurica* Bentham et Hooker, which belongs to the genus Angelica (family Apiaceae), is widely used as a traditional medicine to treat several symptoms including headaches, asthma, hypertension, colds, and toothaches in East Asian countries including Korea, Japan and China (*10-12*). Up to now, various therapeutic activities

of *Angelica dahurica Radix* including anti-microbial, anti-oxidant, anti-inflammatory, and anti-mutagenic effects have been reported (*13-18*). Although recent studies have showed that the extracts and/or compounds isolated *Angelica dahurica Radix* has an anti-tumor effect on human cancer cells (*17,19-22*), the underlying mechanism is not yet well known. Therefore, in this study, as part of a screening program for the discovery of traditional medicine resources with anti-metastatic activity, we investigated the effect of ethanol extract from the *Angelica dahurica Radix* on the metastatic potential of murine melanoma B16F10 cells and attempted to identify the mechanism of action.

2. Materials and Methods

2.1. Preparation of 70% ethanol extract of *Angelica dahurica Radix*

The dried roots of *A. dahurica* (*Angelica dahurica Radix*) were obtained from Dong-eui Korean Medical Center (Busan, Republic of Korea). The roots (100 g) were ground into fine powder, and refluxed with 1 L of 70% ethanol solution by sonication for 24 h. After filtering through a glass filter funnel to remove insoluble matters, the extracts were concentrated with a rotary vacuum evaporator (Buchi Labortechnik, Flawil, Switzerland) and followed by lyophilization. The ethanol extracts of *Angelicae dahuricae Radix* (abbreviated as EEAD hereafter) were then stored at -80°C prior to use. EEAD were dissolved in dimethylsulfoxide (DMSO, Sigma-Aldrich Chemical Co., St. Louis, MO, USA) to a final concentration of 100 mg/mL. The stock solution was diluted with a cell culture medium to the desired concentration before use.

2.2. Cell culture

B16F10 cells that originate in the syngeneic C57BL/6 (H-2b) mouse stain, were obtained from the American Type Culture Collection (Manassas, MD, USA). The cells were maintained in Dulbecco's modified Eagle's medium (DMEM) supplemented with 10% fetal bovine serum (FBS), 100 U/mL penicillin, and 100 μg/mL streptomycin (WelGENE Inc., Daegu, Republic of Korea).

2.3. Cell viability assay

Cell viability was assessed by 3-(4,5-dimethyl-2-thiazolyl)-2,5-diphenyltetra-zolium bromide (MTT) assay, as described previously (*19*). Briefly, B16F10 cells were seeded onto 96-well plates at a density of 1 × 10^4 cells/well, and incubated for overnight. The cells were exposed to a series of concentrations of EEAD for 24 h, and the cells were then incubated with 50 μg/mL MTT solution (Invitrogen, Waltham, MA, USA) at 37°C for 2 h. Subsequently, the medium was removed, and DMSO was added to each well to dissolve the formed blue formazan crystals, followed by measurement at 570 nm in a microplate reader (Molecular Device Co., Sunnyvale, CA, USA). The morphological changes of cells were directly observed and photographed under a phase-contrast microscope (Carl Zeiss, Oberkochen, Germany).

2.4. Nuclear staining assay

The alteration of nuclear morphology in EEAD-treated cells was assessed by 4′,6-diamidino-2-phenylindole (DAPI) staining. In brief, cells were treated with different concentrations of EEAD for 24 h, and then fixed with 4 % paraformaldehyde (Sigma-Aldrich Chemical Co.) at room temperature for 10 min. The cells were washed with phosphate buffered saline (PBS), and stained with 1 μg/m DAPI solution (Sigma-Aldrich Chemical Co.) for 10 min, under light-shielded conditions. The cells were rinsed with PBS, visualized and photographed using a fluorescence microscope (Carl Zeiss).

2.5. Determination of apoptotic cell death by flow cytometric analysis

The magnitude of apoptosis was measured by flow cytometry using the annexin V-fluorescein isothiocyanate (FITC) Apoptosis detection kit (BD Biosciences, San Diego, CA, USA). After treatment with EEAD for 24 h, the cells were suspended in the supplied binding buffer, and then stained with FITC-conjugated annexin V and propidium iodide (PI) for 20 min in the dark at room temperature, by following the manufacturer's protocol. The fluorescent intensities of the cells were detected by flow cytometry (BD Biosciences), and the annexin V^+/PI^- and annexin V^+/PI^+ cell populations were considered indicators of apoptotic cells.

2.6. Measurement of mitochondrial membrane potential (MMP, $\Delta\Psi m$)

To measure MMP ($\Delta\Psi m$), 5,5',6,6'-tetrachloro-1,1',3,3'-tetraethyl-imidacarbocyanine iodide (JC-1) staining was performed. After treatment with EEAD for 24 h, cells were exposed to 10 μM JC-1 (Sigma-Aldrich Chemical Co.) for 30 min at 37°C. The cells were washed with PBS to remove unbound dye, and the cells were collected for each sample. The amounts of MMP ($\Delta\Psi m$) were detected at 488/575 nm using a flow cytometer, according to the manufacturer's instruction.

2.7. Measurement of intracellular reactive oxygen species (ROS) production

The production of ROS was measured using 5,6-carboxy-2',7'-dichlorodihydrofluorescein diacetate

(DCF-DA), as described previously (*23*). After treatment with EEAD for 30 min, the cells were washed with PBS and incubated with 10 μM DCF-DA (Invitrogen) in the dark at 37°C for 20 min. Subsequently, the cells were analyzed for DCF fluorescence by flow cytometry at 480 nm/520 nm.

2.8. Reverse transcription-polymerase chain reaction (RT-PCR)

Total RNA was isolated using TRIzol reagent (Invitrogen) by the manufacturer's recommended protocol. After quantifying the RNA concentration, genes of interest were amplified from cDNA that was reverse-transcribed from 1 μg of total RNA using AccuPower® PCR PreMix (Bioneer, Daejeon, Korea), as described previously (*24*). The PCR was carried out using the Mastercycler (Eppendorf, Hamburg, Germany) under the following conditions: initial denaturation for 3 min at 94°C; 30 cycles of 30 sec at 94°C, 30 sec at 61°C, and 1 min at 72°C; and final extension for 5 min at 72°C. Subsequently, PCR products were separated on 1.0% agarose gel containing ethidium bromide (EtBr; Sigma-Aldrich Chemical Co.) and visualized using ultraviolet light. The glyceraldehyde 3-phosphate dehydrogenase (GAPDH) housekeeping gene transcript was used as a control.

2.9. Protein extraction and Western blot analysis

The whole cellular proteins were prepared using the Bradford protein assay kit (Bio-Rad Laboratories, Hercules, CA, USA) and protein concentration was measured using the Bio-Rad protein assay kit (Bio-Rad Laboratories), according to the manufacturer's instruction. An equal amount of protein from the samples was separated by denaturing sodium dodecyl sulfate (SDS)-polyacrylamide gel electrophoresis, and then transferred onto polyvinylidene difluoride membranes (Schleicher & Schuell, Keene, NH, USA). The membranes were blocked with 5% skim milk in Tris-buffered saline containing 0.1% Triton X-100 (TBST) for 1 h, and then probed with specific primary antibodies (Santa Cruz Biotechnology, Santa Cruz, CA, USA) to react with the blotted membranes at 4°C overnight. After washing with TBST, the membranes were incubated with the appropriate horseradish peroxidase (HRP)-conjugated secondary antibodies (Santa Cruz Biotechnology, Inc.) for 2 h at room temperature. The expression of protein was detected by enhanced chemiluminescence (ECL) kit (GE Healthcare Life Sciences, Little Chalfont, UK), and visualized by Fusion FX Image system (Vilber Lourmat, Torcy, France).

2.10. Wound healing assay

B16F10 cells were seeded in a 6-well plate (1×10^6 cells/well) and incubated to 80-90% confluence. To evaluate cell migration, wound lines in the form of a cross were made by scraping with a plastic 200 μL pipette tip in confluent cells. After wounding, floating cells were washed out with PBS, and were incubated with 1% FBS-containing DMEM supplemented with or without EEAD for 24 h. Subsequently, the width of wound healing was observed and photographed under a phase-contrast microscope.

2.11. Invasion assay

The invasion ability was assessed using the Trans-well chamber system (10 mm diameter, 8 μm pore size with polycarbonate membrane, Corning Costar Corp., Cambridge, MA, USA). After maintaining B16F10 cells in serum-free DMEM for 24 h, the cells (5×10^4 cells/well) were placed in the upper chamber of trans-well insert, and at the same time, 10% FBS-containing complement medium supplemented with or without EEAD was added into the lower chamber, and then cells were incubated for 24 h. Cells that invaded through the filter were fixed with 3.7% paraformaldehyde, and stained with hematoxylin and eosin (Sigma-Aldrich Chemical Co.). The stained colonies were observed and counted under a phase-contrast microscope and photographed.

2.12. Colony formation assay

After treatment with EEAD for 24 h, single-cell suspensions of B16F10 cells were inoculated on 6-well plates (200 cells/well). The cells were cultured for two weeks while replacing the medium every 3 days to form colonies. The colonies were fixed with 3.7% paraformaldehyde and then stained with 0.1% crystal violet solution (Sigma-Aldrich Chemical Co.) at room temperature for 10 min. The stained colonies were observed and counted under a phase-contrast microscope and photographed.

2.13. Matrix metalloproteinase (MMP) activity assay

The cells were treated with EEAD for 24 h, and then cell culture supernatants were collected to measure the activities of MMP-2 and -9. The activities of MMP-2 and -9 were determined using Biotrak Activity Assay system from Amersham Biosciences (Piscataway, NJ, USA), according to the manufacturer's instruction.

2.14. Animal and *in vivo* experimental procedures

C57BL/6 mice (male, 8 weeks old) were obtained from Samtaco Korea (Osan, Korea). The animals were housed under specific pathogen-free conditions at a temperature of 24 ± 1˚C and humidity of 55 ± 5% in a laminar air-flow room with a 12 h light and 12 h dark circle. After

acclimatization for 1 week, 28 mice were injected intravenously *via* tail vein with 3×10^5 B16F10 cells per 100 μL PBS to produce experimental lung metastasis. At the same time, 16 mice were injected in the same area with PBS alone. After 1 day of tumor inoculation, B16F10 cell injected-mice were randomly divided into three groups: the B16 + control group (100 μL of distilled water), the B16 + EEAD 100 group (100 μL of EEAD 100 mg/kg/day), and the B16 + EEAD 200 group (100 μL of EEAD 200 mg/kg/day). Eighteen PBS-injected mice were also randomly divided into two groups: the normal group (100 μ of distilled water); and the EEAD 200 group (200 μL of EEAD 200 mg/kg/day). All treatments were administrated orally once per day in the morning for 21 days. Mice were sacrificed at day 21 after B16F10 melanoma cells injection, and blood was placed in heparinized tubes, centrifuged at 3,000 rpm for 10 min at 4°C, and kept at -80°C for subsequent analysis. After perfusion, organs were immediately surgically excised, including liver, kidney, spleen, lung, and thymus, then weighed, and stored at -80°C. Animal experiments were conducted in accordance with the Guidelines for Animal Experimentation of Dong-eui University (Busan, Republic of Korea), approved by the Institutional Animal Care and Research Advisory Committee of Dong-eui University (Reference no. R2017-004).

2.15. Blood biochemical analysis

After 21 days of the experiment, blood samples were collected from the animals in all groups. Alanine aminotransferase (ALT) and aspartate aminotransferase (AST) levels were measured using commercial colorimetric assay kits (Abcam Inc. (Cambridge, UK). Lactate dehydrogenase (LDH) activity and blood urea nitrogen (BUN) level were analyzed using detection kits according to the manufacturer's instructions, which kits were obtained from BioVision Inc. (Milpitas, CA, USA) and antibodies-online GmbH (Aachen, Germany), respectively.

2.16. Immunohistochemical staining for tumor necrosis factor (TNF)-α

Histological analysis for TNF-α immunohistochemistry analysis of the lung tissue was performed as described previously (*25*). In brief, the sections of 5 μm thickness were deparaffinized, rehydrated, cooked in antigen retrieval solution (Abcam, Inc.), and dipped in 3% hydrogen peroxide solution for 30 min. TNF-α antibody (Abcam, Inc.) was then applied, and incubated for 1 h at room temperature. After washing, the sections were incubated with peroxidase conjugated secondary antibody (HRP-labelled goat anti-rabbit IgG antibody, DAKO Corp, Glostrup, Denmark) for 40 min. After washing with PBS, images of the sections were photographed with a microscope (Carl Zeiss).

2.17. Statistical analysis

The results of quantitative studies are reported as mean ± standard deviation (SD) using GraphPad Prism software (version 5.03; GraphPad Software, Inc., La Jolla, CA, USA). All experiments were repeated at least three times. To compare data, One-way analysis of variance (ANOVA) with Dunnett's *post-hoc* test was used, and $p < 0.05$ was considered to indicate a statistically significant difference.

3. Results

3.1. EEAD inhibited cell viability and induced apoptosis in B16F10 cells

In evaluate the cytotoxicity of EEAD on B16F10 cells, cells were treated with different concentrations of EEAD for 24 h, and cell viability was assessed by MTT assay. Figure 1A shows that EEAD significantly reduced B16F10 cells viability in a concentration-dependent manner. Phase-contrast microscopic examination demonstrated that the phenotypic characteristics of EEAD-treated cells exhibited irregular cell outlines, decrease of cell density, shrinkage, and increase of detached cells (Figure 1B, upper panel). Therefore, DAPI staining was performed to determine whether EEAD-induced growth inhibition was associated with apoptosis induction, and it was found that nuclear fragmentation and chromatin condensation formation were increased in EEAD treated cells (Figure 1B, lower panel). The results of flow cytometric analysis also showed that the percentage of apoptotic cells was significantly increased in EEAD-treated cells in a concentration-dependent manner (Figure 1C and D).

3.2. EEAD increased mitochondrial dysfunction and ROS generation in B16F10 cells

We assessed whether mitochondrial dysfunction was involved in the induction of EEAD-induced apoptosis and found that the MMP ($\Delta\Psi m$)-dependent formation of JC-1 aggregates in mitochondria was maintained at a relatively high rate in cells not treated with EEAD. However, JC-1 aggregates were markedly reduced after treatment with EEAD in a concentration-dependent manner (Figure 2A and B), indicating a significant depletion of MMP ($\Delta\Psi m$) after EEAD treatment. DCF-DA staining was applied to investigate whether EEAD-induced mitochondrial dysfunction was associated with increased production of ROS. As depicted in Figures 2C and D, ROS production significantly increased according to the rise in concentration of EEAD. The effects of EEAD on the expression of Bcl-2 family members, which play a critical role in the mitochondria-mediated intrinsic apoptotic pathway, were also determined. As indicated in Figure 2E and

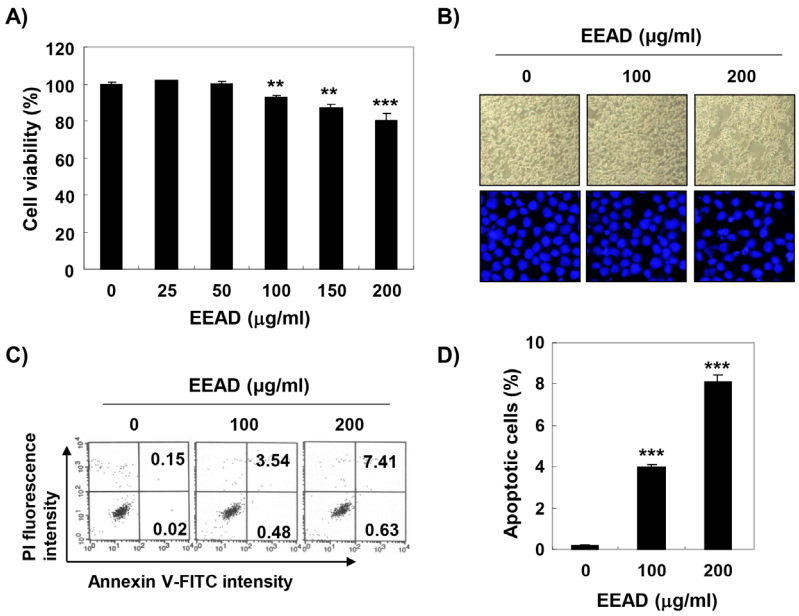

Figure 1. Inhibition of cell viability and induction of apoptosis by EEAD in B16F10 cells. Cells were treated with the indicated concentrations of EEAD for 24 h. **(A)**, The cell viability was assessed by MTT assay. Data are expressed as the mean ± SD. The statistical analyses were conducted using analysis of variance between groups (**$p < 0.001$ and ***$p < 0.0001$ when compared to control). **(B, Upper panel)** Morphological changes of B16F10 cells treated with EEAD for 24 h were observed by a phase-contrast microscope at 40× magnification. **(B, Lower panel)** The nuclear morphological change was observed using DAPI staining, and was photographed under a fluorescence microscope at 400× magnification. Representative photographs of the morphological changes are presented. **(C** and **D)** Apoptosis of B16F10 cells treated with EEAD was measured by flow cytometric analysis using annexin V-FITC and PI. **(C)** Representative profiles. The results show early apoptosis, defined as annexin V^+ and PI^- cells (lower right quadrant), and late apoptosis, defined as annexin V^+ and PI^+ (upper right quadrant) cells. **(D)** The percentages of apoptotic cells were determined by expressing the numbers of Annexin V^+ cells as percentages of all the present cells. The statistical analyses were conducted using analysis of variance between groups (***$p < 0.0001$ when compared to control).

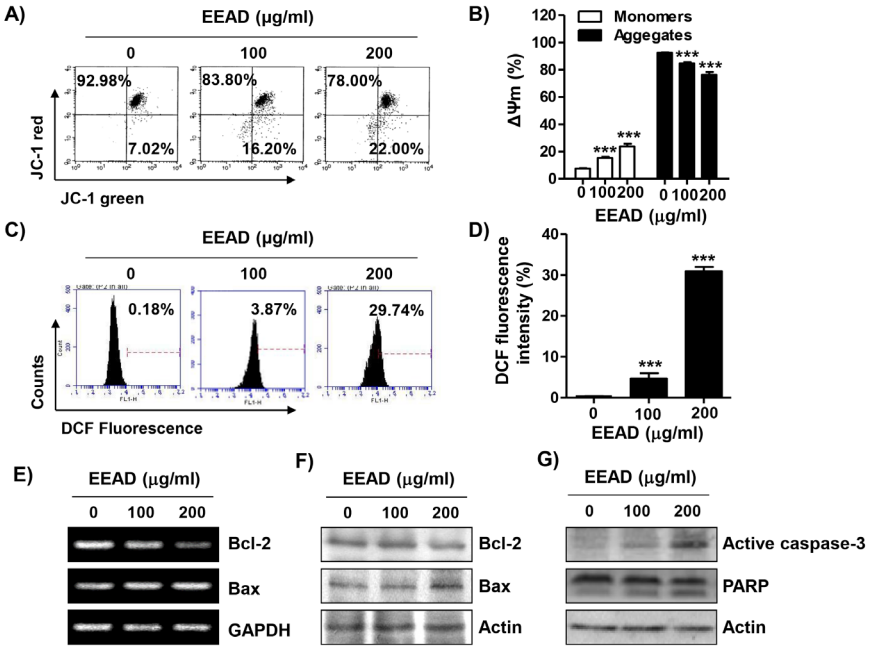

Figure 2. Reduction of MMP (*ΔΨm*) and induction of ROS generation by EEAD in B16F10 cells. (A), After 24 h incubation with the indicated concentrations of EEAD, the cells were stained with JC-1 dye, and were then analyzed by flow cytometry, in order to evaluate the changes in MMP (*ΔΨm*). **(B)** Each bar represents the percentage of cells with JC-1 aggregates and monomers. The quantitative data are expressed in the bar diagram as the mean ± SD. The statistical analyses were conducted using analysis of variance between groups (***$p < 0.0001$ when compared to control). **(C)** The cells were treated with the indicated concentrations of EEAD for 30 min and then intracellular ROS generation was measured by flow cytometry using DCF-DA dye. **(D)** Each bar represents the mean ± SD of three independent experiments (***$p < 0.0001$, when compared to control). **(E)** After treatment with EEAD for 24 h, total RNA was isolated and RT-PCR was performed using the indicated primers. The amplified PCR products were run on 1% agarose gels and visualized with EtBr staining. GAPDH was used as the housekeeping control gene. **(F** and **G)** The cells were lysed and equal amounts of cell lysates were separated by SDS-polyacrylamide gel electrophoresis and transferred to membranes. The membranes were probed with the indicated antibodies and the proteins were visualized using an ECL detection system. The equivalent loading of proteins in each well was confirmed by actin.

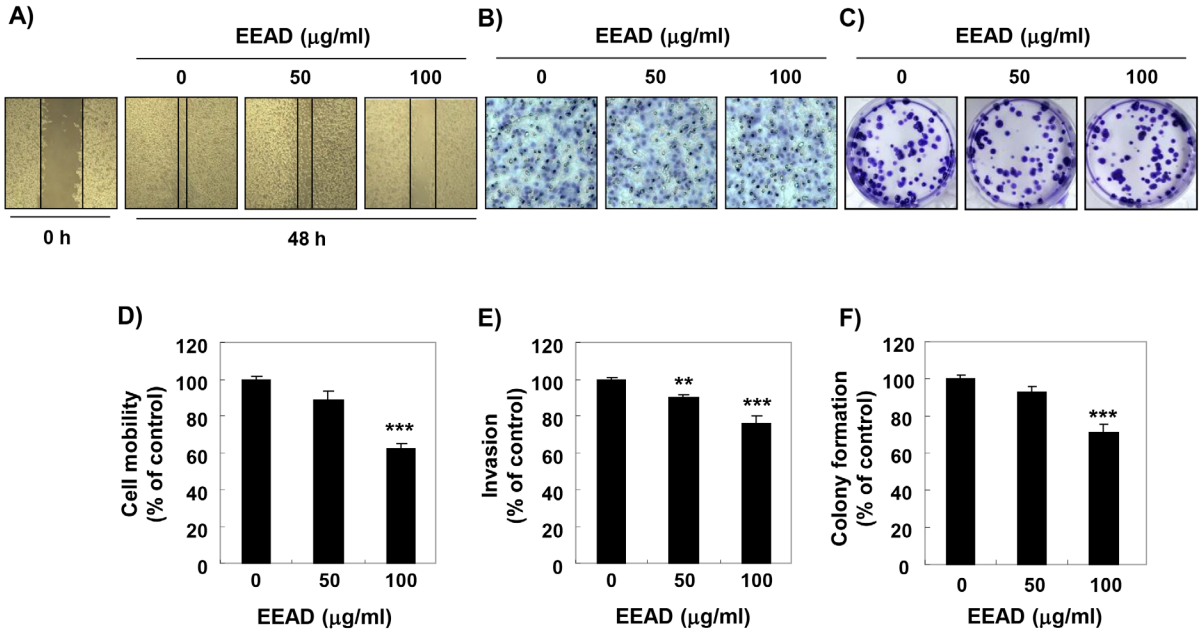

Figure 3. Suppression of cell migration, invasion and colony formation by EEAD in B16F10 cells. (A) Cell migration of B16F10 cells was assessed by wound healing assay at 24 h after EEAD treatment. **(B)** For cell invasion assay using trans-well chamber system, B16F10 cells were placed in the upper chamber of trans-well insert, and complement medium supplemented with EEAD was added in the lower chamber, and then cells were incubated for 24 h. **(C)** B16F10 cells were exposed to EEAD for 15 days, followed by colony formation assay. Cells were stained with 0.1% crystal violet solution, and visualized colonies were observed under a phase-contrast microscope. (A-C) Representative photographs are shown from three independent experiments. **(D)** The mobility of B16F10 cells was calculated for EEAD-treated cells, as compared with the non-treated control cells for each experiment in different field. **(E)** The numbers of invading cells in EEAD-treated cells, as compared with the non-treated control cells, for each experiment. **(F)** Rates of colony formation were detected by microplate reader at 650 nm. The quantitative data are expressed in the bar diagram as the mean ± SD. The statistical analyses were conducted using analysis of variance between groups (**$p < 0.001$ and ***$p < 0.0001$ when compared to control).

F, the levels of pro-apoptotic Bax mRNA and protein were increased, while those of anti-apoptotic Bcl-2 were reduced in EEAD-stimulated cells. EEAD further activated caspase-3 and induced cleavage of poly (ADP-ribose) polymerase (PARP), one of the major substrate proteins of activated caspase-3 (Figure 3G).

3.3. EEAD supprerssed the motility, invasion and colony formation of B16F10 cells *via* the inhibition of MMPs expression and activity

To determine the effect of EEAD on metastatic activity of B16F10 cells, we investigated the cell migration and invasion using wound scratch assay and trans-well system, respectively. Figure 3A and D show that EEAD suppressed the closure rate of the scratch at 24 h treatment, compared with the control cells. Additionally, EEAD apparently decreased the intrusion of B16F10 cells concentration-dependently in trans-well chamber assay (Figure 3B and E), consistent with the result of the wound scratch assay. We also found that the colony forming ability of B16F10 cells was markedly decreased by EEAD relative to the control (Figure 3C and F). Because the degradation of extracellular matrix (ECM) is an essential step in cancer cell metastasis, we investigated whether EEAD regulates the activity and expression of matrix MMPs. Our RT-PCR and immunoblotting results indicated that EEAD effectively decreased the mRNA and protein expression of MMP-2 and -9 (Figure 4A and B), which was associated with a decrease in their enzymatic activity (Figure 4C). However, EEAD concentration-dependently increased the mRNA and protein expression of tissue inhibitor matrix metalloproteinase (TIMP)-1 and -2 (Figure 4A and B).

3.4. EEAD administration reduced the lung metastasis of B16F10 cells in C57BL/6 mice

To examine the effect of EEAD on lung metastasis *in vivo*, we used the lung metastatic mouse model, by which B16F10 melanoma cells were injected into the tail vein of C57BL/6 mice. A total of 44 mice were involved in the present experiment. Twenty-eight mice were injected with B16F10 cells, and 16 mice were injected with PBS as vehicle. From one day after, EEAD 100 mg/kg, EEAD 200 mg/kg, or distilled water were administrated orally once per day in the morning for 21 days. One day after tumor cell inoculation, one animal died in the control group, and one in the EEAD 200 mg/kg group. In the control group, two of them died 14 days after tumor inoculation, and the survival rate on the 21 days was 83.33%. However, the survival rate was not significantly different between

the control and EEAD groups. At day 21, 100% of the normal mice and the EEAD 200 mg/kg treated mice without B16F10 cell inoculation were still alive. During the experimental period, the initial and final body weight did not differ between all the groups (Data not shown). Mice were sacrificed at day 21 of treatment, and their organs were surgically excised. As shown in Table 1, the weight of thymus, spleen, liver and kidney were not significantly different between all groups, exclusive of lung. The B16F10 cells-injected control mice markedly increased lung hypertrophy (2.87-fold of lung weight in normal), whereas it was substantially decreased by EEAD 200 mg/kg treatment. In addition, the levels of BUN showed no significant differences for all groups (Table 2). In contrast, the activities of plasma ALT and AST were elevated in 34.20 and 324.11 U/L, respectively, in B16F10 cells-injected control mice, compared to 23.75 and 126.55 U/L in the normal group, whereas the activities of these enzymes were decreased, following the administration of EEAD. Meanwhile, the LDH activity was apparently increased to 1,042.85 U/L in B16F10 cells-injected control mice (757.60 U/L). However, the LDH activity was meaningfully decreased by the administration of EEAD 200 mg/kg, and its activity was similar to that of the normal mice. Next, we investigated the effect of EEAD on the histopathological alteration of lung metastatic tissue following B16F10 inoculation. The number of metastatic tumor nodules in B16F10-injected control mice was apparently increased in comparison with normal mice visually (Figure 5A), as well as numerically (Figure 5B). In contrast, the number of metastatic tumor nodules was significantly reduced by the oral administration of EEAD, in a concentration-dependent manner. In addition, we evaluated whether EEAD could suppress lung inflammation in these mice. Similar to the results from the count of metastatic tumor, Figure 5C shows that TNF-α of lung metastatic tissue was overexpressed in B16F10 cell inoculated-mice, but completely inhibited in EEAD-treated mice.

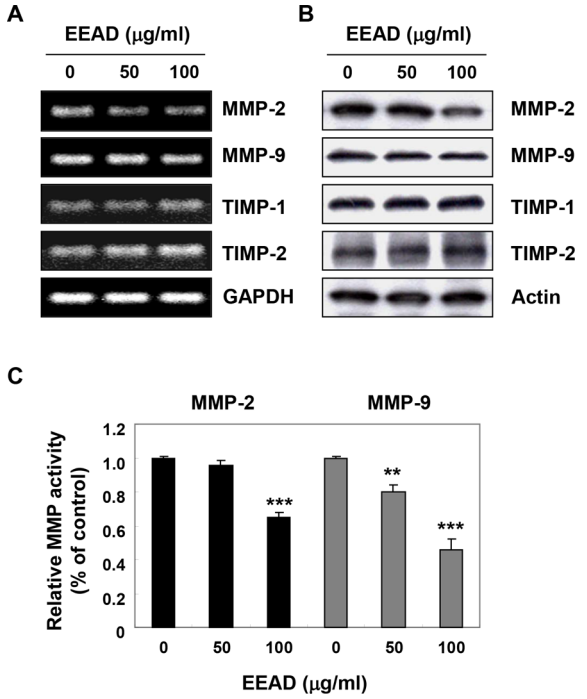

Figure 4. Inhibition of the expression and activity of MMP-2 and -9 by EEAD in B16F10 cells. (A) After treatment with EEAD for 24 h, total RNA was isolated and RT-PCR was performed using the indicated primers. The amplified PCR products were run on 1% agarose gels and visualized with EtBr staining. GAPDH was used as the housekeeping control gene. **(B)** The cells were lysed and equal amounts of cell lysates were separated by SDS-polyacrylamide gel electrophoresis and transferred to membranes. The membranes were probed with the indicated antibodies and the proteins were visualized using an ECL detection system. The equivalent loading of proteins in each well was confirmed by actin. **(C)** *In vitro* activity of MMP-2 and -9 in cell culture supernatant was measured using a MMP-2 and -9 gelatinase activity assay kit. Data are mean ± SD deviation from three independent experiments and are presented as fold change compared with vector control (**$p < 0.001$ and ***$p < 0.0001$ when compared to control).

4. Discussion

Apoptosis, a well known programmed cell death, is an essential mechanism to maintain cell homeostasis and maintains a balance between cell survival and apoptosis (*26,27*). Cancer develops as a result of a

Table 1. The effects of oral administration of EEAD on organ weights in B16F10 cells-inoculated C57BL/6 mice

Group	No. of animals	Organ weights (g)				
		Thymus	Lung	Spleen	Liver	Kidney
Normal	8	0.050 ± 0.094	0.15 ± 0.01	0.075 ± 0.008	1.38 ± 0.06	0.37 ± 0.06
EEAD 200	8	0.049 ± 0.011	0.15 ± 0.02	0.075 ± 0.009	1.32 ± 0.03	0.37 ± 0.01
B16 + control	8	0.045 ± 0.009	0.43 ± 0.15	0.086 ± 0.017	1.39 ± 0.10	0.37 ± 0.03
B16 + EEAD 100	8	0.043 ± 0.007	0.35 ± 0.25	0.086 ± 0.019	1.34 ± 0.09	0.36 ± 0.04
B16 + EEAD 200	8	0.044 ± 0.009	0.20 ± 0.17	0.080 ± 0.024	1.37 ± 0.05	0.37 ± 0.02

After 1 day of tumor inoculation, B16F10 cell injected-mice were randomly divided into three groups: the B16+control group (100 μl of distilled water), the B16+EEAD 100 group 100 μL of EEAD 100 mg/kg/day), and the B16+EEAD 200 group (100 μL of EEAD 200 mg/kg/day). PBS-injected mice were also randomly divided into two groups: the normal group (100 μ of distilled water); and the EEAD 200 group (200 μL of EEAD 200 mg/kg/day). Mice were sacrificed at day 21 after B16F10 melanoma cells injection, and thymus, lung, spleen, liver, and kidney were immediately surgically excised, and then measured the weight. Data are presented as means ± SD.

Table 2. The effects of oral administration of EEAD to AST, ALT, BUN, and LDH values of serum samples obtained from B16F10 cells-inoculated C57BL/6 mice

Group	No. of animals	ALT (U/L)	AST (U/L)	BUN (mg/dL)	LDH (U/L)
Normal	8	23.75 ± 3.10	126.55 ± 55.86	20.11 ± 2.38	757.60 ± 87.08
EEAD 200	8	22.94 ± 2.47	123.09 ± 31.17	20.19 ± 3.14	699.47 ± 89.41
B16 + control	8	34.20 ± 6.63	324.11 ± 90.03	20.66 ± 7.24	1042.85 ± 57.03
B16 + EEAD 100	8	31.11 ± 9.59	299.11 ± 87.17	20.79 ± 2.47	1001.00 ± 12.47
B16 + EEAD 200	8	28.97 ± 7.14	227.67 ± 97.17	19.98 ± 2.77	874.95 ± 93.14

After 1 day of tumor inoculation, B16F10 cell injected-mice were randomly divided into three groups: the B16 + control group (100 μl of distilled water), the B16 + EEAD 100 group (100 μl of EEAD 100 mg/kg/day), and the B16 + EEAD 200 group (100 μL of EEAD 200 mg/kg/day). PBS-injected mice were also randomly divided into two groups: the normal group (100 μ of distilled water); and the EEAD 200 group (200 μL of EEAD 200 mg/kg/day). The whole blood of mice was collected after 21 day treatment with or without EEAD. The values of ALT, AST, BUN, and LDH were measured. Data are presented as means ± SD.

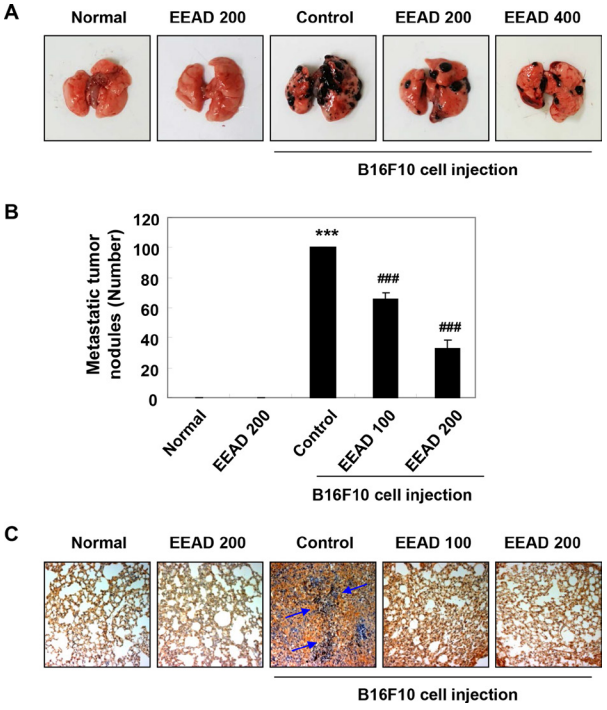

Figure 5. Effects of EEAD on pulmonary metastasis of B16F10 melanoma cells *in vivo*. (A) Representatives of metastatic nodules on the surface of the lungs in C57BL/6 mice induced by injecting 3×10^5 cells intravenously, which were then treated daily with 100 and 150 mg/kg EEAD. On day 21, the mice were sacrificed, and their lungs were then removed and fixed. Metastatic foci at the lung surfaces were photographed. **(B)** The number of metastatic nodules in each group were counted, and data presented as the mean ± SD (n = 8). The statistical analyses were conducted using analysis of variance between groups (***$p < 0.0001$ when compared to normal group. ###$p < 0.0001$ when compared to B16F10 cell-injected control group). **(C)** Tumor tissues of lung metastasis were immunohistochemistry stained with TNF-α. Blue arrow indicates the TNF-α-expressed area shown in brown color, and marks the metastasis nodule (Original magnification, 200×).

series of genetic changes, during which normal cells are converted to malignant cells that are involved in abnormal growth and uncontrolled growth of cells (*28,29*). Hence, most chemotherapeutic agents function by inducing apoptosis in malignant cells, so the induction of apoptosis is a major strategy for cancer treatment and one of the most actively studied areas (*30,31*). In the present study, we have verified that EEAD, ethanol extract from the *Angelica dahurica Radix*, suppressed B16F10 cell proliferation in a concentration-dependent manner. Additionally, EEAD significantly increased the percentage of annexin V^+-positive cells. Furthermore, EEAD-treated cells showed the typical morphological hallmarks of apoptotic cells, such as chromatin condensation, nuclear fragmentation, and cell shrinkage. These results suggest that the inhibition of cell growth by EEAD is associated with the induction of apoptosis in B16F10 melanoma cells.

Apoptosis is largely divided into death receptor (DR)-mediated extrinsic and mitochondria-mediated intrinsic pathways (*26,28*). The extrinsic pathway begins with the activation of caspase-8 by the formation of the death-inducing signaling complex through the binding of death ligand to the cell surface DR (*27,32*). On the other hand, the intrinsic apoptosis signal pathway is initiated by genetic damage, oxidative stress, hypoxia, and high concentration of cytosolic Ca^{2+}, which converge at the mitochondria (*28,33*). This pathway is the result of a mitochondrial dysfunction that includes loss of MMP ($\Delta\psi m$), production of ROS, opening of the permeability transition pore, and release of cytochrome *c* from the mitochondria to the cytoplasm, which is strictly regulated by a group of proteins that are composed of pro- and anti-apoptotic proteins, such as Bcl-2 protein family proteins (*33,34*). The release of cytochrome *c* eventually activates caspase-3 *via* the formation of apoptosome, which consists of cytochrome *c*, caspase-9, and Apaf-1 (*28,34*). Caspase-3 converges both intrinsic and extrinsic pathways, and degrades various substrate proteins, such as PARP (*27,34*). In the current study, we investigated whether apoptosis by EEAD was associated with mitochondria dysfunction. Our results showed that EEAD significantly increased MMP ($\Delta\psi m$) loss, as well as intracellular accumulation of ROS, in B16F10 melanoma cells. Moreover, EEAD increased the expression of pro-apoptotic Bax and inhibited the expression of anti-apoptotic Bcl-2. Additionally, EEAD induced the activation of caspase-3, and the degradation of PARP. Therefore, these results demonstrate that

EEAD induced apoptosis through a mitochondria-mediated intrinsic pathway in B16F10 melanoma cells.

Melanoma, one of the most aggressive malignancies, is a skin cancer with a resistance to cytotoxic anti-tumor drugs, and high capacity for invasion and metastasis (*1,2*). Therefore, the rate of response of standard therapies is low and prognosis is also poor. This is estimated to be because melanocytes originate from highly motile cells that have enhanced survival properties (35,36). Metastasis is caused by the movement of cancer cells from the primary tumor to target organs, thus blocking cancer cell migration and invasion, which are most important for the treatment of melanoma (*37,38*). Herein, we found that EEAD suppressed the migration and invasion of B16F10 cells through the results of wound scratch assay and trans-well assay, in the concentration range of non-toxic conditions. In addition, we confirmed that EEAD also inhibited anchorage-dependent colony formation that is a characteristic of tumor cells (*39,40*). These results indicate that EEAD blocked the migration and invasion, key steps of the metastasis of cancer cell, as well as the establishment of anchorage-dependent colony formation from a single cell. Degradation and remodeling of the ECM and basement membranes are essential steps in the metastasis of melanoma. These processes are mediated by proteolytic enzymes, such as MMPs and their tissue inhibitors, TIMPs, and the regulation of their expression and/or activation on invasion and migration in many types of tumors has been widely reviewed *in vitro* and *in vivo* (*41,42*). In particular, MMP-2 and -9 are well known to induce cancer progression and the metastasis of melanoma through the degradation of type IV collagen, which is the major component of the basement membrane (*43,44*). In this regard, we demonstrated that EEAD markedly decreased the activity of MMP-2 and -9. Furthermore, our results proved that EEAD induced the down-regulated expression of MMP-2 and -9, as well as the up-regulated expression of TIMP-1 and -2 in mRNA and protein levels. Based on these findings, we suggest that EEAD promotes an increase of TIMP/MMPs ratio as a critical factor in the regulation of the motility of melanoma cells, which may subsequently lead to the suppression of cell migration and invasion associated metastasis.

Furthermore, we have re-confirmed the efficacy of EEAD on the suppression of metastasis in B16F10 cell inoculated-mice. Interestingly, B16F10 cells have been metastasized specifically to the lung following the injection into the tail vein, and most of the cells have been found in the pulmonary tissue (*45*). Therefore, the murine B16F10 melanoma is most accepted as a useful model for metastatic lung tumor, its application having been used to evaluate the metastatic mechanisms of melanoma and the development of anti-cancer therapies (*45,46*). Numerous studies reported the experimental pulmonary metastasis model by B16F10 cell inoculation in C57BL/6 mice, and investigated the efficacy of new potential anti-cancer agents in this murine model (*47-49*). In the current study, we identified that B16F10 cell inoculated-mice have induced lung hypertrophy and increase of the number and expression of metastatic tumor nodules in lung tissue, whereas these were significantly decreased by the oral administration of EEAD. Additionally, the oral administration of EEAD reduced serum LDH activity, as the most consistent marker of the aggressive carcinogenesis (*50*), without weight loss or nephrotoxicity. Similarly, plasma levels of ALT and AST, which are considered to be important indicators for measuring liver damage (*51,52*), in B16F10 cell-inoculated mice were higher than those of the normal group. However, they were dose-dependently reduced by oral administration of EEAD. These results suggest that EEAD can be a considerably safe therapeutic candidate for metastatic melanoma through its low toxicity, and efficacy in the suppression of metastasis. Moreover, our study also provided that B16F10 inoculation enhanced the expression of TNF-α in the metastatic region, but was suppressed by EEAD. It is well known that inflammation plays principal roles at different stages of tumor development, including initiation, promotion, malignant conversion, invasion, and metastasis (*53,54*). El Rayes *et al*. (*55*) demonstrated that lung inflammation promotes metastasis, and Yu et al. (*56*) reported pro-inflammatory cytokines, including TNF-α, interleukin (IL)-1 and IL-6, accelerate MMPs expression, invasiveness, and metastasis. In this respect, our results provide the possibility of EEAD suppressing inflammation, a hallmark of cancer contributing to tumor development, and may lead to the inhibition of metastasis in lung cancer.

As has been mentioned, melanoma is a tumor with a resistance to drugs therapies (*1,2*). To solve this problem, a lot of researches are getting identification of the mechanisms by which melanoma initiation can be triggered and sustained. Recently, there are well known that melanoma may trigger not only the activation of RAS/MEK singling pathway, but also other pathways such as phosphoinositide 3-kinase (PI3K)/Akt and Wnt signaling pathways (*57,58*). In present study, we found that exposure to EEAD led to decrease protein expression of Akt and β-catenin in B16F10 cells (Supplementary Figure S1, *http://www.biosciencetrends.com/action/getSupplementalData.php?ID=55*). These results suggested that EEAD suppressed tumor growth *via* down-regulation of Akt and β-catenin pathway, but not RAS/MEK pathway. Although we have partially identified the underlying mechanism of EEAD on suppression of melanoma tumor, action mechanism and efficacy of bioactive components from *Angelica dahurica Radix* needs to be confirmed. Recent discoveries reported that coumarin

and pyrrole 2-carbaldedhyde derived alkaloids from *Angelica dahurica Radix* were identified and have bioactivity (*59,60*). In this context, further studies are need to investigate whether these active compounds also have anti-cancer effects for melanoma, as well as identify the underlying actin mechanism.

In summary, EEAD inhibited B16F10 melanoma cell growth through the induction of mitochondria-mediated intrinsic apoptosis pathway. EEAD also promoted down-regulation of MMPs activity and expression, which is a critical factor in the regulation of the motility of melanoma cells, and may subsequently lead to the suppression of cell migration and invasion-associated metastasis. In the metastatic lung cancer mouse, EEAD inhibited lung hypertrophy and metastatic tumor nodule, as well as inflammation in lung tissue without toxicity. Although the identification of bioactive components of EEAD should be performed, the results of this study suggest that EEAD may be a potential anti-invasive candidate for treatment strategies for metastatic melanoma tumors.

Acknowledgements

This research was funded by Basic Science Research Program through the National Research Foundation of Korea (NRF) grant funded by the Korea government (2018R1A2B2005705).

References

1. Read T, Lonne M, Sparks DS, David M, Wagels M, Schaider H, Soyer HP, Smithers BM. A systematic review and meta-analysis of locoregional treatments for in-transit melanoma. J Surg Oncol. 2019; 119: 887-896.
2. Weitman ES, Zager JS. Regional therapies for locoregionally advanced and unresectable melanoma. Clin Exp Metastasis. 2018; 35:495-502.
3. Almeida FV, Douglass SM, Fane ME, Weeraratna AT. Bad company: Microenvironmentally mediated resistance to targeted therapy in melanoma. Pigment Cell Melanoma Res. 2019; 32:237-247.
4. Swe T, Kim KB. Update on systemic therapy for advanced cutaneous melanoma and recent development of novel drugs. Clin Exp Metastasis. 2018; 35:503-520.
5. Herrington CS, Poulsom R, Coates PJ. Recent advances in pathology: the 2019 annual review issue of the journal of pathology. J Pathol. 2019; 247:535-538.
6. Amaral T, Meraz-Torres F, Garbe C. Immunotherapy in managing metastatic melanoma: which treatment when? Expert Opin Biol Ther. 2017; 17:1523-1538.
7. Danciu C, Soica C, Antal D, Alexa E, Pavel IZ, Ghiulai R, Ardelean F, Babuta RM, Popescu A, Dehelean CA. Natural compounds in the chemoprevention of malignant melanoma. Anticancer Agents Med Chem. 2018; 18:631-644.
8. Albuquerque KRS, Pacheco NM, Del Rosario Loyo Casao T, de Melo FCSA, Novaes RD, Gonçalves RV. Applicability of plant extracts in preclinical studies of melanoma: A systematic review. Mediators Inflamm. 2018; 2018:6797924.
9. Prieto JM, Silveira D. Natural cytotoxic diterpenoids, a potential source of drug leads for melanoma therapy. Curr Pharm Des. 2018; 24:4237-4250.
10. Wei H, Xiao Y, Tong Y, Chen Y, Luo X, Wang Y, Jin P, Ma C, Fu Z, Guo H, Zhao X, Li Y. Therapeutic effect of angelica and its compound formulas for hypertension and the complications: Evidence mapping. Phytomedicine. 2019; 59:152767.
11. Sowndhararajan K, Deepa P, Kim M, Park SJ, Kim S. A review of the composition of the essential oils and biological activities of *Angelica* species. Sci Pharm. 2017; 85:E33.
12. Sarker SD, Nahar L. Natural medicine: the genus Angelica. Curr Med Chem. 2004; 11:1479-1500.
13. Li D, Wu L. Coumarins from the roots of *Angelica dahurica* cause anti-allergic inflammation. Exp Ther Med. 2017; 14:874-880.
14. Wang GH, Chen CY, Tsai TH, Chen CK, Cheng CY, Huang YH, Hsieh MC, Chung YC. Evaluation of tyrosinase inhibitory and antioxidant activities of *Angelica dahurica* root extracts for four different probiotic bacteria fermentations. J Biosci Bioeng. 2017; 123:679-684.
15. Lee HJ, Lee H, Kim MH, Choi YY, Ahn KS, Um JY, Lee SG, Yang WM. *Angelica dahurica* ameliorates the inflammation of gingival tissue *via* regulation of pro-inflammatory mediators in experimental model for periodontitis. J Ethnopharmacol. 2017; 205:16-21.
16. Lee MY, Lee JA, Seo CS, Ha H, Lee H, Son JK, Shin HK. Anti-inflammatory activity of *Angelica dahurica* ethanolic extract on RAW264.7 cells *via* upregulation of heme oxygenase-1. Food Chem Toxicol. 2011; 49:1047-1055.
17. Zheng YM, Shen JZ, Wang Y, Lu AX, Ho WS. Anti-oxidant and anti-cancer activities of *Angelica dahurica* extract *via* induction of apoptosis in colon cancer cells. Phytomedicine. 2016; 23:1267-1274.
18. Yang WQ, Song YL, Zhu ZX, Su C, Zhang X, Wang J, Shi SP, Tu PF. Anti-inflammatory dimeric furanocoumarins from the roots of *Angelica dahurica*. Fitoterapia. 2015; 105:187-193.
19. Mi C, Ma J, Wang KS, Zuo HX, Wang Z, Li MY, Piao LX, Xu GH, Li X, Quan ZS, Jin X. Imperatorin suppresses proliferation and angiogenesis of human colon cancer cell by targeting HIF-1α *via* the mTOR/p70S6K/4E-BP1 and MAPK pathways. J Ethnopharmacol. 2017; 203:27-38.
20. Wu M, Li T, Chen L, Peng S, Liao W, Bai R, Zhao X, Yang H, Wu C, Zeng H, Liu Y. Essential oils from *Inula japonica* and *Angelicae dahuricae* enhance sensitivity of MCF-7/ADR breast cancer cells to doxorubicin *via* multiple mechanisms. J Ethnopharmacol. 2016; 180:18-27.
21. Li X, Zeng X, Sun J, Li H, Wu P, Fung KP, Liu F. Imperatorin induces Mcl-1 degradation to cooperatively trigger Bax translocation and Bak activation to suppress drug-resistant human hepatoma. Cancer Lett. 2014; 348:146-155.
22. Choochuay K, Chunhacha P, Pongrakhananon V, Luechapudiporn R, Chanvorachote P. Imperatorin sensitizes anoikis and inhibits anchorage-independent growth of lung cancer cells. J Nat Med. 2013; 67:599-606.
23. Koh EM, Lee EK, Song CH, Song J, Chung HY, Chae CH, Jung KJ. Ferulate, an active component of wheat

germ, ameliorates oxidative stress-induced PTK/PTP imbalance and PP2A inactivation. Toxicol Res. 2018, 34:333-341.
24. Kang JB, Kim DK, Park DJ, Shah MA, Kim MO, Jung EJ, Lee HS, Koh PO. Hyperglycemia aggravates decrease in alpha-synuclein expression in a middle cerebral artery occlusion model. Lab Anim Res. 2018; 34:195-202.
25. Kwon HJ, Jung HY, Hahn KR, Kim W, Kim JW, Yoo DY, Yoon YS, Hwang IK, Kim DW. *Bacopa monnieri* extract improves novel object recognition, cell proliferation, neuroblast differentiation, brain-derived neurotrophic factor, and phosphorylation of cAMP response element-binding protein in the dentate gyrus. Lab Anim Res. 2018; 34:239-247.
26. Pfeffer CM, Singh ATK. Apoptosis: A target for anticancer therapy. Int J Mol Sci. 2018, 19:448.
27. Hassan M, Watari H, AbuAlmaaty A, Ohba Y, Sakuragi N. Apoptosis and molecular targeting therapy in cancer. Biomed Res Int. 2014; 2014:150845.
28. Kiraz Y, Adan A, Kartal Yandim M, Baran Y. Major apoptotic mechanisms and genes involved in apoptosis. Tumour Biol. 2016; 37:8471-8486.
29. Hanahan D, Weinberg RA. Hallmarks of cancer: the next generation. Cell. 2011; 144:646-674.
30. Bolhassani, A. Cancer chemoprevention by natural carotenoids as an efficient strategy. Anticancer Agents Med Chem. 2015; 15:1026-1231.
31. Medema RH, Macůrek L. Checkpoint control and cancer. Oncogene. 2012; 31:2601-2613.
32. Kantari C, Walczak H. Caspase-8 and bid: caught in the act between death receptors and mitochondria. Biochim Biophys Acta. 2011, 1813:558-563.
33. Schultz, DR, Harrington WJ Jr. Apoptosis: programmed cell death at a molecular level. Semin. Arthritis Rheum. 2003, 32:345-369.
34. Edlich F. BCL-2 proteins and apoptosis: Recent insights and unknowns. Biochem Biophys Res Commun. 2018, 500:26-34.
35. Helgadottir H, Rocha Trocoli Drakensjö I, Girnita A. Personalized medicine in malignant melanoma: Towards patient tailored treatment. Front Oncol. 2018; 8:202.
36. Gray-Schopfer V, Wellbrock C, Marais R. Melanoma biology and new targeted therapy. Nature. 2007; 445:851-857.
37. Huang R, Rofstad EK. Integrins as therapeutic targets in the organ-specific metastasis of human malignant melanoma. J Exp Clin Cancer Res. 2018; 37:92.
38. Arena GO, Arena V, Arena M, Abdouh M. Transfer of malignant traits as opposed to migration of cells: A novel concept to explain metastatic disease. Med Hypotheses. 2017; 100:82-86.
39. Achkova D, Maher J. Role of the colony-stimulating factor (CSF)/CSF-1 receptor axis in cancer. Biochem Soc Trans. 2016; 44:333-341.
40. Russo J, Russo IH. The role of the basal stem cell of the human breast in normal development and cancer. Adv Exp Med Biol. 2011; 720:121-134.
41. Gonzalez-Avila G, Sommer B, Mendoza-Posada DA, Ramos C, Garcia-Hernandez AA, Falfan-Valencia R. Matrix metalloproteinases participation in the metastatic process and their diagnostic and therapeutic applications in cancer. Crit Rev Oncol Hematol. 2019; 137:57-83.
42. Deryugina EI, Quigley JP. Tumor angiogenesis: MMP-mediated induction of intravasation- and metastasis-sustaining neovasculature. Matrix Biol. 2015; 44-46:94-112.
43. Jabłońska-Trypuć A, Matejczyk M, Rosochacki S. Matrix metalloproteinases (MMPs), the main extracellular matrix (ECM) enzymes in collagen degradation, as a target for anticancer drugs. J Enzyme Inhib Med Chem. 2016; 31:177-183.
44. Sampieri CL, León-Córdoba K, Remes-Troche JM. Matrix metalloproteinases and their tissue inhibitors in gastric cancer as molecular markers. J Cancer Res Ther. 2013; 9:356-363.
45. Fidler IJ. The relationship of embolic homogeneity, number, size and viability to the incidence of experimental metastasis. Eur J Cancer. 1973; 9:223-227.
46. Giavazzi R, Decio A. Syngeneic murine metastasis models: B16 melanoma. Methods Mol Biol. 2014; 1070:131-140.
47. Pal S, Amin PJ, Sainis KB, Shankar BS. Potential role of TRAIL in metastasis of mutant KRAS expressing lung adenocarcinoma. Cancer Microenviron. 2016; 9: 77-84.
48. Gautam A, Densmore CL, Waldrep JC. Inhibition of experimental lung metastasis by aerosol delivery of PEI-p53 complexes. Mol Ther. 2000; 2:318-323.
49. Siddikuzzaman, Grace VM. Inhibition of metastatic lung cancer in C57BL/6 mice by liposome encapsulated all trans retinoic acid (ATRA). Int Immunopharmacol. 2012; 14:570-579.
50. Chaube B, Malvi P, Singh SV, Mohammad N, Meena AS, Bhat MK. Targeting metabolic flexibility by simultaneously inhibiting respiratory complex I and lactate generation retards melanoma progression. Oncotarget. 2015; 6:37281-37299.
51. Liu Y, Zhao P, Cheng M, Yu L, Cheng Z, Fan L, Chen C. AST to ALT ratio and arterial stiffness in non-fatty liver Japanese population: a secondary analysis based on a cross-sectional study. Lipids Health Dis. 2018; 17:275.
52. Webster GF, Webster TG, Grimes LR. Laboratory tests in patients treated with isotretinoin: occurrence of liver and muscle abnormalities and failure of AST and ALT to predict liver abnormality. Dermatol Online J. 2017; 23:13030.
53. Ham B, Fernandez MC, D'Costa Z, Brodt P. The diverse roles of the TNF axis in cancer progression and metastasis. Trends Cancer Res. 2016; 11:1-27.
54. Nenu I, Tudor D, Filip AG, Baldea I. Current position of TNF-α in melanomagenesis. Tumour Biol. 2015; 36:6589-6602.
55. El Rayes T, Catena R, Lee S, Stawowczyk M, Joshi N, Fischbach C, Powell CA, Dannenberg AJ, Altorki NK, Gao D, Mittal V. Lung inflammation promotes metastasis through neutrophil protease-mediated degradation of Tsp-1. Proc Natl Acad Sci U S A. 2015; 112:16000-16005.
56. Yu H, Kortylewski M, Pardoll D. Crosstalk between cancer and immune cells: role of STAT3 in the tumour microenvironment. Nat Rev Immunol. 2007; 7:41-51.
57. Dantonio PM, Klein MO, Freire MRVB, Araujo CN, Chiacetti AC, Correa RG. Exploring major signaling cascades in melanomagenesis: a rationale route for targetted skin cancer therapy. Biosci Rep. 2018; 38:BSR20180511.
58. Gray-Schopfer V, Wellbrock C, Marais R. Melanoma biology and new targeted therapy. Nature 2007: 445:851-857.
59. Wang J, Peng L, Shi M, Li C, Zhang Y, Kang W.

Spectrum effect relationship and component knock-out in *Angelica Dahurica Radix* by high performance liquid chromatography-Q exactive hybrid quadrupole-qrbitrap mass spectrometer. Molecules. 2017; 22:E1231.
60. Qi B, Yang W, Ding N, Luo Y, Jia F, Liu X, Wang J, Wang X, Tu P, Shi S. Pyrrole 2-carbaldehyde derived alkaloids from the roots of *Angelica dahurica*. J Nat Med. 2019; 73:769-776.

Received August 25, 2019; Revised December 26, 2019; Accepted January 25, 2020.

**Address correspondence to:*
Yung Hyun Choi, Department of Biochemistry, Dongeui University College of Korean Medicine, 52-57, Yangjeong-ro, Busanjin-gu, Busan 47227, Korea.
E-mail: choiyh@deu.ac.kr

Released online in J-STAGE as advance publication February 25, 2020.

Original Article

DOI: 10.5582/bst.2019.01296

Fast time perception is associated with high levels of anxiety in cancer patients prior to starting chemotherapy

Ivan Shterev Donev[1], Martina Stoyanova Ivanova[2,3], Nikolay Vladimirov Conev[2,4,*]

[1] Clinic of Medical Oncology, MHAT "Nadezhda", Sofia, Bulgaria;
[2] Clinic of Medical Oncology, UMHAT "St. Marina", Varna, Bulgaria;
[3] Department of Nursing Care, Medical University of Varna, Bulgaria;
[4] Department of Propedeutics of Internal Diseases, Medical University of Varna, Bulgaria.

SUMMARY Our study explored the potential relationship between time perception and the level of anxiety in cancer patients prior to starting chemotherapy. Time perception was assessed in 162 chemonaïve patients with solid tumors by evaluating each subject's prospective estimation of how fast one minute passed compared to the actual amount of time passed. The median value of time perception was used to stratify the patients into two categories of fast and slow time perception. We used the generalized anxiety disorder questionnaire (GAD-7) as a screening tool for detecting levels of anxiety. Scores ≥ 10 were considered high. In total, 45 (27.8%) patients had high levels of anxiety. The pattern of the time perception distributions significantly changed according to the reported levels on the GAD-7 scale. Scores ≥ 10 correlated with fast time perception and the female gender. Patients with a fast time perception had significantly higher levels of anxiety (8.44 ± 5.1) than patients with a slow time perception (3.49 ± 4.3). ROC analysis revealed that at the optimal cut-off value of time perception, clinically significant levels of anxiety can be discriminated with an AUC = 0.78 (95% CI: 0.70-0.85, $p < 0.001$), a sensitivity of 82.2% and a specificity of 64.1%. Moreover, in a multivariate logistic regression model, fast time perception was an independent predictor of clinically significant levels of anxiety (OR: 8.24; 95% CI: 3.16-21.41, $p < 0.001$). Time perception is a novel potent indicator for high levels of anxiety in cancer patients.

Keywords Oncology, cancer, anxiety, time perception

1. Introduction

Cancer patients are battling a life-threatening disease and experience severe treatment side effects that ultimately lead to high levels of distress as well as symptoms of depression and anxiety. Anxiety disorders are the most prevalent pathological conditions among cancer patients, with incidence rates ranging from 10 to 65% (*1,2*). Anxiety disorders are involved in cognitive, physiological and physical reactions as a response to unpleasant stimuli. Anxiety has been shown to cause many detrimental effects, such as fatigue, nonadherence to the prescribed treatment and poor overall quality of life (*3-5*). Cancer patients are preoccupied with stress-inducing events and experience anxiety symptoms due to fear of negative outcomes and treatment side effects (*6,7*). Despite these facts, several surveys showed that anxiety disorders and distress remained underdiagnosed and undertreated (*8-10*). Moreover there is not a specific cause leading to anxiety disorder, but only population groups like cancer patients that are at risk of suffering it (*11-13*).

Time flows at different speed for each of us - an hour may fly-by, while a couple of minutes may seem to drag. There is a sound relation between a person's current emotional status and their perception of time: entertainment activities appear to accelerate time flow, while the monotony of uneventful circumstances seems to instinctively decelerate time (*14,15*). Subsequently, when time appears to flow rapidly, one is left with the impression that less time has passed than what the clock shows. Alternatively, when time seems to drag, we have the feeling that more time has passed than what the clock shows. Thus the emotional state is a crucial modifier of time perception (*16,17*). There are no reports in the literature on the relationship between the experience of time and the levels of anxiety reported by cancer patients.

To improve the detection of high levels of anxiety in busy clinical practices, we searched for a relationship

between time perception and levels of anxiety prior to starting chemotherapy.

2. Patients and Methods

2.1. Patient selection

Our report includes 162 in patients who were treated at the Clinic of Medical Oncology at MHAT "Nadezhda" Sofia and UMHAT "St. Marina" in Varna, Bulgaria, from February 2018 to January 2019. The inclusion criteria for the patients were as follows: the presence of histologically verified cancer, an age greater than 18 years, an understanding of the Bulgarian language, the absence of psychiatric disorders, and the absence of clinical conditions that could limit the patient's understanding of the provided materials and tasks. The exclusion criteria were as follows: patients who reported chronic use of drugs such as sedatives, stimulants, pain killers or opioids, and patients with decompensated chronic disease such as hypo- and hyperthyroidism, heart diseases, etc. None of the patients had limitations to their activities of daily life. Basic sociodemographic and clinicopathological data were collected, along with an assessment of anxiety with the GAD-7 (generalized anxiety disorder questionnaire) questionnaire and a measurement of time perception. The procedure was approved by the Scientific Research Ethics Committee of "Prof. Dr. Paraskev Stoyanov" at the Medical University in Varna and MHAT "Nadezhda", Sofia, Bulgaria.

2.2. Measurement of time perception

Time perception was assessed by the subjects' individual prospective estimations of how quickly one minute passed compared to the actual amount of time passed. Time perception assessment, was performed before patients' first medical appointment for chemotherapy initiation. The assessments were performed in separate research area by a dedicated specially trained study nurse. The patient received instructions to estimate a duration of one minute after a start signal. When the subject gave a stop signal, the interpreter stopped the chronometer, and the estimated time was recorded. For our patients, the estimation of one minute ranged from 7 to 90 sec. The median value of time perception (37 sec) was used to stratify the patients into the two categories of fast (≤ median) and slow (> median) time perception.

2.3. Assessment of the levels of anxiety

The GAD-7 questionnaire was used to assess the levels of anxiety in cancer patients. The GAD-7 anxiety severity score is calculated by assigning the scores of 0, 1, 2, and 3 to the response categories of "not at all", several days", "more than half the days" , and "nearly every day", respectively. In our study, the GAD-7 total score for the seven items ranges from 0 to 21: 0-4: minimal anxiety (n = 73); 5-9: mild anxiety (n = 44); 10-14: moderate anxiety (n = 29); and 15-21: severe anxiety (n = 16) (*18*). Moderate and severe anxiety were considered high levels of anxiety. The questionnaire was validated against other mental health measurements and against a mental health practitioner interview. A clinical cut-off of 10 was recommended for diagnosing generalized anxiety disorder with a sensitivity of 89% and a specificity of 82% (18). However, a later study evaluated GAD-7 as a broader instrument to test for any anxiety disorder and determined an acceptable AUC of 0.86. From this AUC, a lower cut-off of 8 for any anxiety disorder was recommended, which gave a sensitivity of 77% and a specificity of 82% (*19*).

2.4. Statistical analysis

Data were managed and analyzed using IBM SPSS Statistics software ver. 23. The Mann-Whitney U test, χ^2 test and Spearman correlation coefficients were used to compare and evaluate the relationship between the levels of anxiety and clinicopathological characteristics of the patients, such as age, gender, primary tumor location and time perception. For the interpretation of correlation test results, rho values were interpreted as follows, < 0.19, very weak; 0.19-0.39, weak; 0.40-0.59, moderate; 0.60-0.79, strong; and > 0.80 very strong. The diagnostic accuracy of the subjective time perception was also determined by obtaining the largest possible area under the curve (AUC) in receiver operating characteristic (ROC) curve analysis. Trends in the changes of time perception across different levels of anxiety were assessed using the Jonckheere-Terpstra test. The minimum sample size for regression analysis was determined to be 150 patients to provide 80% power at a 5% significance level. The calculation was based on the six covariates and a 40% proportion of positive cases (*20*). Odds ratios (ORs) with confidence intervals (CIs) for categorical outcomes were calculated using a binary logistic regression model. Nagelkerke R-Square is reported for the logistic regression analysis. A $p \leq 0.05$ (two-tailed) was considered significant.

3. Results

3.1. Patient characteristics

A total of 162 patients with malignant solid tumors participated in the study; 60 (37%) were men, and 102 (63%) were women. The median age was 62 years, and the mean age of the group was 59.3 ± 10.6 years with an age range of 27 to 78 years. The sample included subjects with a variety of cancer types: 25 (15.4%) cases of lung cancer, 60 (37%) cases of breast cancer,

38 (23.5%) cases of colorectal cancer, and 39 (24.1%, representing more than 10 different histology types) cases of other cancers. Detailed descriptions of the patients' characteristics can be found in Table 1.

Table 1. Sociodemographic and clinicopathological patient characteristics

Patient characteristics	*n* (%)
Sex	
Male	60 (37%)
Female	102 (63%)
Ethnicity	
Bulgarian	153 (94.4%)
Turkish	9 (5.6%)
Religion	
Christian	149 (92.0%)
Muslim	9 (5.6%)
Atheist	3 (1.9%)
Unspecified	1 (0.5%)
Marital status	
Married	110 (67.7%)
Not married	52 (32.3%)
Cancer type	
Lung cancer	25 (15.4%)
Breast cancer	60 (37.0%)
Colorectal cancer	38 (23.5%)
Other*	39 (24.1%)
Stage	
II and III	99 (61.5%)
IV	63 (38.5%)
Education level	
Secondary**	107 (66%)
Tertiary***	55 (34%)

*Other: more than 10 types of cancer. **Secondary: up to 13 years of education. ***Tertiary: 13+ years of education.

3.2. Relationship between time perception, level of anxiety and patient characteristics

The mean anxiety score was 6.09 ± 5.3. A total of 45 (27.8%) patients had high levels of anxiety (cut-off ≥ 10), and their mean score was 13.2 ± 3.1. At a cut-off score of ≥ 8, 59 (36.4%) patients had high levels of anxiety with a mean score of 12.1 ± 3.4. A fast time perception and the female gender were related with high levels of anxiety (Table 2). Patients with breast cancer (7.48 ± 5.2) had significantly higher levels of anxiety in comparison to patients with colon cancer (4.07 ± 4.2) and trended towards higher anxiety levels compared to patients with lung (5.7 ± 5.8) and other (6.1 ± 5.5) types of cancer. Women (7.32±5.2) had significantly higher levels of anxiety than men (4.0 ± 4.7) ($p < 0.001$). No significant differences in the levels of anxiety were observed regarding age, marital status, education or stage of disease.

Women estimated one-minute intervals faster than men (33.3 ± 15.3 sec *vs*. 45.9 ± 17.9 sec; $p < 0.001$). No significant differences in time perception were observed regarding education level, marital status, stage of disease or type of cancer. Patients with a fast time perception had significantly higher levels of anxiety (8.44 ± 5.1) than patients with a slow time perception (3.49 ± 4.3) ($p = 0.001$) (Figure 1). Time perception differs significantly among patients with minimal ($n = 73$), mild ($n = 44$), moderate ($n = 29$) and severe anxiety ($n = 16$) (Figure 2). ROC analysis revealed that at the optimal cut-off value of time perception, patients with low and high anxiety levels can be discriminated with an AUC = 0.78 (95%

Table 2. Relationship between levels of anxiety and patient characteristics

Variable	Low anxiety, *n* (%) GAD score ≤ 10	High anxiety, *n* (%) GAD score ≥ 10	*p*	Low anxiety, *n* (%) GAD score ≤ 8	High anxiety, *n* (%) GAD score ≥ 8	*p*
Gender			< 0.001			0.001
Male	53 (88.3)	7 (11.7)		48 (80.0)	12 (20.0)	
Female	64 (62.7)	38 (37.3)		55 (53.9)	47 (46.1)	
Age			0.76			0.46
≤ 65	77 (71.3)	31 (28.7)		67 (62.0)	41 (38.0)	
> 65	39 (73.6)	14 (26.4)		36 (67.9)	17 (32.1)	
Marital status			0.58			0.49
Married	80 (73.4)	29 (26.6)		71 (65.1)	38 (34.9)	
Not married	36 (69.2)	16 (30.8)		31 (59.6)	21 (40.4)	
Cancer type			0.12			0.029
Lung cancer	20 (80.0)	5 (20.0)		17 (68.0)	8 (32.0)	
Breast cancer	37 (61.7)	23 (38.3)		30 (50.0)	30 (50.0)	
Colorectal cancer	31 (81.6)	7 (18.4)		30 (78.9)	8 (21.1)	
Other*	29 (74.4)	10 (25.6)		26 (66.7)	13 (33.3)	
Stage			0.58			0.75
II and III	70 (70.7)	29 (29.3)		62 (62.6)	37 (37.4)	
IV	47 (74.6)	16 (25.4)		41 (65.1)	22 (34.9)	
Time perception			< 0.001			< 0.001
Fast	46 (54.1)	39 (45.9)		37 (43.5)	48 (56.5)	
Slow	71 (92.2)	6 (7.8)		66 (85.7)	11 (14.3)	
Education level			0.68			0.78
Secondary**	76 (71.0)	31 (29.0)		67 (62.6)	40 (37.4)	
Tertiary***	41 (74.1)	14 (25.9)		35 (64.8)	19 (35.2)	

*Other: more than 10 types of cancer. **Secondary: up to 13 years of education. ***Tertiary: 13+ years of education.

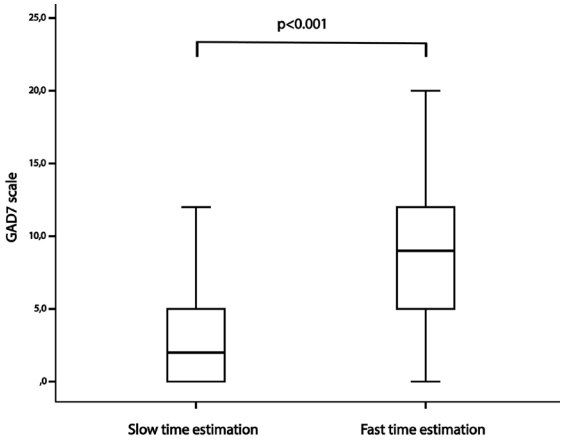

Figure 1. A bar graph depicting the level of anxiety in patients with slow and fast time perception. The Mann-Whitney *U* test was used to detect significant differences in the levels of anxiety between the groups.

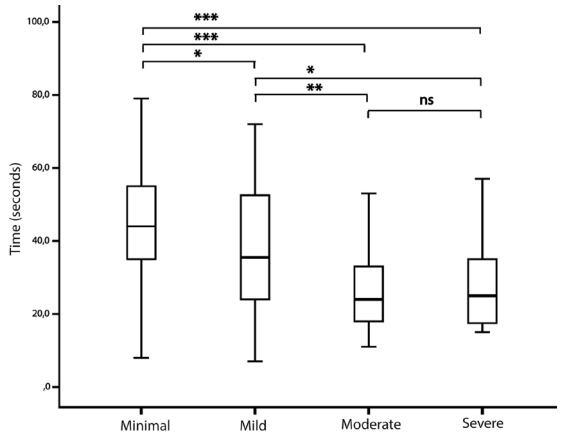

Figure 2. A bar graph depicting time perception among patients with minimal (*n* = 73), mild (*n* = 44), moderate (*n* = 29) and severe anxiety (*n* = 16). The Mann-Whitney *U* test was used to detect significant differences in the levels of anxiety between the groups; *indicates *p* value < 0.05, **indicates *p* value < 0.01 and ***indicates *p* value < 0.001.

CI: 0.70-0.85, $p < 0.001$) and with a sensitivity of 82.2% and specificity of 64.1% (Figure 3A). When we used the median as a cut-off the sensitivity and specificity was 86.7% and 60.7% respectively. A similar AUC = 0.74 was found when we used a GAD-7 score cut-off of ≥ 8 for high levels of anxiety (Figure 3B). There was a moderate, negative correlation (Spearman rho = -0.48, $p < 0.001$) between time perception and levels of anxiety.

3.3. Predictors of high levels of anxiety

In a univariate logistic regression analysis of women, patients with fast time perception and breast cancer were associated with high levels of anxiety. In a stepwise backward multiple logistic regression model, the female gender and fast time perception were independent predictors of high levels of anxiety (Table 3). In addition, the model accounted for 30.9% (Nagelkerke) of the variance in anxiety level. Similar results were found when we used a GAD-7 score cut-off of ≥ 8 for high levels of anxiety. These results were confirmed in an ordinal logistic regression model, where dependent factors were the four levels of anxiety (minimal, mild, moderate and severe) and time perception was used as a continuous independent covariate (data not shown).

4. Discussion

In this study, we investigated the association between time perception and levels of anxiety among patients with malignant solid tumors. The subjective passage of time was faster in patients with moderate and severe anxiety. The prospective time perception test revealed that patients with a faster perception of time were associated with an increased risk of high levels of anxiety.

A cancer diagnosis can lead to detrimental effects on physical and mental health. The diagnosis can

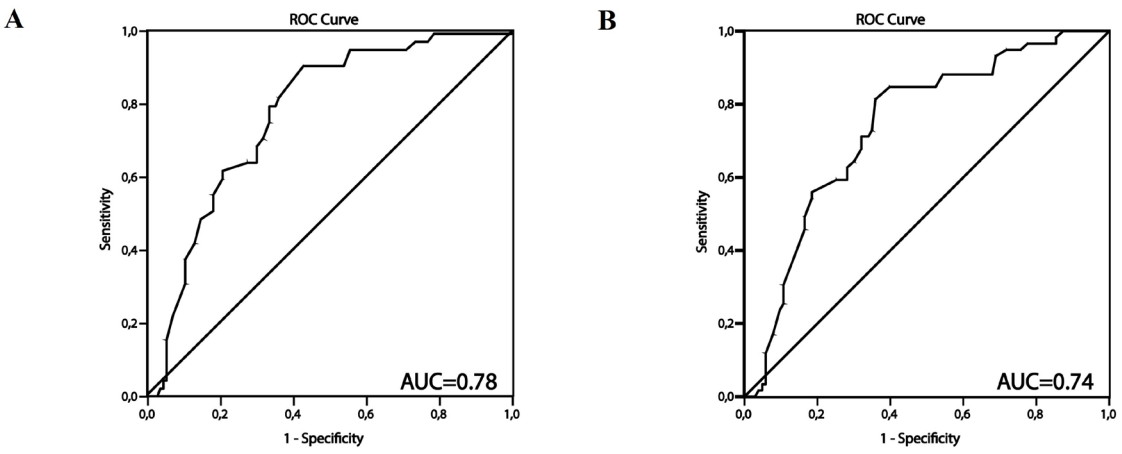

Figure 3. Receiver operating characteristic (ROC) curve analysis in which time perception was used to differentiate between patients with low and high levels of anxiety. The diagnostic accuracy of time perception was determined by obtaining the largest possible area under the curve (AUC) in ROC analysis. **(A)**, GAD-7 scores ≥ 10 were considered high levels of anxiety, AUC = 0.78 (95% CI: 0.70 - 0.85, $p < 0.001$); **(B)**, GAD-7 scores ≥ 8 were considered high levels of anxiety, AUC = 0.74 (95% CI: 0.66 - 0.81, $p < 0.001$).

Table 3. Univariate and stepwise backward multivariate regression analyses for predicting high anxiety levels (GAD-7 scores ≥10)

Variable	Univariate analysis			Multivariate analysis		
	Odds ratio	95% CI	*p*	Odds ratio	95% CI	*p*
Age						
≤ 65 y *vs*. > 65 y	0.89	0.42-1.86	0.76			
Gender						
Women *vs*. Men	4.46	1.85-10.28	0.001	3.01	1.16-7.77	0.023
Cancer type						
Breast cancer	2.26	1.12-4.53	0.02			
Stage						
IV *vs*. II and III	1.27	0.59-2.48	0.59			
Marital status						
Married *vs*. Not married	0.81	0.39-1.68	0.58			
Time perception						
Fast *vs*. slow	10.03	3.9-25.5	< 0.001	8.24	3.16-21.41	< 0.001
Education						
Secondary* *vs*. Tertiary**	1.16	0.56-2.43	0.68			

*Secondary: up to 13 years of education. **Tertiary: 13+ years of education.

negatively affect social functioning and inevitably cause distress over the course of the disease. A meta-analysis showed that a combination of mood disorders can occur in 30-40% of patients admitted to a hospital (*21*). Numerous papers have shown that the most important risk factors for anxiety are low socioeconomic status, low educational level, poor physical health, gender, type of cancer and age (*22-26*). Approximately 30% of these patients needed medical interventions (*27*), and these high levels of anxiety were not transient but remained for a longer period of time in more than 20% of patients (*28*). Stress and anxiety lead to neuroendocrine changes that can negatively affect patient outcomes (*29,30*). Thus, improving the early diagnosis of anxiety may lead to better survival and quality of life. The time point before the start of chemotherapy was identified as one of the most anxiety-provoking time periods and may call for interventions (*31*). Our method for assessing time perception by prospective estimation of a one-minute interval is relatively simple and fast to perform. It ensures higher compliance for both the patient and physician and avoids emotions inevitably linked to one's past or future. To the best of our knowledge, the present study is the first to discover an association between fast perception of time and high levels of anxiety among patients with solid tumors prior to starting chemotherapy. The need for additional predictive factors to explain the variations seen in self-reports of anxiety is well-known (*2*). Time perception has the potential to be such a factor, and because of this potential relationship, our model reached an R^2 value of more than 0.30.

Clinical practice is in need of a reliable, reasonably-priced and effective mechanism to recognize people who may gain from a further or more profound assessment. Our research suggests the conditional estimation of one-minute time intervals as a new possible indicator of anxiety in cancer patients. The suggested method ensures an efficient fast screening for abnormally high anxiety levels in cancer patients. It is a proven fact that a great number of patients do not report their actual levels of anxiety due to frustration or concern of being slandered for having a mental issue (*32*). Moreover, oncologists are not psychologists; they often lack the skills and/or training to tackle emotional issues. In view of the above, a basic screening tool that can be used in the intense everyday environment of a regular clinical practice is gravely needed. Under such circumstances, reviewing the perception of time by means of the method suggested by us can enable physicians to effectively detect patients at risk due to elevated anxiety levels.

Research data shows that the perception of speed of time in patients with advanced cancer is different from that in patients with no evidence of the disease, i.e., to patients suffering from advanced cancer a week seemed to pass much more slowly than to those who had no evidence of the disease (*33*). A recent study shows that the level of distress undoubtedly affects time perception and its distribution patterns. The one-minute time period of evaluation, suggested herein, is therefore a new efficient marker of elevated levels of distress in cancer patients (*34*). All things considered, time perception can be affected by the circumstances - personality, state of mind and level of activity during the testing period are just few of them. Assessments made at longer time periods may prove quite inaccurate and unreliable (*35*). We as humans tend to estimate "short" intervals of time as longer and "long" time durations as shorter (*36)*. Time perception results can be made more accurate in an experimental setting similar to ours in which patients were expected to estimate time duration (*37*). Numerous psychophysical methods have been used in various studies for assessing the perceived duration of a time interval. The outcomes, however, have been inconsistent and incomparable. The

data collected as well as the interpretations that come with it, have often been inconsistent and contradictory (*38*). It is common belief that time goes quickly only when you are having fun. This idea was questioned in an experimental model, where the estimation of time appeared faster when participants were awaiting a negative experience (*39*). Consistent with this finding, our results suggest that time perception appeared faster for patients with high levels of anxiety before starting their treatment, which is often with uncertain outcome.

Several limitations of our study should be noted. First, the GAD-7 scale focuses only on 1 anxiety disorder, even though there are many patients with other anxiety disorders, such as social phobia and posttraumatic stress disorder, who also need clinical attention. Clinicians and researchers usually do not look for depression or anxiety alone. Considering the frequency with which depression and anxiety occur together (up to 60%), a search for one condition should always be accompanied by an assessment of the other. Nevertheless, GAD is one of the most common mental disorders seen in outpatient practices. The Global Burden of Disease Study examined major depressive and anxiety disorders separately, and it was reported that anxiety disorders are the seventh most burdensome condition of all diseases worldwide today (*12*). Our study is cross-sectional and thus accurate predictions cannot be definitely made. Another limitation of our study is that the GAD-7 scale provides only probable diagnoses that should be confirmed by further evaluation.

It is well-known that the diagnosis of anxiety disorders is challenging due to a lack of objective biomarkers, and the diagnosis is based only on symptoms (*40*). Our study proposes a potential marker for anxiety for the first time, and further studies are warranted to confirm our results. Emotional concerns are a risk factor for nonadherence to treatment. Thus, early identification of such concerns is crucial for developing a management plan. The method we propose for detecting emotional concerns is an easily performed, time-saving, nonintrusive, ultrashort screening tool that is even suitable for patients who are not willing to reveal their level of anxiety via direct questionnaires.

References

1. Kessler RC, Chiu WT, Demler O, Merikangas KR, Walters EE. Prevalence, severity, and comorbidity of 12-month DSM-IV disorders in the National Comorbidity Survey Replication. Arch Gen Psychiatry. 2005; 62:617-627.
2. Salvo N, Zeng L, Zhang L, Leung M, Khan L, Presutti R, Nguyen J, Holden L, Culleton S, Chow E. Frequency of reporting and predictive factors for anxiety and depression in patients with advanced cancer. Clin Oncol (R Coll Radiol). 2012; 24:139-148.
3. McGregor BA, Antoni MH. Psychological intervention and health outcomes among women treated for breast cancer: a review of stress pathways and biological mediators. Brain Behav Immun. 2009; 23:159-166.
4. Andersen BL, DeRubeis RJ, Berman BS, Gruman J, Champion VL, Massie MJ, Holland JC, Partridge AH, Bak K, Somerfield MR, Rowland JH, American Society of Clinical O. Screening, assessment, and care of anxiety and depressive symptoms in adults with cancer: an American Society of Clinical Oncology guideline adaptation. J Clin Oncol. 2014; 32:1605-1619.
5. Skarstein J, Aass N, Fossa SD, Skovlund E, Dahl AA. Anxiety and depression in cancer patients: relation between the Hospital Anxiety and Depression Scale and the European Organization for Research and Treatment of Cancer Core Quality of Life Questionnaire. J Psychosom Res. 2000; 49:27-34.
6. Mehnert A, Hartung TJ, Friedrich M, Vehling S, Brahler E, Harter M, Keller M, Schulz H, Wegscheider K, Weis J, Koch U, Faller H. One in two cancer patients is significantly distressed: Prevalence and indicators of distress. Psychooncology. 2018; 27:75-82.
7. Walker LG, Heys SD, Walker MB, Ogston K, Miller ID, Hutcheon AW, Sarkar TK, Ah-See AK, Eremin O. Psychological factors can predict the response to primary chemotherapy in patients with locally advanced breast cancer. Eur J Cancer. 1999; 35:1783-1788.
8. Fernandez A, Rubio-Valera M, Bellon JA, Pinto-Meza A, Luciano JV, Mendive JM, Haro JM, Palao DJ, Serrano-Blanco A, investigators D. Recognition of anxiety disorders by the general practitioner: results from the DASMAP study. Gen Hosp Psychiatry. 2012; 34:227-233.
9. Fallowfield L, Ratcliffe D, Jenkins V, Saul J. Psychiatric morbidity and its recognition by doctors in patients with cancer. Br J Cancer. 2001; 84:1011-1015.
10. Delgado-Guay M, Parsons HA, Li Z, Palmer JL, Bruera E. Symptom distress in advanced cancer patients with anxiety and depression in the palliative care setting. Support Care Cancer. 2009; 17:573-579.
11. Ruiz MA, Zamorano E, Garcia-Campayo J, Pardo A, Freire O, Rejas J. Validity of the GAD-7 scale as an outcome measure of disability in patients with generalized anxiety disorders in primary care. J Affect Disord. 2011; 128:277-286.
12. Vos T, Flaxman AD, Naghavi M, et al. Years lived with disability (YLDs) for 1160 sequelae of 289 diseases and injuries 1990-2010: a systematic analysis for the Global Burden of Disease Study 2010. Lancet. 2012; 380:2163-2196.
13. Bandelow B, Michaelis S. Epidemiology of anxiety disorders in the 21st century. Dialogues Clin Neurosci. 2015; 17:327-335.
14. Baum SK, Boxley RL, Sokolowski M. Time perception and psychological well-being in the elderly. Psychiatr Q. 1984; 56:54-61.
15. Fraisse P. Perception and estimation of time. Annu Rev Psychol. 1984; 35:1-36.
16. Droit-Volet S, Gil S. The time-emotion paradox. Philos Trans R Soc Lond B Biol Sci. 2009; 364:1943-1953.
17. Donev IS, Stoyanov DS, Panayotova TV, Ivanova MS, Kashlov YK, Efraim ME, Conev NV. One-minute time interval estimation as a novel potent indicator of emotional concerns in cancer patients prior to starting chemotherapy. Current Psychology. 2019; 1-7.
18. Spitzer RL, Kroenke K, Williams JB, Lowe B. A brief measure for assessing generalized anxiety disorder: the GAD-7. Arch Intern Med. 2006; 166:1092-1097.

19. Kroenke K, Spitzer RL, Williams JB, Monahan PO, Lowe B. Anxiety disorders in primary care: prevalence, impairment, comorbidity, and detection. Ann Intern Med. 2007; 146:317-325.
20. Peduzzi P, Concato J, Kemper E, Holford TR, Feinstein AR. A simulation study of the number of events per variable in logistic regression analysis. J Clin Epidemiol. 1996; 49:1373-1379.
21. Mitchell AJ, Chan M, Bhatti H, Halton M, Grassi L, Johansen C, Meader N. Prevalence of depression, anxiety, and adjustment disorder in oncological, haematological, and palliative-care settings: a meta-analysis of 94 interview-based studies. Lancet Oncol. 2011; 12:160-174.
22. Dean C. Psychiatric morbidity following mastectomy: preoperative predictors and types of illness. J Psychosom Res. 1987; 31:385-392.
23. Kyranou M, Puntillo K, Dunn LB, Aouizerat BE, Paul SM, Cooper BA, Neuhaus J, West C, Dodd M, Miaskowski C. Predictors of initial levels and trajectories of anxiety in women before and for 6 months after breast cancer surgery. Cancer Nurs. 2014; 37:406-417.
24. Jacobsen PB, Bovbjerg DH, Redd WH. Anticipatory anxiety in women receiving chemotherapy for breast cancer. Health Psychol. 1993; 12:469-475.
25. Cohen M. Depression, anxiety, and somatic symptoms in older cancer patients: a comparison across age groups. Psychooncology. 2014; 23:151-157.
26. Lima MP, Longatto-Filho A, Osorio FL. Predictor variables and screening protocol for depressive and anxiety disorders in cancer outpatients. PloS One. 2016; 11:e0149421.
27. Carlson LE, Angen M, Cullum J, Goodey E, Koopmans J, Lamont L, MacRae JH, Martin M, Pelletier G, Robinson J, Simpson JS, Speca M, Tillotson L, Bultz BD. High levels of untreated distress and fatigue in cancer patients. Br J Cancer. 2004; 90:2297-2304.
28. Burgess C, Cornelius V, Love S, Graham J, Richards M, Ramirez A. Depression and anxiety in women with early breast cancer: five year observational cohort study. BMJ. 2005; 330:702.
29. Miller GE, Chen E, Zhou ES. If it goes up, must it come down? Chronic stress and the hypothalamic-pituitary-adrenocortical axis in humans. Psychol Bull. 2007; 133:25-45.
30. Chida Y, Hamer M, Wardle J, Steptoe A. Do stress-related psychosocial factors contribute to cancer incidence and survival? Nat Clin Pract Oncol. 2008; 5:466-475.
31. Schneider A, Kotronoulas G, Papadopoulou C, McCann L, Miller M, McBride J, Polly Z, Bettles S, Whitehouse A, Kearney N, Maguire R. Trajectories and predictors of state and trait anxiety in patients receiving chemotherapy for breast and colorectal cancer: Results from a longitudinal study. Eur J Oncol Nurs. 2016; 24:1-7.
32. Steele R, Fitch MI. Why patients with lung cancer do not want help with some needs. Support Care Cancer. 2008; 16:251-259.
33. van Laarhoven HW, Schilderman J, Verhagen CA, Prins JB. Time perception of cancer patients without evidence of disease and advanced cancer patients in a palliative, end-of-life-care setting. Cancer Nurs. 2011; 34:453-463.
34. Conev NV, Donev IS, Stoyanov DS. One-minute time interval estimation as a novel ultrashort tool for distress screening. Support Care Cancer. 2019; 27:2031-2037.
35. Foley H, Matlin M. Sensation and perception. 5th Edition, Psychology Press, 2015.
36. Zakay D. The evasive art of subjective time measurement: Some methodological dilemmas. In R. A. Block (Ed.), Cognitive models of psychological time. 1990; p.59-84.
37. Brown SW, Stubbs DA. The psychophysics of retrospective and prospective timing. Perception. 1988; 17:297-310.
38. Fraisse P. Perception and estimation of time. Annu Rev Psychol. 1984;35:1-36.
39. Edmonds EM, Cahoon D, Bridges B. The estimation of time as a function of positive, neutral, or negative expectancies. Bulletin of the Psychonomic Society. 1981; 17:259-260.
40. Rose M, Devine J. Assessment of patient-reported symptoms of anxiety. Dialogues Clin Neurosci. 2014; 16:197-211.

Received October 29, 2019; Revised January 3, 2020; Accepted January 25, 2020.

Address correspondence to:
Nikolay Vladimirov Conev, Clinic of Medical Oncology, UMHAT "St. Marina", 1 "Hristo Smirnenski" Blvd., Varna 9000, Bulgaria.
E-mail: nikolay_conev@yahoo.com

Released online in J-STAGE as advance publication February 6, 2020.

Original Article

DOI: 10.5582/bst.2019.01313

Long-term outcomes of living donor liver transplantation in patients with a prior history of nonhepatic malignancy

Hidekazu Yamamoto*, Yuzuru Sambommatsu, Sho Ibuki, Keita Shimata, Yasuhiko Sugawara, Taizo Hibi

Department of Pediatric Surgery and Transplantation, Kumamoto University Graduate School of Medical Sciences, Kumamoto, Japan.

SUMMARY Posttransplant malignancy has become a significant cause of mortality. Data on the long-term outcomes of patients with pretransplant nonhepatic malignancy (PTM) after living donor liver transplantation (LDLT) are scarce, although the recipients of other organs with PTM have been reported to have a poor survival. Fifteen patients with PTM (4.4%) among the 342 adult recipients were identified in our LDLT programs. The outcomes of the patients with PTM after LDLT were compared to those of patients without PTM in terms of the all-cause mortality and cancer-specific mortality (defined as mortality related to malignancy expect for hepatocellular carcinoma, cholangiocarcinoma, or neuroendocrine tumor). The sites of PTM included the breast in six, stomach in two, and colon, lung, kidney, uterine, thyroid, larynx, and acute myelogenous leukemia in one each. The median interval from the PTM treatment to LDLT was 57 months (range, 2-298). The patients who received the curative treatment for PTM were selected as the recipients. No patients with PTM had recurrence during the follow-up period. The 1-, 5-, and 10-year patient survival rates were 100%, 92.9%, and 92.9% in the PTM group and 86.2%, 76.7%, and 68.5% in the non-PTM group, respectively ($p = 0.142$). Likewise, there was no significant difference between the two groups in the cancer-specific mortality. In conclusion, the patients with PTM had comparable outcomes with regard to mortality and cancer-specific mortality compared with those without PTM. This study showed that the patients with PTM can obtain an acceptable outcome after LDLT when carefully selected.

Keywords pretransplant malignancy, living donor liver transplantation, all-cause mortality, cancer-specific mortality

1. Introduction

The survival in liver transplantation (LT) has improved significantly over time. The age of the recipients has increased steadily (*1,2*), and it is expected that more patients might have a history of pretransplant nonhepatic malignancy (PTM).

Solid organ transplant recipients are at an increased risk for the development of posttransplant malignancies including the recurrence of PTM and *de novo* malignancy due to the immunosuppression, compared with the general population (*3-8*). Cancer after transplantation causes considerable morbidity and mortality. There are some reports that PTM is a relative contraindication to solid organ transplantation (*9,10*). Organ transplantation for patients with PTM has been described from renal experiences (*11-21*). In addition, there are several reports describing about the outcomes of LT in patients with PTM (*22-25*), however, there are no reports on the outcomes after living donor LT (LDLT).

The present study explored the clinical outcomes, including cancer recurrence, in LDLT patients with PTM.

2. Patients and Methods

2.1. Patients and study design

A total of 342 adult patients with end-stage liver disease who underwent LDLT at Kumamoto University Hospital from January 1999 to December 2018 were enrolled in this study. Fifteen patients with PTM were identified retrospectively. Data were collected on patient characteristics, pre-LDLT malignancy, treatment, and post-LDLT recurrence by a clinical examination. The all-cause mortality was examined

as the patient survival. In addition, the cancer-specific mortality (defined as death related to the recurrence of PTM, and *de novo* malignancy; all other deaths, including those from recurrence of hepatocellular carcinoma [HCC], intrahepatic cholangiocarcinoma, and neuroendocrine tumor liver metastases identified before LDLT, were censored) was investigated in the patients with and without PTM (n = 327).

This study was conducted in accordance with the Declaration of Helsinki after approval from our institutional ethics board. Written informed consent was obtained from all patients.

2.2. Selection for LDLT

The patients with PTM were considered as LDLT candidates when all of the following factors were satisfied: (1) Patients had received the curative treatment for PTM, and (2) the expected 5-year survival rate related to PTM after treatment was 70-80% or greater.

2.3. Immunosuppression

Basic immunosuppressants included tacrolimus and steroid after LDLT. The immunosuppression regimen for the patients with PTM was indicated as the same standard regimen used for the patients without PTM. All patients began tacrolimus within 24 h after graft perfusion. Target trough levels of tacrolimus were 10 to 15 ng/mL during the second week postoperatively and then around 10 ng/mL during the first month postoperatively, 5 to 10 ng/mL until 3 months, and around 5 ng/mL thereafter. Steroids were given with tapering within 3 months (methylprednisolone 1 mg/kg/day 1-3 days after operation and 0.5 mg/kg/day 4-6 days and 0.3 mg/kg/day 7 day and prednisone 0.3 mg/kg/day in the first month and then tapered). If acute cellular rejection was diagnosed, patients were treated with bolus dose steroids followed by a tapered dose or the addition of mycophenolate mofetil.

2.4. Statistical analysis

The values were presented as the median and range. The Kruskal-Wallis test was applied respectively for paired and unpaired multiple comparisons. The Mann-Whitney test was applied respectively for paired and unpaired comparisons between two groups. The correlation of the categorical data and numerical data was evaluated using the chi-square test and Spearman's test, respectively. Cumulative survival rates were calculated using the Kaplan-Meier method, and differences between curves were evaluated using the log-rank test. A P-value < 0.05 was recognized as significant. All statistical analyses were performed using the SPSS ver. 18 statistical software program (IBM, Tokyo, Japan).

3. Results

3.1. Patient's characteristics

Of the 342 patients, 15 (4.4 %) were found to have PTM before LDLT (Table 1). The underlying liver diseases for transplantation included hepatitis C virus-related liver cirrhosis (LC) (n = 7), hepatitis B virus-related LC (n = 1), alcoholic LC (n = 1), primary biliary cirrhosis (n = 1), nonalcoholic steatohepatitis (n = 1), cryptogenic LC (n = 1), secondary sclerosing cholangitis (n = 1), idiopathic portal hypertension (n = 1), and Budd-Chiari syndrome (n = 1). Eight of these patients had HCC. The median age at LDLT was 60 years old (range, 45-69 years old) and the median Model for End-stage Liver Disease (MELD) score was 17.0 was (range, 8.0-27.0). The median age at the time of the cancer diagnosis was

Table 1. Characteristics of LT patients with preexisting nonhepatic malignancy

Patient No.	Age at transplant (years)	gender	Liver disease	MELD score	Age at malignancy (years)
1	54	M	HBV-LC	20	54
2	57	F	SSC	17	52
3	66	F	cryptogenic LC, HCC	13	66
4	55	F	HCV-LC, HCC	9	37
5	66	M	HCV-LC, HCC	10	51
6	68	M	HCV-LC, HCC	8	65
7	65	M	ALC, HCC	19	63
8	62	M	IPH	17	48
9	59	F	HCV-LC	27	42
10	69	F	HCV-LC, HCC	8	52
11	57	F	HCV-LC	21	48
12	55	F	PBC	19	51
13	60	F	NASH, HCC	14	56
14	62	F	Budd-Chiari syndrome	9	61
15	45	M	HCV-LC, HCC	17	20

LT, liver transplantation; MELD, Model for end-stage liver disease; SCC, secondary sclerosing cholangitis; HBV- and HCV-LC, hepatitis B and hepatitis C-related liver cirrhosis; HCC, hepatocellular carcinoma; ALC, alcoholic liver cirrhosis; IPH, idiopathic portal hypertension; PBC, primary biliary cirrhosis; NASH, nonalcoholic steatohepatitis.

Table 2. Clinical data on LT patients with preexisting nonhepatic malignancy

Patient No.	Malignancy	Type/stage	Treatment	Interval to LT (months)	Follow-up post LT (months)	Tumor Recurrence	Survival
1	Larynx	T1N0M0(stage I)	Radiation	2	68	No	Alive
2	Thyroid	n.a.	Right lobectomy	57	98	No	Alive
3	Lung	T1aN0M0(stage IA)	Resection	3	76	No	Alive
4	Uterine	CIS	Hysterectomy	216	136	No	Alive
5	Stomach	T1aN0M0(stage IA)	Endoscopic resection	192	59	No	Alive
6	Stomach	T1aN0M0(stage IA)	Endoscopic resection	36	20	No	Dead
7	Colon	T3N1M0(stage IIIA)	Resection+Chemotherapy	19	27	No	Alive
8	Kidney	T1aN0M0(stage IA)	Nephrectomy	165	43	No	Alive
9	Breast	n.a.	Mastectomy	204	63	No	Alive
10	Breast	n.a.	Mastectomy	204	57	No	Alive
11	Breast	T3N2M0(stage IIIA)	Mastectomy+Radiation +Chemotherapy	115	92	No	Alive
12	Breast	T2N1M0(stage IIB)	Mastectomy	51	58	No	Alive
13	Breast	T2N0M0(stage IIA)	Mastectomy+Radiation	48	44	No	Alive
14	Breast	T2N0M0(stage IIA)	Mastectomy+Chemotherapy	9	7	No	Alive
15	AML	n.a.	Chemotherapy	298	77	No	Alive

LT, liver transplantation; CIS, carcinoma in situ; AML, acute myelogenous leukemia

52 years old (range, 20-66 years old). Six patients were male, and nine were female.

The PTM consisted of a total of 15 cancers: breast cancer (n = 6), gastric cancer (n = 2), colon cancer (n = 1), thyroid cancer (n = 1), laryngeal cancer (n = 1), lung cancer (n = 1), renal cancer (n = 1), uterus cancer (n = 1), and acute myelogenous leukemia (AML) (n = 1).

3.2. Pretransplant cancer status

The median interval from treatment of cancer to LDLT was 57 months (range, 2-298 months) (Table 2). Laryngeal and lung cancer were found during the pretransplant examination. Because the liver function in the patients with laryngeal and lung cancer were considered to be stable enough to postpone transplantation, they underwent LDLT two and three months later, respectively, following treatment for their early-stage cancers (laryngeal cancer/stage I, lung cancer/stage IA). Two patients with gastric mucosal cancer underwent radical endoscopic mucosal resection (EMR) and received LDLT at more than three years after EMR. The deteriorated liver function of the patient with advanced colon cancer did not allow us to delay transplantation and this patient underwent LDLT 19 months after the curative treatment for cancer. In the patients with breast cancer, the median interval between the treatment and LDLT was 83 months (range, 9-204 months). The patient with AML underwent LDLT over 20 years after achieving a complete response with chemotherapy. No patients with PTM experienced recurrence after primary treatment of cancer before LDLT.

3.3. Immunosuppression and rejection after LDLT

Primary immunosuppression consisted of tacrolimus and steroids in all the patients. Mycophenolate mofetil was added in seven patients. No patients developed rejection that required steroid bolus therapy.

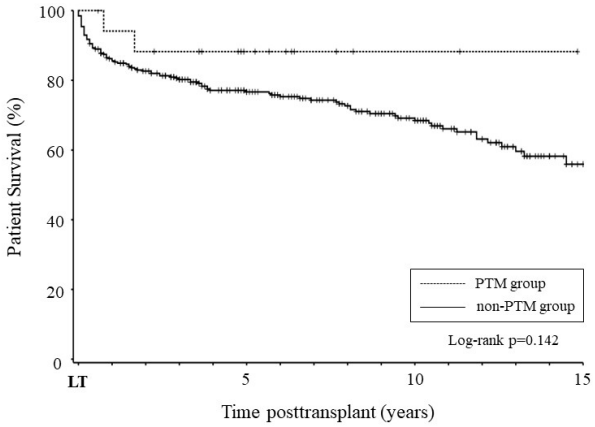

Figure 1. The cumulative patient survival following liver transplantation.

3.4. Posttransplant outcomes

No patients with PTM experienced recurrence for a median follow-up of 59 months (range, 8-136 months) after LDLT. One of the 15 PTM patients (6.7%) died during the follow-up periods due to sepsis 20 months after transplantation, an event that was not related to PTM. A total of 98 of the 327 non-PTM patients (30%) died during the follow-up period. The 1-, 3-, and 5-year patient survival rates were 100%, 92.9%, and 92.9% in the PTM group and 86.2%, 80.2%, and 76.7% in the non-PTM group, respectively, without a statistically significant difference (p = 0.142; Figure 1). No patients died of *de novo* malignancy or PTM recurrence in the PTM group, while eight died of *de novo* malignancy in the non-PTM group. There was no significant difference in the cancer-specific mortality rate between the two groups (p = 0.251).

4. Discussion

In this study, we identified the 15 patients with PTM (4.4%). This study showed that selected patients with PTM were suitable as LDLT candidates because the recurrence rate of the PTM was low. If the 5-year survival rates related to PTM after curative treatment are expected to be 70-80% or more, regardless of early or advanced cancer, LDLT might be considered, irrespective of the cancer-free interval and cancer type. From this perspective, it is necessary to hold multidisciplinary discussions about the indication of LDLT among hepatologists, transplant surgeons, and oncologists. This is the first report to describe the long-term outcomes of patients with PTM after LDLT.

In renal transplantation, the recurrence rate of PTM ranged from 13.7% to 22% (*12,17,18,20,26*). Penn et.al. reported that almost of these recurrences occurred in the first 2 years after transplantation (*12*). In the previous literature, which was limited in number, the recurrence rate of the PTM after LT ranged from 2.7% to 13.8% (*22-25*). The median duration from LT to the time of diagnosis of the recurrence of the PMT was 12 months (range, 6-36) (*22-25*). In our study, no recurrence of PTM developed for a median follow-up of 59 months (range, 8-136) after LDLT.

The optimal cancer-free interval between the treatment of cancer and transplantation has not yet been established. Some reports showed that the shorter cancer-free intervals were associated with a higher risk of cancer recurrence and cancer-specific mortality (*12,27,28*). Sigurdardottir *et al*. reported that a cancer-free survival for ≥ 5 years before the transplantation was associated with the lowest risk of recurrence in lung and heart transplantation (*27*). In addition, a minimum of two-year waiting period until transplantation has been recommended in some guidelines of renal transplantation, based on the understanding that recurrence tends to occur within two years of treatment in general (*11,28,29*).

However, others have found no association between the cancer-free interval and recurrent cancer mortality. Dahle *et al*. showed that short waiting periods between treatment of pretransplant cancer and transplantation were not associated with recurrent cancer or all-cause mortality (*18*). Acuna *et al*. reported that there was no association between prolonged remission times before transplantation and a reduced risk of recurrence or death from malignancy (*17*). Similarly, we found no association between a prolonged cancer-free period and posttransplant cancer recurrence. In LT, it is difficult to postpone the timing of transplantation because of there is no other alternative treatment for liver failure.

The guidelines in renal transplantation recommend waiting two years after cancer remission in case of low-risk malignancy (*i.e*. prostate, thyroid, testicular, renal cancer). For colorectal cancer, the interval between cancer remission and transplantation was suggested to be 0-5 years (depending on the stage) by the American society of Transplant Physicians (AST) and over 5 years by the European Best Practice Guidelines (EBPG) for Renal Transplantation, respectively (*29,30*). The interval between cancer remission and transplantation of breast cancer was recommended to be 2-5 years by the AST and over 3 years by the EBPG. For malignant melanoma, the interval was recommended to be 2-5 years by the AST and over 2 years by the EBPG (*29,30*). In our series, almost all patients had early or low TMN (stage I-II) stage of each malignancy. Although three patients with an early TMN (stage I-II) stage underwent LT within one year from cancer treatment in our series, no recurrence occurred. The intervals from PTM treatment to LT in the patients with advanced-stage colon cancer and breast cancer was 19 months and 9 years, and neither has experienced recurrence during the follow-up period. 5-year disease free survival rate in the patients with Stage IIIA colon cancer which was curatively resected and received chemotherapy was over 70% in the literature (*31,32*). We accepted the patient with advanced colon cancer as the candidate of transplant recipient.

PTM is reportedly associated with an increased risk of all-cause mortality and cancer-specific mortality, including PTM recurrence and *de novo* malignancies after transplantation, compared to those without PTM, especially case of heart and renal transplantation (*17,26,28,33,34*). However, the findings of other studies as well as our own work were not compatible with this observation (*18,35*). Viecelli *et al*. reported that a history of malignancy did not have an additive effect on the all-cause mortality or cancer-specific mortality in the large cohort (*35*). In contrast, we found that the all-cause mortality and cancer-specific mortality in the patients with PTM were comparable to those in the patients without PTM in our study.

Two limitations associated with our study deserve further comment: namely, the retrospective nature and small sample size. Ideally, prospective and multicenter studies, or otherwise meta-analyses given the rarity of disease are therefore needed in order to clarify the indication of LDLT while taking into consideration the cancer type, cancer stage, and interval between the treatment of PTM and LDLT. Despite these limitations, we believe that this study provides useful information regarding the clinical outcomes of patients with PTM after LDLT.

In conclusion, the recurrence rate of PTM after LDLT is low, and PTM is not associated with an increased risk of all-cause mortality or cancer-specific mortality. The results of our study suggest that patients with PTM can be considered as candidates for LDLT if appropriately selected.

References

1. Niazi S, Schneekloth T, Taner CB. Elderly recipients

of liver transplantation: impact of age and psychosocial variables on outcome. Curr Opin Organ Transplant. 2017; 22:588-592.
2. Aduen JF, Sujay B, Dickson RC, Heckman MG, Hewitt WR, Stapelfeldt WH, Steers JL, Harnois DM, Kramer DJ. Outcomes after liver transplant in patients aged 70 years or older compared with those younger than 60 years. Mayo Clin Proc. 2009; 84:973-978.
3. Dantal J, Soulillou JP. Immunosuppressive drugs and the risk of cancer after organ transplantation. N Engl J Med. 2005; 352:1371-1373.
4. Hall EC, Pfeiffer RM, Segev DL, Engels EA. Cumulative incidence of cancer after solid organ transplantation. Cancer. 2013; 119:2300-2308.
5. Collett D, Mumford L, Banner NR, Neuberger J, Watson C. Comparison of the incidence of malignancy in recipients of different types of organ: a UK Registry audit. Am J Transplant. 2010; 10:1889-1896.
6. Aberg F, Pukkala E, Hockerstedt K, Sankila R, Isoniemi H. Risk of malignant neoplasms after liver transplantation: a population-based study. Liver Transpl. 2008; 14:1428-1436.
7. Chatrath H, Berman K, Vuppalanchi R, Slaven J, Kwo P, Tector AJ, Chalasani N, Ghabril M. *De novo* malignancy post-liver transplantation: a single center, population controlled study. Clin Transplant. 2013; 27:582-590.
8. Engels EA, Pfeiffer RM, Fraumeni JF, Jr., *et al*. Spectrum of cancer risk among US solid organ transplant recipients. JAMA. 2011; 306:1891-1901.
9. Oechslin E, Kiowski W, Schneider J, Follath F, Turina M, Gallino A. Pretransplant malignancy in candidates and posttransplant malignancy in recipients of cardiac transplantation. Ann Oncol. 1996; 7:1059-1063.
10. Murray KF, Carithers RL, Jr. AASLD practice guidelines: Evaluation of the patient for liver transplantation. Hepatology. 2005; 41:1407-1432.
11. Batabyal P, Chapman JR, Wong G, Craig JC, Tong A. Clinical practice guidelines on wait-listing for kidney transplantation: consistent and equitable? Transplantation. 2012; 94:703-713.
12. Penn I. Evaluation of transplant candidates with pre-existing malignancies. Ann Transplant. 1997; 2:14-17.
13. Chapman JR, Sheil AG, Disney AP. Recurrence of cancer after renal transplantation. Transplant Proc. 2001; 33:1830-1831.
14. Chiu HF, Chung MC, Chung CJ, Yu TM, Shu KH, Wu MJ. Prognosis of kidney transplant recipients with pretransplantation malignancy: a nationwide population-based cohort study in Taiwan. Transplant Proc. 2016; 48:918-920.
15. Knoll G, Cockfield S, Blydt-Hansen T, Baran D, Kiberd B, Landsberg D, Rush D, Cole E. Canadian Society of Transplantation consensus guidelines on eligibility for kidney transplantation. CMAJ. 2005; 173:1181-1184.
16. Kalble T, Lucan M, Nicita G, Sells R, Burgos Revilla FJ, Wiesel M. EAU guidelines on renal transplantation. Eur Urol. 2005; 47:156-166.
17. Acuna SA, Sutradhar R, Kim SJ, Baxter NN. Solid organ transplantation in patients with preexisting malignancies in remission: a propensity score matched cohort study. Transplantation. 2018; 102:1156-1164.
18. Dahle DO, Grotmol T, Leivestad T, Hartmann A, Midtvedt K, Reisaeter AV, Mjoen G, Pihlstrom HK, Naess H, Holdaas H. Association between pretransplant cancer and survival in kidney transplant recipients. Transplantation. 2017; 101:2599-2605.
19. Watschinger B, Budde K, Crespo M, Heemann U, Hilbrands L, Maggiore U, Mariat C, Oberbauer R, Oniscu GC, Peruzzi L, Sorensen SS, Viklicky O, Abramowicz D. Pre-existing malignancies in renal transplant candidates-time to reconsider waiting times. Nephrol Dial Transplant. 2019.
20. Unterrainer C, Opelz G, Dohler B, Susal C, Collaborative Transplant S. Pretransplant Cancer in Kidney Recipients in Relation to Recurrent and *De Novo* Cancer Incidence Posttransplantation and Implications for Graft and Patient Survival. Transplantation. 2019; 103:581-587.
21. Acuna SA, Huang JW, Daly C, Shah PS, Kim SJ, Baxter NN. Outcomes of solid organ transplant recipients with preexisting malignancies in remission: a systematic review and meta-analysis. Transplantation. 2017; 101:471-481.
22. Kelly DM, Emre S, Guy SR, Miller CM, Schwartz ME, Sheiner PA. Liver transplant recipients are not at increased risk for nonlymphoid solid organ tumors. Cancer. 1998; 83:1237-1243.
23. Saigal S, Norris S, Srinivasan P, Muiesan P, Rela M, Heaton N, O'Grady J. Successful outcome of orthotopic liver transplantation in patients with preexisting malignant states. Liver Transpl. 2001; 7:11-15.
24. Benten D, Sterneck M, Panse J, Rogiers X, Lohse AW. Low recurrence of preexisting extrahepatic malignancies after liver transplantation. Liver Transpl. 2008; 14:789-798.
25. Jain A, Fiaz O, Sheikh B, Sharma R, Safadjou S, Kashyap R, Bryan L, Batzold P, Orloff M. Recurrent nonhepatic and *de novo* malignancies after liver transplantation. Transplantation. 2009; 88:706-710.
26. Hellstrom V, Lorant T, Dohler B, Tufveson G, Enblad G. High posttransplant cancer incidence in renal transplanted patients with pretransplant cancer. Transplantation. 2017; 101:1295-1302.
27. Sigurdardottir V, Bjortuft O, Eiskjaer H, Ekmehag B, Gude E, Gustafsson F, Hagerman I, Halme M, Lommi J, Mared L, Riise GC, Simonsen S. Long-term follow-up of lung and heart transplant recipients with pre-transplant malignancies. J Heart Lung Transplant. 2012; 31:1276-1280.
28. Brattstrom C, Granath F, Edgren G, Smedby KE, Wilczek HE. Overall and cause-specific mortality in transplant recipients with a pretransplantation cancer history. Transplantation. 2013; 96:297-305.
29. Girndt M, Kohler H. Waiting time for patients with history of malignant disease before listing for organ transplantation. Transplantation. 2005; 80:S167-170.
30. Campistol JM, Cuervas-Mons V, Manito N, *et al*. New concepts and best practices for management of pre- and post-transplantation cancer. Transplant Rev (Orlando). 2012; 26:261-279.
31. Shimada Y, Hamaguchi T, Mizusawa J, *et al*. Randomised phase III trial of adjuvant chemotherapy with oral uracil and tegafur plus leucovorin versus intravenous fluorouracil and levofolinate in patients with stage III colorectal cancer who have undergone Japanese D2/D3 lymph node dissection: final results of JCOG0205. Eur J Cancer. 2014; 50:2231-2240.
32. Kusumoto T, Ishiguro M, Nakatani E, *et al*. Updated 5-year survival and exploratory T x N subset analyses of ACTS-CC trial: a randomised controlled trial of S-1 versus tegafur-uracil/leucovorin as adjuvant

chemotherapy for stage III colon cancer. ESMO Open. 2018; 3:e000428.
33. Yoosabai A, Mehta A, Kang W, Chaiwatcharayut W, Sampaio M, Huang E, Bunnapradist S. Pretransplant malignancy as a risk factor for posttransplant malignancy after heart transplantation. Transplantation. 2015; 99:345-350.
34. Webster AC, Craig JC, Simpson JM, Jones MP, Chapman JR. Identifying high risk groups and quantifying absolute risk of cancer after kidney transplantation: a cohort study of 15,183 recipients. Am J Transplant. 2007; 7:2140-2151.
35. Viecelli AK, Lim WH, Macaskill P, Chapman JR, Craig JC, Clayton P, Cohney S, Carroll R, Wong G. Cancer-specific and all-cause mortality in kidney transplant recipients with and without previous cancer. Transplantation. 2015; 99:2586-2592.

Received November 25, 2019; Revised January 16, 2020; Accepted January 31, 2020.

*Address correspondence to:
Hidekazu Yamamoto, Department of Pediatric Surgery and Transplantation, Kumamoto University Graduate School of Medical Sciences. 1-1-1, Honjo, Chuo-ku, Kumamoto 860-8556, Japan.
E-mail: yamahide@kuh.kumamoto-u.ac.jp

Released online in J-STAGE as advance publication February 5, 2020.

Original Article

DOI: 10.5582/bst.2019.01279

Neutrophil to lymphocyte ratio as a potential predictive marker for treatment with pembrolizumab as a second line treatment in patients with non-small cell lung cancer

Mila P. Petrova[1], Mariyana I. Eneva[2], Jeliazko I. Arabadjiev[3], Nikolay V. Conev[4], Eleonora G. Dimitrova[4], Krassimir D. Koynov[5], Teodora S. Karanikolova[1], Spartak S. Valev[1], Radostina B. Gencheva[1], Georgi A. Zhbantov[1], Anika I. Ivanova[1], Iva I. Sarbianova[6], Constanta V. Timcheva[1], Ivan S. Donev[1,*]

[1] Clinic of Medical Oncology, MHAT "Nadezhda", Sofia, Bulgaria;
[2] Hospital Pharmacy "Nadezhda" Sofia, Bulgaria;
[3] Department of Medical Oncology, MHAT "Tokuda", Sofia, Bulgaria;
[4] Clinic of Medical Oncology, UMHAT "St. Marina", Varna, Bulgaria;
[5] Department of Medical Oncology, MHAT "Serdika", Sofia, Bulgaria;
[6] Department of Intensive Care Unit, MHAT "Nadezhda", Sofia, Bulgaria.

SUMMARY The aim of this multicentric retrospective study is to evaluate the predictive and prognostic performance of neutrophil to lymphocyte ratio (NLR), platelet-lymphocyte ratio (PLR) and their dynamics in patients with non-small cell lung cancer (NSCLC) treated with pembrolizumab as a second line. Patients with metastatic NSCLC (n = 119), whose tumors expressed programmed death-ligand 1 (PD-L1) ≥ 1%, were retrospectively analyzed between Apr 2017 and Apr 2019. All patients received platinum-containing chemotherapy as a first line treatment. Pre-treatment NLR was calculated by dividing the number of neutrophils by the number of lymphocytes in peripheral blood before the first pembrolizumab infusion. Progression free survival (PFS) and overall survival (OS) was compared by Kaplan-Meier method and Cox Proportional Hazard model. Patients with NLR > 5 before immunotherapy showed significantly shorter mean PFS of 6.86 months (95% CI: 5.81-7.90) as compared to those with NLR ≤ 5 of 18.82 months (95% CI: 15.87-21.78) (long rank test p < 0.001). Furthermore in the multivariate analysis, only NLR > 5 was an independent predictive factor for shorter PFS (HR: 4.47, 95% CI: 2.20-9.07, p < 0.001). In multivariate analysis, presence of bone metastases (HR: 2.08, 95% CI: 1.10-4.94, p = 0.030), NLR > 5 before chemotherapy (HR: 8.09, 95% CI: 2.35-27.81, p = 0.001) and high PLR before chemotherapy (HR: 2.81, 95% CI: 1.13-6.97, p = 0.025) were found to be independent negative prognostic factors for poor OS. Our data suggests that NLR ≤ 5 is a potential predictive marker, which may identify patients appropriate for immunotherapy as a second line treatment.

Keywords neutrophil to lymphocyte ratio, predictive marker, immunotherapy

1. Introduction

Lung cancer is the leading cause of cancer death worldwide (*1*). Non-small cell lung cancer (NSCLC) accounts for about 80% of lung cancers. Recently, immunotherapy has turned out to be of great interest to researchers, especially with its promise to treat various forms of cancer including NSCLC (*2*). Human immune checkpoint-inhibitor antibodies inhibit the program death (PD-1) receptor or its ligand PD-L1. This helps to improve antitumor immunity. However, for different reasons, platinum-based chemotherapy still remains the first-line treatment or at least part of it for the majority of patients without targetable oncogenic driver alterations (*3,4*). In the phase II/III KEYNOTE-010 study, pembrolizumab significantly prolonged overall survival over docetaxel as second line therapy in advanced NSCLC (*5*). Despite these advances in treatment and the increased knowledge of the molecular pathways, our understanding why some people benefit from treatment with immunotherapy while others do not, is not well clarified (*6,7*). Durable responses can be observed in these populations, although the percentage was often found to be lower than 20% (*8,9*). This is why it is

important to identify a biomarker, which will predict the response to checkpoint blockades so as to optimize patient clinical benefit.

Overexpression of PD-L1 is an important and widely-explored predictive biomarker for the response to PD-1/PD-L1 antibodies (*10*). Immune cells which are most commonly associated with tumor progression and poor prognosis include neutrophils, platelets, macrophages and regulatory T cells (*11,12*). Neutrophil-to-lymphocyte ratio (NLR) and platelet-to-lymphocyte ratio (PLR) which are easily and usually performed in clinical practice, prove to be established strong prognostic markers associated with the worse OS in several tumor types including NSCLC in the pre-immunotherapy era (*13,14*). Limited studies suggested that high NLR and PLR predict poor response to nivolumab as a second line treatment (*15-17*).

The purpose of this retrospective study is to evaluate the predictive and prognostic performance of NLR, PLR and their dynamics in patients with NSCLC treated with pembrolizumab as a second line.

2. Materials and Methods

2.1. Patient selection

In this retrospective study we reviewed the cases of 119 patients from four centers in Bulgaria with metastatic NSCLC treated with pembrolizumab who have progressed after first line platinum-based chemotherapy between April 1, 2017 and April 30, 2019. The procedure was approved by the Scientific Research Ethics Committee at the Hospital "Nadezhda" in Sofia. Patients were eligible if they were ≥18 years old, and had histologically confirmed diagnosis of NSCLC in metastatic stage. Patients were Epidermal Growth Factor Receptor/Anaplastic lymphoma kinase (ALK) wildtype. All patients were in Eastern Cooperative Oncology Group -Performance status (ECOG-PS) < 2, and had disease progression after receiving one prior platinium-based systemic therapy for metastatic disease, with blood cell count and blood samples available. Patients were excluded if they had brain metastases (since the use of corticosteroids may compromise therapy), had autoimmune disease, symptomatic interstitial lung disease, systemic immunosuppression, or prior treatment with immune-stimulatory antitumor agents including checkpoint inhibitors. Patients did not show any clinical or computed tomography signs of active infection. Tumor PD-L1 status was required. Before starting a pembrolizumab treatment patients had at least 3 weeks free of treatment. Pembrolizumab was initially administered at 2 mg/kg intravenously (*i.v.*) over 60 minutes every 3 weeks and later at 200 mg *i.v.*, flat dose, every 3 weeks.

2.2. Data collection

Data collected included: demographics; smoking history; weight, height and body-mass index (BMI), histology; PD-L1 status; metastatic sites at initial diagnosis; description of first line treatment; date of progression (or last follow-up) as determined by radiology reports; and date of death or last follow-up. Peripheral blood samples were collected from patients included in the study the day of the first line chemotherapy administration at baseline and the day of first immunotherapy infusion upon progression. Hematological and biochemistry parameters of interest were absolute leukocyte (Leu), RDW (red blood cell distribution width), absolute neutrophil (ANC), absolute lymphocyte (ALC) and platelet (APC) counts, enabling calculation of NLR (Neutrophil to Lymphocyte Ratio – ANC/ALC) and PLR (Platelet to Lymphocyte ratio-APC/ALC). NLR1 and PLR1 were calculated before the first cycle of chemotherapy, NLR2 and PLR 2 – before the first pembrolizumab infusion. ΔNLR (NLR2-NLR1) and ΔPLR (PLR2-PLR1) were calculated. An NLR > 5 was considered elevated in accordance with earlier reports (*15,18,19*). The median value of NLR1 was 4.96. The median value of PLR was used to group cases into two categories of low (≤ median-200) and high (> median). Relative NLR and PLR change was analyzed: (calculated as % change ({[NLR2 / NLR1] -1} *100) and subsequently grouped in two groups (≥ 25% and < 25% increase).

The tumor PD-L1 protein expression level was examined in archived biopsy samples of the tumors using the PD-L1 immunohistochemistry (IHC) 28-8 pharmDx (Dako) kit (Agilent Technology). According to the manufacturer's kit criteria, cases with positive membranous staining of 1% or more of the tumor cells were defined as positive. In addition, we subdivided the positive group into expression categories - 50% or more, between 25-49% and between 1-24%.

2.3. Endpoints

The tumor response was assessed according to the Response Evaluation Criteria in Solid Tumors (ver.1.1) (RECIST 1.1) and clinical tumor response was assessed every 3 months. Patients were staged before treatment by performing computed tomography (CT). Clinical benefit rate (CBR) was defined as the proportion of patients with a partial response or stable disease for at least six months since no patients with complete response were recorded. Patients without clinical benefit (CB) were defined by a progression less than six months after treatment (chemotherapy or immunotherapy); patients with CB – the proportion of patients with radiological response or stabilization more than six months. Progression-free survival (PFS) was defined as the time elapsed between treatment initiation and tumor progression or death from any cause. Overall survival (OS) was defined as the interval between diagnosis

of the disease and death or date of last follow-up evaluation.

2.4. Statistical design and analysis

Data was managed and analyzed using SPSS software ver. 23. The demographic characteristics were expressed as frequencies and percentages for categorical variables and as medians and means with standard deviations for quantitative variables. The Mann–Whitney U test, χ^2 test and Spearman correlation were used to compare and evaluate the correlations between the biomarkers and the clinicopathological characteristics of the patients such as age, gender, PS (ECOG) - performance status (Eastern Cooperative Oncology Group). For interpretation of correlation test results, rho values were interpreted as follows, < 0.39, weak; 0.40-0.59, moderate; 0.60-0.79, strong; and ≥ 0.80, very strong. The Wilcoxon and McNemar tests were used to compare quantitative and categorical biomarkers values and their dynamics. The diagnostic accuracy of biomarkers was determined by obtaining the largest possible area under the curve (AUC) in receiver operating characteristic curve (ROC) analysis. AUC values: ≥ 0.9 are considered "excellent"; ≥ 0.80, "good"; ≥ 0.7, "fair"; and < 0.70, "poor". Survival curves according to the cutoff values of NLR and PLR were estimated using the Kaplan-Meier method, and differences were assessed using the log-rank test. Hazard ratios (HRs) and 95 percent confidence intervals for univariate and multivariate models were computed with the use of Cox proportional-hazards regression models. Two-tailed *p*-values (< 0.05) were considered significant.

3. Results

3.1. Baseline characteristics

This study includes 119 patients who after failure of first line chemotherapy have received anti PD-1-treatment with pembrolizumab. The clinical characteristics of the patients are summarized in Table 1. The mean age was 62.3 ± 7.9 years - most of the patients were men (62.2%), with nonsquamous histology (57.1%) and all patients exhibited ECOG PS 1. Lung was the most common metastatic site (78.2%), followed by pleural effusion (60.5%) and bone (40.3%). All patients were eligible for the examination of the tumor PD-L1 expression, of which 10 patients (8.4%) had more than 50% expression, 55 patients (46.2%) – between 25-49% expression and 54 patients (45.4%) – between 1-24%. Of all clinical-pathological characteristics of the patients only the presence of bone metastases was significantly related to CBR – Table 1.

3.2. Relation between CBR and immunological biomarkers

Blood biomarker results before first cycle of chemotherapy and before first pembrolizumab infusion are given at Table 2. Patients without CB in both chemotherapy and immunotherapy groups were characterized by significantly higher Leu, ANC, ALC and APC as compared to patients with CB. However, only NLR and PLR2 were related with CBR (Table 2).

The Wilcoxon test showed that ALC and APC did not change significantly from chemotherapy. Still, Leu

Table 1. Relations between baseline clinical-pathological characteristics of patients and Clinical Benefit (CB)

Characteristics		Immunotherapy			Chemotherapy		
	General Population (*n* = 119)	Patients without CB (*n* = 44)	Patients with CB (*n* = 75)	*p* value	Patients without CB (*n* = 30)	Patients with CB (*n* = 89)	*p* value
Age	62.3 ± 7.9	62.6 ± 7.3	62.0 ± 8.1	0.55	61.3 ± 7.1	62.7 ± 8.1	0.27
Gender				0.20			0.77
Men, *n* (%)	74 (62.2)	24	50		18 (60)	56 (62.9)	
Women, *n* (%)	45 (37.8)	20	25		12 (40)	33 (37.1)	
BMI	1.82 ± 0.14	1.74 ± 0.12	1.78 ± 0.15	0.21	1.86 ± 0.13	1.81 ± 0.14	0.068
ECOG PS							0.28
0	0	0	0		3	116	
1	119	74	45		73	46	
Histology				0.99			0.62
Non-squamous	68 (57.1)	25 (56.8)	43 (56.7)		16 (53.3)	52 (58.4)	
Squamous	51 (42.9)	19 (43.2)	32 (43.3)		14 (46.7)	37 (41.6)	
PD-L1 expression (%)				0.52			0.29
100-50	10 (8.4)	5 (11.4)	5 (6.8)		1 (3.3)	9 (10.1)	
49-25	55 (46.2)	18 (40.9)	37 (50)		17 (56.7)	38 (42.7)	
24-1	54 (45.4)	21(47.7)	33 (43.2)		12 (40)	42 (47.2)	
Metastatic sites							
Lung, *n* (%)	93 (78.2)	36 (81.8)	57 (75.7)	0.43	24 (80)	69 (77.5)	0.77
Pleura, *n* (%)	72 (60.5)	28 (63.6)	44 (58.1)	0.55	21 (70)	51 (57.3)	0.21
Liver, *n* (%)	29 (24.4)	12 (27.3)	17 (21.6)	0.48	7 (23.3)	22 (24.7)	0.87
Adrenal glands, *n* (%)	20 (16.8)	9 (20.5)	11 (13.5)	0.32	5 (16.7)	15 (16.9)	0.97
Bone, *n* (%)	48 (40.3)	24 (54.5)	24 (31.3)	0.012	18 (60)	30 (33.7)	0.011

Table 2. Patients' blood biomarker values before chemotherapy and immunotherapy and Clinical Benefit (CB)

Biomarker	Just before 1st CT				Just before 1st Pembrolizumab			
	General Population	Patients without CB (*n* = 30)	Patients with CB (*n* = 89)	*p* value	General Population	Patients without CB (*n* = 44)	Patients with CB (*n* = 75)	*p* value
Leu, mean ± SD	9.4 ± 2.6	10.2 ± 2.5	8.8 ± 2.6	0.002	10.1 ± 3.6	11.4 ± 3.6	9.4 ± 3.5	0.003
ANC, mean ± SD	6.5 ± 2.47	7.4 ± 2.2	5.8 ± 2.4	< 0.001	7.2 ± 3.4	8.7 ± 3.1	6.2 ± 3.3	< 0.001
ALC, mean ± SD	1.62 ± 0.64	1.41 ± 0.59	1.75 ± 0.64	0.001	1.64 ± 0.67	1.37 ± 0.56	1.82 ± 0.68	< 0.001
APC, mean ± SD	313.1 ± 85.1	311.3 ± 84.1	312 ± 88.2	0.84	323.1 ± 102.3	356.8 ± 103.6	304.1 ± 97.3	0.004
NLR, *n* (%)				< 0.001				< 0.001
≤ 5	61(50.8)	10 (22.7)	51 (68.5)		57 (47.9)	8 (18.2)	49 (66.2)	
> 5	58 (49.2)	34 (77.3)	24 (31.5)		62 (52.1)	36 (81.8)	26 (33.8)	
PLR				0.46				< 0.001
High		13 (43.3)	45 (51.1)			32 (72.7)	27 (36.5)	
Low		17 (56.7)	44 (48.9)			12 (27.3)	48 (63.5)	

Table 3. Receiver operating curve (ROC) analysis, using Neutrophil to Lymphocyte Ratio (NLR), Platelet-Lymphocyte Ratio (PLR) and their dynamics to differentiate patients between patients with and without clinical benefit. Diagnostic accuracy of biomarkers was determined by obtaining the largest possible area under the curve (AUC) in ROC analysis

Items	Biomarker	AUC 95% CI	*p* value	Sensitivity (%)	Specificity (%)
Chemotherapy Group	NLR1	0.651 (0.54-0.76)	0.014	64.8	63.3
	PLR1	0.575 (0.45-0.69)	0.21	61.4	56.7
Immunotherapy Group	NLR2	0.75 (0.66-0.85)	< 0.001	77.0	61.4
	PLR2	0.72 (0.63-0.82)	< 0.001	75.7	63.6
	ΔNLR	0.64 (0.53-0.75)	0.013	63.5	61.4
	ΔPLR	0.65 (0.54-0.75)	0.009	64.9	59.1

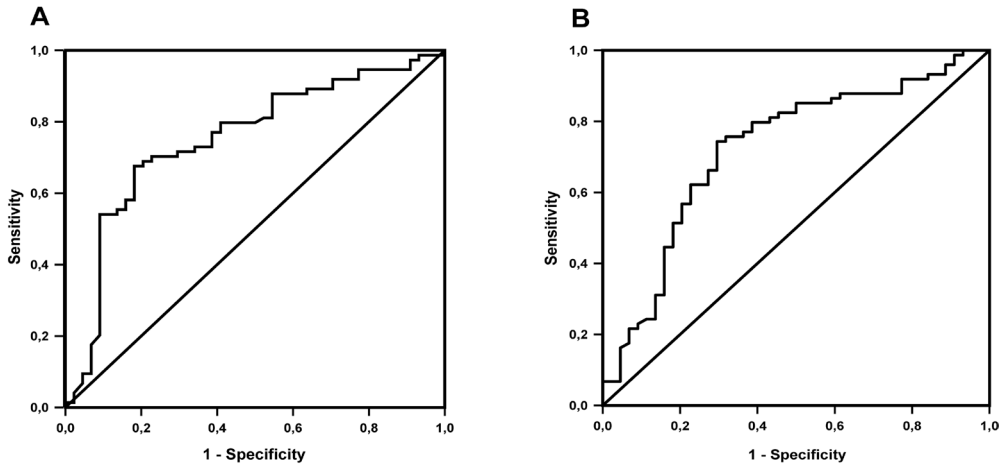

Figure 1. Receiver operating curve (ROC) analysis, using Neutrophil to Lymphocyte Ratio (NLR), Platelet-Lymphocyte Ratio (PLR) to differentiate between patients with and without clinical benefit. (A), NLR2; (B), PLR2.

and ANC significantly differ between the first cycle of chemotherapy and the first pembrolizumab infusion. The McNemar test showed that the proportion of patients with NLR > 5 and high PLR did not change significantly with chemotherapy treatment.

Significantly strong correlation was detected between NLR1 and PLR1 (rho = 0.737), NLR2 and PLR2 (rho = 0.774), and moderate correlation between Δ NLR and ΔPLR (rho = 0.494).

3.3. Immunological biomarkers and CBR

For the chemotherapy group CBR was 74.8%; for the immunotherapy group – 62.7%. ROC analysis was performed to explore the potential role of these biomarkers - NLR1, NLR2, PLR1, PLR2, ΔNLR, ΔPLR, as noninvasive ones for discrimination between patients with CB and without CB (Table 3). At the optimal cutoff values of the NLR1 and PLR1, only NLR1 could significantly, but poorly distinguish between patients with or without CB (AUC = 0.651, 95% CI: 0.54-0.76, p = 0.014) with a sensitivity of 64.8% and a specificity of 63.3%. In the immunotherapy group both biomarkers – NLR2 and PLR2, allowed significant but fair discrimination between patients with and without CB (Figure 1). NLR

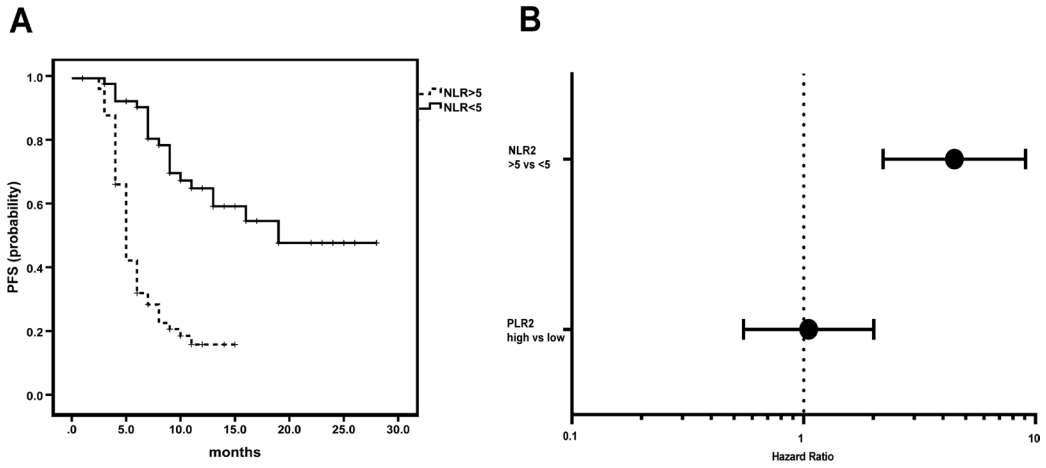

Figure 2. Kaplan-Maier estimates of progression free survival (PFS) in patients with NLR > 5 and NLR ≤ 5. (A), Patients with NLR > 5 showed significantly shorter mean PFS of 6.86 months (95% CI: 5.81-7.90) as compared to those with NLR ≤ 5 of 18.82 months (95% CI: 15.87-21.78) (long rank test $p < 0.001$); **(B)**, Forest plot showed progression-free survival across patients' subgroups. Hazard ratios are adjusted for gender, age, histology, PD-L1 expression, and ΔNLR and ΔPLR.

showed positive predictive value – 59% and negative predictive value – 86%. ΔNLR and ΔPLR could also discriminate between patients with and without CB, but poorly (Table 3).

Patients without CB had significantly higher values of ΔNLR (1.12 ± 2.2) and ΔPLR (49.6 ± 126.5) than patients with CB - ΔNLR (0.32 ± 1.95; $p = 0.013$) and ΔPLR (-7.7 ± 95.1; $p = 0.009$). The McNemar test showed that patients with CB differ between treatment with chemotherapy and immunotherapy ($p = 0.033$). Sixteen patients did not have clinical benefit either to chemotherapy, or to immunotherapy. They had significantly higher values of NLR (7.8 ± 2.08) and PLR (334.7 ± 91.9) than the rest of the patients (5.0 ± 3.4 and 221.4 ± 138.1). Twelve of them (75%) had bone metastasis.

3.4. Predictive and prognostic role of NLR and PLR in patients treated with pembrolizumab

Patients with NLR > 5 before immunotherapy showed significantly shorter mean PFS of 6.86 months (95% CI: 5.81-7.90) as compared to those with NLR ≤ 5 of 18.82 months (95% CI: 15.87-21.78) (long rank test $p < 0.001$) (Figure 2A). Patients with high PLR before immunotherapy showed also significantly shorter mean PFS of 11.01 months (95% CI: 8.46-13.57) as compared to those with low PLR of 15.96 months (95% CI: 13.08-18.84) (long rank test $p = 0.001$). Furthermore in the multivariate analysis, only NLR > 5 was an independent predictive factor for shorter PFS (HR: 4.47, 95% CI: 2.20-9.07, $p < 0.001$) (Table 4 and Figure 2B).

Patients with NLR > 5 had significantly shorter mean OS - 19.42 months (95% CI: 16.36-22.47) as compared to those with NLR ≤ 5 – 40.59 months (95% CI: 36.01-45.16) (log-rank test $p < 0.001$) (Figure 3A). Patients with high PLR had also shorter mean OS of 22.05 months (95% CI: 18.23-25.87) compared to patients with low PLR – 38.47 months (95% CI: 33.67-43.27) (long rank test $p < 0.001$) (Figure 3B). In univariate analysis squamous histology, presence of bone metastases, NLR > 5 and high PLR before chemo and immunotherapy, high RDW before chemotherapy, ΔNLR ≥ 25% and ΔPLR ≥ 25% were associated with worse OS. In multivariate analysis, however only presence of bone metastases (HR: 2.08, 95% CI: 1.10-4.94, $p = 0.030$), NLR > 5 before chemotherapy (HR: 8.09, 95% CI: 2.35-27.81, $p = 0.001$) and high PLR before chemotherapy (HR: 2.81, 95% CI: 1.13-6.97, $p = 0.025$) remained independent negative prognostic factors for poor OS (Table 5 and Figure 3D).

Table 4. Multivariate Cox regression analysis for predicting progression free survival

Marker	HR[a]-adjusted	95% CI	*p* value
NLR: > 5 *vs*. ≤ 5	4.47	2.20-9.07	< 0.001
PLR: High *vs*. Low	1.05	0.55-2.01	0.86

[a]Adjusted for gender, age, histology, PD-L1 expression, and ΔNLR and ΔPLR

4. Discussion

The current study found that patients with NLR > 5 had significantly shorter OS and PFS. Our study suggests that the proportion of patients with NLR > 5 and high PLR did not change significantly as a result of chemotherapy treatment and that NLR has an independent predictive value in NSCLC patients, treated with pembrolizumab as a second-line therapy. Patients with NLR > 5 had a lower chance to receive clinical benefit from immunotherapy. Furthermore, we demonstrated the negative prognostic role of high

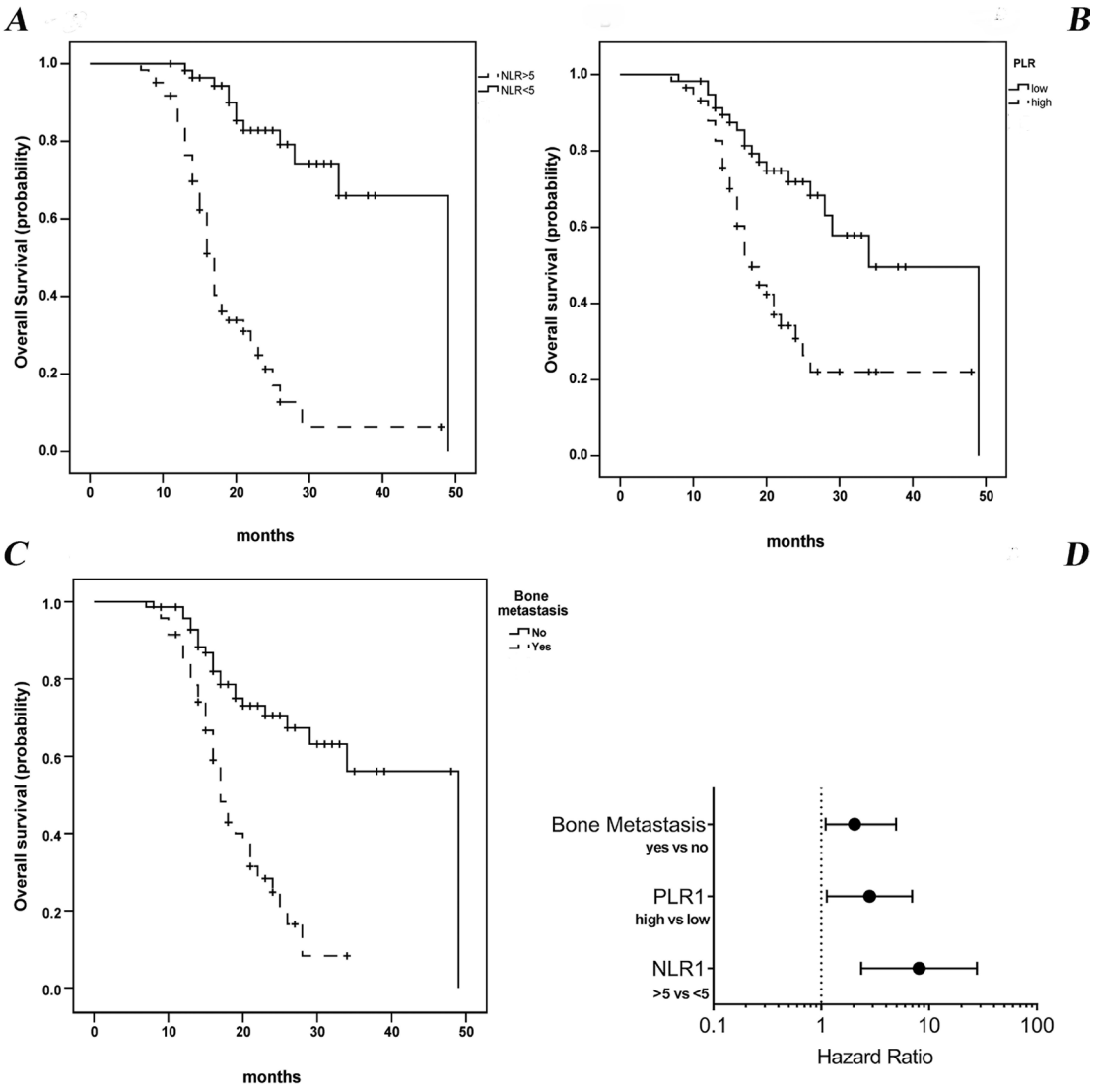

Figure 3. Kaplan-Maier estimates of overall survival (OS). (A), Patients with NLR > 5 had significantly shorter mean OS - 19.42 months (95% CI: 16.36-22.47) as compared to those with NLR ≤ 5 – 40.59 months (95% CI: 36.01-45.16) (log-rank test $p < 0.001$); **(B)**, Patients with high PLR had shorter mean OS of 22.05 months (95% CI: 18.23-25.87) compared to patients with low PLR – 38.47 months (95% CI: 33.67-43.27) (long rank test $p < 0.001$); **(C)**, Patients with bone metastasis had shorter mean OS of 19.24 months (95% CI: 17.01-21.45) compared to patients without bone metastasis – 36.60 months (95% CI: 32.12-41.07) (long rank test $p < 0.001$); **(D)**, Forest plot showed overall survival across patients' subgroups.

Table 5. Cox regression analysis for predicting overall survival

Variable	Univariate analysis		Multivariate analysis	
	HR (95% CI)	*p* value	HR (95% CI)	*p* value
Age	1.015 (0.98-1.05)	0.39		
Gender: Female vs. Male	0.79 (0.46-1.38)	0.42		
Smoking: Yes vs. No	0.57 (0.29-1.11)	0.10		
Histology: Non-squamous vs. Squamous	0.49 (0.28-0.83)	0.009		
PD-L1 expression: ≥ 50% vs. < 50%	0.92 (0.36-2.33)	0.87		
Bone metastasis: Yes vs. No	2.28 (2.09-6.43)	< 0.001	2.08 (1.10-4.94)	0.030
Just before CT				
NLR1: > 5 vs. ≤ 5	8.56 (4.34-16.93)	< 0.001	8.09 (2.35-27.81)	0.001
PLR1: High vs. Low	2.89 (1.63-5.15)	< 0.001	2.81 (1.13-6.97)	0.025
RDW: High vs. Low	1.831 (1.048-3.197)	0.034		
Just before Immunotherapy				
NLR2: > 5 vs. ≤ 5	7.94 (3.99-15.78)	< 0.001		
PLR2: High vs. Low	5.08 (2.72-9.50)	< 0.001		
ΔNLR: ≥ 25% vs. < 25%	2.27 (1.32-3.89)	0.003		
ΔPLR: ≥ 25% vs. < 25%	1.83 (1.06-3.20)	0.031		

pre-treatment PLR and presence of bone metastasis in NSCLC patients treated with pembrolizumab.

Until now, many research studies have examined and evaluated the predictive and prognostic value of blood NLR and PLR in patients with various solid tumors, who received immune checkpoints inhibitors (*20,21*). The retrospective review of a recent phase 1 clinical trial reported that high baseline NLR and PLR values were linked significantly with worse OS and PFS in 90 advanced-stage cancer patients, who received treatment on an immunotherapy-based regimen (*20*). In addition, an increase in NLR and PLR values 6 weeks after baseline was associated with shorter OS and PFS.

In conjunction with other studies, our results further support the evidence that NLR (member of the markers of systemic inflammation) may predict poor response to checkpoint inhibitors and poor outcome in patients with NSCLC (*16,22,23*). However, no direct relation was found between distinct NLR cutoff values and PFS benefit (*6*). In the subsequent analysis of NLR cutoff values and OS/PFS benefit, it turned out that higher NLR cutoff was linked to a lower chance of OS benefit. Another study reports that higher cutoff value was linked with worse PFS (*24*). This suggests that the relation between NLR and prognosis could be gradual rather than a threshold one.

Recent studies report that blood neutrophils, identified by the NLR were directly linked with the number of intratumoral neutrophil populations, which may have the potential to compromise the antitumor immune response (*25,26*). Lower counts of lymphocytes usually reflect an impairment of cell-mediated immunity. It has been shown that increased infiltration of lymphocytes in the tumor region is associated with better responsiveness to treatment and prognosis in patients with solid tumors (*27*). Usually neutrophilia represents a response to systematic inflammation (*28*).

Although the biological foundation for these findings requires further elucidation, a number of recent research studies provide some explanations that should be strongly considered. It has been established that neutrophils and platelets play an important role in the development and progression of tumors as well as metastases, either by exercising a direct effect on tumor cells or by indirectly affecting other components of the tumor microenvironment. This effect is achieved through the secretion and release of various chemokines and cytokines, including transforming growth factor-beta, vascular endothelial growth factor, IL-6, IL-8 and matrix metalloproteinases (*29,30*). In addition, the latest findings of a study demonstrate that there is an association between a higher neutrophil count and decreased CD8+ content in lung cancer tumor cells (*31*), identifying neutrophilia as an inflammatory response, which suppress the antitumor immune response through inhibition of the cytotoxic activity of immune cells, in particular, that of activated CD8+T cells. Consequently, this may lower the chance of response to immunotherapy.

Consistent with the results of other research studies, we found that high PLR and presence of bone metastasis, which are common in patients with advanced NSCLC, are associated with shorter survival (*32-34*).

Several limitations were identified in our study. First of all, our study is retrospective and has a relatively small sample size. Moreover, the predictive value of NLR was not compared to new predictive markers like tumor mutational burden or microsatellite instability.

Despite these limitations, the results suggest that patients with NLR > 5 are at high risk for early progression and short overall survival. This may be helpful to clinicians in their choice of treatment, especially for patients with high pretreatment NLR - perhaps a combination of chemotherapy and immunotherapy or new molecules in clinical trials. Drugs, which are capable of transforming neutrophils into a functional state with antitumor activity, are needed in order to improve patients' outcome.

References

1. Torre LA, Siegel RL, Ward EM, Jemal A. Global cancer incidence and mortality rates and trends--An update. Cancer Epidemiol Biomarkers Prev. 2016; 25:16-27.
2. Nixon NA, Blais N, Ernst S, Kollmannsberger C, Bebb G, Butler M, Smylie M, Verma S. Current landscape of immunotherapy in the treatment of solid tumours, with future opportunities and challenges. Curr Oncol. 2018; 25:e373-e384.
3. Prabhash K. Treatment of advanced nonsmall cell lung cancer: First line, maintenance and second line - Indian consensus statement update. South Asian J Cancer. 2019; 8:1-17.
4. Wu YL, Planchard D, Lu S, *et al*. Pan-Asian adapted Clinical Practice Guidelines for the management of patients with metastatic non-small-cell lung cancer: a CSCO-ESMO initiative endorsed by JSMO, KSMO, MOS, SSO and TOS. Ann Oncol. 2019; 30:171-210.
5. Herbst RS, Baas P, Kim DW, *et al*. Pembrolizumab versus docetaxel for previously treated, PD-L1-positive, advanced non-small-cell lung cancer (KEYNOTE-010): a randomised controlled trial. Lancet. 2016; 387:1540-1550.
6. Jiang T, Bai Y, Zhou F, Li W, Gao G, Su C, Ren S, Chen X, Zhou C. Clinical value of neutrophil-to-lymphocyte ratio in patients with non-small-cell lung cancer treated with PD-1/PD-L1 inhibitors. Lung Cancer. 2019; 130:76-83.
7. Rizvi NA, Hellmann MD, Snyder A, *et al*. Cancer immunology. Mutational landscape determines sensitivity to PD-1 blockade in non-small cell lung cancer. Science. 2015; 348:124-128.
8. Vokes EE, Ready N, Felip E, *et al*. Nivolumab versus docetaxel in previously treated advanced non-small-cell lung cancer (CheckMate 017 and CheckMate 057): 3-year update and outcomes in patients with liver metastases. Ann Oncol. 2018; 29:959-965.
9. Reck M, Rodriguez-Abreu D, Robinson AG, *et al*. Updated Analysis of KEYNOTE-024: Pembrolizumab

Versus Platinum-Based Chemotherapy for Advanced Non-Small-Cell Lung Cancer With PD-L1 Tumor Proportion Score of 50% or Greater. J Clin Oncol. 2019; 37:537-546.
10. Meng X, Huang Z, Teng F, Xing L, Yu J. Predictive biomarkers in PD-1/PD-L1 checkpoint blockade immunotherapy. Cancer Treat Rev. 2015; 41:868-876.
11. Diakos CI, Charles KA, McMillan DC, Clarke SJ. Cancer-related inflammation and treatment effectiveness. Lancet Oncol. 2014; 15:e493-503.
12. Tao H, Mimura Y, Aoe K, Kobayashi S, Yamamoto H, Matsuda E, Okabe K, Matsumoto T, Sugi K, Ueoka H. Prognostic potential of FOXP3 expression in non-small cell lung cancer cells combined with tumor-infiltrating regulatory T cells. Lung Cancer. 2012; 75:95-101.
13. Proctor MJ, McMillan DC, Morrison DS, Fletcher CD, Horgan PG, Clarke SJ. A derived neutrophil to lymphocyte ratio predicts survival in patients with cancer. Br J Cancer. 2012; 107:695-699.
14. Templeton AJ, McNamara MG, Seruga B, Vera-Badillo FE, Aneja P, Ocana A, Leibowitz-Amit R, Sonpavde G, Knox JJ, Tran B, Tannock IF, Amir E. Prognostic role of neutrophil-to-lymphocyte ratio in solid tumors: a systematic review and meta-analysis. J Nat Cancer Inst. 2014; 106:dju124.
15. Park W, Kwon D, Saravia D, *et al*. Developing a Predictive Model for Clinical Outcomes of Advanced Non-Small Cell Lung Cancer Patients Treated With Nivolumab. Clin Lung cancer. 2018; 19:280-288. e4.
16. Diem S, Schmid S, Krapf M, Flatz L, Born D, Jochum W, Templeton AJ, Fruh M. Neutrophil-to-Lymphocyte ratio (NLR) and Platelet-to-Lymphocyte ratio (PLR) as prognostic markers in patients with non-small cell lung cancer (NSCLC) treated with nivolumab. Lung Cancer. 2017; 111:176-181.
17. Russo A, Franchina T, Ricciardi GRR, Battaglia A, Scimone A, Berenato R, Giordano A, Adamo V. Baseline neutrophilia, derived neutrophil-to-lymphocyte ratio (dNLR), platelet-to-lymphocyte ratio (PLR), and outcome in non small cell lung cancer (NSCLC) treated with Nivolumab or Docetaxel. J Cell Physiol. 2018; 233:6337-6343.
18. Bagley SJ, Kothari S, Aggarwal C, *et al*. Pretreatment neutrophil-to-lymphocyte ratio as a marker of outcomes in nivolumab-treated patients with advanced non-small-cell lung cancer. Lung Cancer. 2017; 106:1-7.
19. Cedres S, Torrejon D, Martinez A, Martinez P, Navarro A, Zamora E, Mulet-Margalef N, Felip E. Neutrophil to lymphocyte ratio (NLR) as an indicator of poor prognosis in stage IV non-small cell lung cancer. Clin Transl Oncol. 2012; 14:864-869.
20. Bilen MA, Martini DJ, Liu Y, *et al*. The prognostic and predictive impact of inflammatory biomarkers in patients who have advanced-stage cancer treated with immunotherapy. Cancer. 2019; 125:127-134.
21. Capone M, Giannarelli D, Mallardo D, Madonna G, Festino L, Grimaldi AM, Vanella V, Simeone E, Paone M, Palmieri G, Cavalcanti E, Caraco C, Ascierto PA. Baseline neutrophil-to-lymphocyte ratio (NLR) and derived NLR could predict overall survival in patients with advanced melanoma treated with nivolumab. J Immunother Cancer. 2018; 6:74.
22. Ren F, Zhao T, Liu B, Pan L. Neutrophil-lymphocyte ratio (NLR) predicted prognosis for advanced non-small-cell lung cancer (NSCLC) patients who received immune checkpoint blockade (ICB). Onco Targets Ther. 2019; 12:4235-4244.
23. Passiglia F, Galvano A, Castiglia M, Incorvaia L, Calo V, Listi A, Mazzarisi S, Perez A, Gallina G, Rizzo S, Soto Parra H, Bazan V, Russo A. Monitoring blood biomarkers to predict nivolumab effectiveness in NSCLC patients. Ther Adv Med Oncol. 2019; 11:1758835919839928.
24. Mei Z, Shi L, Wang B, Yang J, Xiao Z, Du P, Wang Q, Yang W. Prognostic role of pretreatment blood neutrophil-to-lymphocyte ratio in advanced cancer survivors: A systematic review and meta-analysis of 66 cohort studies. Cancer Treat Rev. 2017; 58:1-13.
25. Moses K, Brandau S. Human neutrophils: Their role in cancer and relation to myeloid-derived suppressor cells. Semin Immunol. 2016; 28:187-196.
26. Dumitru CA, Lang S, Brandau S. Modulation of neutrophil granulocytes in the tumor microenvironment: mechanisms and consequences for tumor progression. Semin Cancer Biol. 2013; 23:141-148.
27. Gooden MJ, de Bock GH, Leffers N, Daemen T, Nijman HW. The prognostic influence of tumour-infiltrating lymphocytes in cancer: a systematic review with meta-analysis. Br J Cancer. 2011; 105:93-103.
28. Grivennikov SI, Greten FR, Karin M. Immunity, inflammation, and cancer. Cell. 2010; 140:883-899.
29. Klinger MH, Jelkmann W. Role of blood platelets in infection and inflammation. J Interferon Cytokine Res. 2002; 22:913-922.
30. Treffers LW, Hiemstra IH, Kuijpers TW, van den Berg TK, Matlung HL. Neutrophils in cancer. Immunol Rev. 2016; 273:312-328.
31. Kargl J, Busch SE, Yang GH, Kim KH, Hanke ML, Metz HE, Hubbard JJ, Lee SM, Madtes DK, McIntosh MW, Houghton AM. Neutrophils dominate the immune cell composition in non-small cell lung cancer. Nat Commun. 2017; 8:14381.
32. Kuchuk M, Kuchuk I, Sabri E, Hutton B, Clemons M, Wheatley-Price P. The incidence and clinical impact of bone metastases in non-small cell lung cancer. Lung Cancer. 2015; 89:197-202.
33. Liu W, Wu J. Lung cancer with bone metastases in the United States: an analysis from the Surveillance, Epidemiologic, and End Results database. Clin Exp Metastasis. 2018; 35:753-761.
34. Gu X, Sun S, Gao XS, Xiong W, Qin S, Qi X, Ma M, Li X, Zhou D, Wang W, Yu H. Prognostic value of platelet to lymphocyte ratio in non-small cell lung cancer: evidence from 3,430 patients. Sci Rep. 2016; 6:23893.

Received October 12, 2019; Revised January 7, 2020; Accepted January 21, 2020.

**Address correspondence to:*
Ivan Shterev Donev, Clinic of Medical Oncology, MHAT "Nadezhda", "Blaga Vest" 3 str., Sofia 1000, Bulgaria.
E-mail: ivan_donev75@abv.bg

Released online in J-STAGE as advance publication February 4, 2020.

Original Article

DOI: 10.5582/bst.2019.01329

Technical details of and prognosis for the "China stitch", a novel technique for totally laparoscopic hand-sewn esophagojejunostomy

Zhipeng Sun[§], Xuejing Zheng[§], Guanyang Chen, Liang Wang, Qing Sang, Guangzhong Xu, Nengwei Zhang[*], Aminbuhe[*]

Oncology Surgery Department, Beijing Shijitan Hospital, Capital Medical University (Peking University Ninth School of Clinical Medicine), Beijing, China.

SUMMARY The current study describes the technical details of and the clinical prognosis for the "China stitch", a novel technique for hand-sewn esophagojejunostomy in totally laparoscopic total gastrectomy. This study also explores the feasibility and safety of the technique. Clinical data of 20 patients with esophagogastric junction cancer in Beijing Shijitan Hospital, Capital Medical University from January 2017 to April 2018 were retrospectively analyzed. All 20 patients underwent esophagojejunostomy via a novel hand-sewn technique that uses traction to turn the left or right wall of the esophagus into an anterior wall. This avoids the difficulty of suturing the posterior wall. All patients were followed until June 2019. All 20 patients successfully underwent the procedure. The mean operating time was 216.5 ± 24.9 (176-254) min, the mean hand-sewn reconstruction time was 44.4 ± 9.4 (26-61) min, intraoperative bleeding was 141.2 ± 24.9 (130-160) mL, and the number of resected lymph nodes was 23 ± 8 (14-33). After surgery, there was one case of anastomotic leakage and one case of anastomotic stenosis, but both were alleviated with conservative treatment. The mean duration of follow-up was 15 (4-33) months. There was no significant difference in postoperative complications of and short-term oncologic prognosis for the 20 patients who underwent hand-sewn esophagojejunostomy and the 21 patients who underwent mechanical esophagojejunostomy during the same period. In conclusion, the "China stitch", a novel hand-sewn technique, is a cost-effective, safe, and reliable method for esophagojejunostomy in totally laparoscopic total gastrectomy.

Keywords hand-sewn esophagojejunostomy, laparoscopic total gastrectomy, gastric cancer

1. Introduction

Laparoscopic total gastrectomy (LTG) is considered to be an effective option for treatment of esophagogastric junction (EGJ) cancer. LTG involves laparoscopic lymph node dissection and digestive tract reconstruction via open surgery. During totally laparoscopic total gastrectomy (TLTG), however, the entire surgery (including lymph node dissection and digestive tract reconstruction) is performed laparoscopically; an incision is made only to collect specimens, resulting in a smaller incision and a faster recovery.

Recent studies have indicated that TLTG is safe, feasible, and minimally invasive (*1,2*). However, the technique for laparoscopic esophagojejunostomy remains a major challenge. esophagojejunostomy is usually performed mechanically; techniques include end-to-side anastomosis using a traditional circular stapler, end-to-side anastomosis using a trans-orally inserted stapler anvil (OrVil™) (*3*), and side-to-side anastomosis using a linear stapler (*4*). However, these techniques still have many flaws such as the difficulty of placing anvil in esophageal stump laparoscopically, an unconfirmed resection margin, and expense (*5*). Recent studies have cited several flaws of hand-sewn esophagojejunostomy, including the difficulty of suturing the posterior wall due to technical complexity and the high level of suture skill (*6,7*).

In light of these circumstances, the current authors devised a novel suture technique for laparoscopic hand-sewn esophagojejunostomy. This technique can avoid the difficulty of suturing the posterior wall through an optimized procedure.

2. Materials and Methods

2.1. Patients

Potential subjects were patients diagnosed with Siewert II or Siewert III EGJ cancer who underwent TLTG

using the novel "China stitch" technique for hand-sewn esophagojejunostomy by the same surgeon at Beijing Shijitan Hospital from January 2017 to April 2018. Subjects were 20 patients who provided informed consent. The patients had an average age of 59 (45-89) years; 65% (13/20) of them were male. The control group consisted of patients who underwent TLTG with using mechanical esophagojejunostomy during the same period.

All patients underwent routine preoperative examinations, gastroscopy, endoscopic ultrasonography, and chest, abdomen, and pelvis CT scans to determine the clinical stage and pathological type. Patients who had distant metastases or peripheral tissue invasion were excluded. Of 20 patients in total, 2 had Siewert II EGJ cancer and 18 had Siewert III EGJ cancer. There were no significant differences in the preoperative baseline data for the hand-sewn esophagojejunostomy group and the control group (Table 1).

This study was approved by the Ethics Committee of Beijing Shijitan Hospital. All patients provided written informed consent for participation in this study.

2.2. Protocol

2.2.1. Procedure

The 20 patients underwent TLTG and esophagojejunostomy using the novel "China stitch" technique for laparoscopic hand-sewn esophagojejunostomy.

2.2.2. Body position

Patients were placed in the supine position under endotracheal intubation and general anesthesia. The surgeon stood on the patient's right side, the first assistant on his left side, and the laparoscopic assistant between his legs.

2.2.3. Placement of trocars

After establishing pneumoperitoneum, the first 10-mm trocar was inserted below the umbilicus, and a 12-mm trocar and three 5-mm trocars were inserted into the right abdomen, right upper abdomen, and left abdomen, respectively. Carbon dioxide pneumoperitoneum was set at 12-15 mmHg.

2.2.4. Total gastrectomy

Laparoscopic total gastrectomy was performed depending on the TNM stage preoperatively, followed by lymph node dissection. Surgery was standardized in accordance with the Guidelines for Laparoscopic Gastrectomy for Gastric Cancer (2016) of the Chinese Society of Surgery, Chinese Medical Association (*8*).

Table 1. Patient characteristics.

Variables	China stitch group (n = 20)	Mechanical suturing group (n = 21)	P value
Age (y, mean ± SD)	59.0 ± 8.9	58.4 ± 7.7	0.799
Gender (n)			
Male	13	15	0.986
Female	7	6	0.875
BMI (kg/m^2, mean ± SD)	24.5 ± 2.5	23.9 ± 3.7	0.646
Siewert Classification			
Type II	2	2	0.956
Type III	18	19	0.921
ECOG score, n (%)			
0	14	15	0.943
1	4	5	0.936
2	2	1	0.867
Comorbidity, n (%)			
Hypertension	8	6	0.248
Diabetes mellitus	1	3	0.687
Cardiac disease	1	2	0.587
Pulmonary disease	1	0	0.536
Hepatic disease	2	1	0.687
Renal disease	0	1	0.432
Tumor location, n			
EGJ	16	18	0.777
Non-EGJ	4	3	
Tumor size (cm, mean ± SD)	4.8 ± 2.0	4.6 ± 1.8	0.761
Tumor stage*			
I	0	2	0.163
II	4	3	0.458
III	14	15	0.421
IV	2	1	0.687

EGJ = Esophagogastric junction. * Seventh edition of the Union for International Cancer Control TNM classification.

2.2.5. The "China Stitch", a novel technique for laparoscopic hand-sewn esophagojejunostomy (Video 1, *https://pan.baidu.com/s/1o3zl3AC8AACVsko6ne9B9Q* Serial number: kkr2).

After specimen collection, the esophageal stump was removed by ultrasonic scalpel and taken as biopsy for frozen-section examination.

The jejunum was disconnected 15 cm distal from Treitz's ligament using the Endo-GIA stapler, the mesentery was freed, and then the distal jejunum was elevated to the esophageal hiatus above the colon.

If the resection margins were positive, the distal esophagus was resected for frozen-section examination again. Once a negative resection margin was confirmed, an end-to-side esophagojejunostomy was performed.

1) Prepare an anastomotic stoma on the jejunal side. Make a 3-cm incision 2 cm away from the jejunal stump, and dissect the seromuscular layer. Lift the mucous membrane from the seromuscular layer, and then remove the mucous membrane (Figure 1).

2) Place one suture on the center of the posterior wall of the esophagus and the center of the posterior wall of the jejunum using 3-0 absorbable suture, tie a knot, and fix the suture as a traction suture.

3) Place one suture on the center of the anterior wall of the esophagus and the center of the anterior wall of the jejunum using 3-0 absorbable suture, tie a knot, and fix the suture as a traction suture (Figure 2).

4) The assistant pulls the traction sutures outwards and turns the left wall of the anastomotic stoma into the anterior wall. Place a continuous full-thickness suture on the "anterior wall" using the right traction suture. Place 6 sutures in total about 1 cm apart, and tie a knot with the left traction suture.

5) The assistant switches to the other traction suture. The assistant pulls outwards, turning the right wall of the anastomotic stoma into an anterior wall. Place a continuous full-thickness suture on the "anterior wall" using the right traction suture. Place 6 sutures in total about 1 cm apart, and tie a knot with the left traction suture. With this, full-thickness suturing of the esophagus and jejunum is finished (Figure 3).

6) Use horizontal mattress sutures to continue suturing the seromuscular layer of the "anterior wall" with the right traction suture.

7) The assistant switches to the other traction suture. The assistant pulls outwards again, turning the left wall of the anastomotic stoma into an anterior wall. Use single horizontal mattress sutures to suture the seromuscular layer of the "anterior wall" with the right traction suture. Once done, suturing of the seromuscular layer for anastomosis is done (Figure 4).

Afterwards, completed Roux-en-Y digestive tract reconstruction using the Endo-GIA stapler, performed side-to-side jejunojejunostomy at the choledochopancreatic branch of the proximal jejunum 50 cm away from the esophagogastric anastomotic stroma, and closed the joint opening. Lastly, closed the mesenteric hiatus of the small intestine.

2.2.6. Postoperative X-ray radiography

Each patient underwent gastrointestinal radiography on the second or third day post-operatively. Each patient started drinking water after that and started eating the next day.

2.2.7. Follow-up

All patients underwent follow-up on an outpatient basis or by phone until June 2019. The follow-up included the patient's oncologic prognosis and gastroscopy, abdominal CT, tumor markers, and laboratory results. The follow-up also included changes in body weight, nutritional status, eating patterns, and the frequency of meals, the occurrence of dysphagia, and the occurrence of a burning sensation over the sternum and its severity.

3. Results

3.1. Surgery details

The 20 patients underwent esophagojejunostomy via the "China stitch" and TLTG. The operating time was 216.5 ± 24.9 (176-254) min, intracorporeal suturing time was 44.4 ± 9.4 (26-41) min, intraoperative bleeding was 141.2 ± 24.9 (130-160) mL, and the number of resected lymph nodes was 23 ± 8 (14-33). Patients who underwent hand-sewn esophagojejunostomy did not differ significantly from those who underwent conventional mechanical esophagojejunostomy (Table 2).

3.2. Postoperative details

Postoperative routine gastrointestinal imaging revealed a case of anastomotic leakage, and a case of anastomotic stenosis was found about 6 months postoperatively, but there were no cases of postoperative hemorrhaging. The patient with anastomotic leakage underwent hand-sewn esophagojejunostomy since mechanical esophagojejunostomy failed. As a result, the blood supply to the anastomotic stoma was relatively poor. A drainage tube was inserted across the anastomotic stoma. Postoperative drainage was adequate without any signs of infection. After a month of conservative treatment, the drainage tube was gradually removed and the patient was discharged (Figure 5). The patient with anastomotic stenosis had a high anastomotic stoma; the upper margin of the neoplasm was 1 cm above the Z-line, and the resection line was about 4 cm above the Z-line. Therefore, the anastomotic stoma was under considerable tension. The patient experienced

Figure 1. Prepare an anastomotic stoma on the jejunal side. A. Make a 3-cm incision 2 cm away from the jejunal stump, and dissect the seromuscular layer. Lift the mucous membrane from the seromuscular layer. **B**. Remove the mucous membrane. **C**. Diagram of dissection of the seromuscular layer and removal of the mucous membrane.

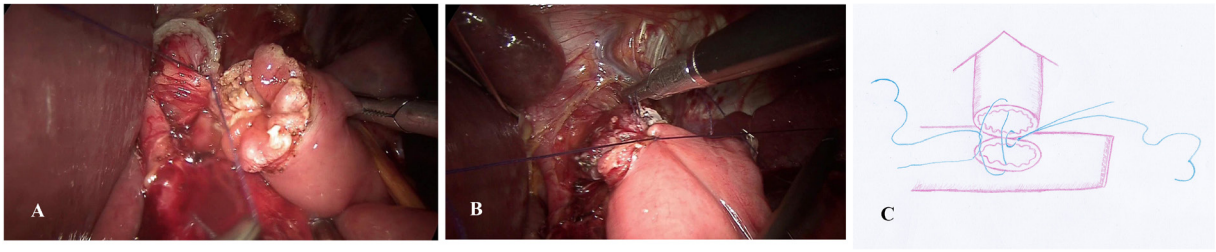

Figure 2. Place a fixation suture on the anterior and posterior walls. A. Place one suture on the center of the posterior wall of the esophagus and the center of the posterior wall of the jejunal stoma using 3-0 absorbable suture, tie a knot, and fix the suture as a traction suture. Remove the stump of the esophagus and perform a rapid frozen section pathological examination. **B**. Place one suture on the center of the anterior wall of the esophagus and the center of the anterior wall of the jejunum using 3-0 absorbable suture, tie a knot, and fix the suture as another traction suture. **C**. Diagram of the fixation sutures on the anterior and posterior walls.

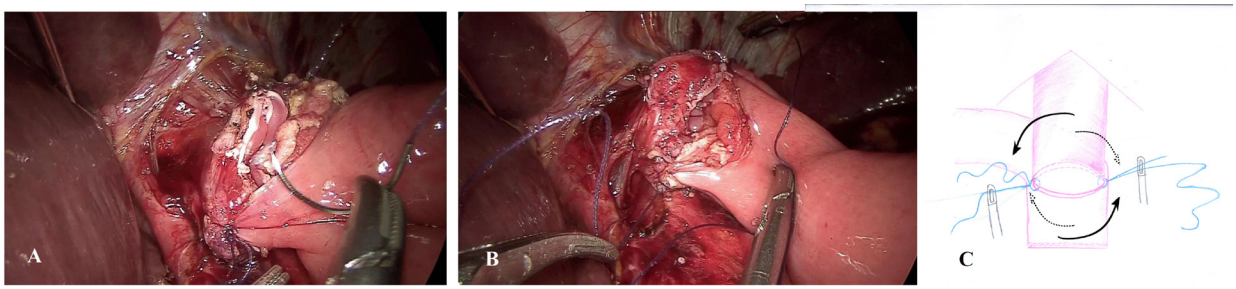

Figure 3. Esophagojejunostomy with full-thickness sutures all in the anterior wall. A. The assistant pulls the traction suture outwards and turns the left wall of the anastomotic stoma into an anterior wall. Place a continuous full-thickness suture on the "anterior wall" using the right traction suture; place 6 sutures in total, and tie a knot with the left traction suture. **B**. The assistant switches to the other traction suture. The assistant pulls outwards, turning the right wall of the anastomotic stoma into an anterior wall. Place a continuous full-thickness suture on the "anterior wall" using the right traction suture. Place 6 sutures in total about 1 cm apart, and tie a knot with the left traction suture. With this, full-thickness suturing of the esophagus and jejunum is finished. **C**. Diagram of esophagojejunostomy with full-thickness sutures all in the anterior wall. The solid line is the direction of pull that rotates the stoma 90 degrees, turning the left wall of the esophagus into an anterior wall. The dashed line is the direction of pull to turn the right wall of the esophagus into an anterior wall.

Table 2. Surgical outcomes

Variables	China stitch group (n = 20)	Mechanical suturing group (n = 21)	P value
Lymphadenectomy			
D2 + no. 10	3	2	0.556
D2	17	19	0.716
Lymph nodes acquired	23 ± 8	24 ± 7	0.842
Total operating time (min, mean ± SD)	216.5 ± 24.9	203.2 ± 30.5	0.344
Reconstruction (min, mean ± SD)	44.4 ± 9.4	40.1 ± 5.4	0.012
Estimated blood loss (ml, mean ± SD)	141.2 ± 24.9	138.8 ± 79.9	0.934
Incision length (cm, mean ± SD)	6.6 ± 0.4	7.2 ± 1.7	0.125
Proximal margin (mm, mean ± SD)	30.6 ± 16.4	28.0 ± 19.4	0.611
Time to first ambulation (d, mean ± SD)	2.6 ± 0.8	3.0 ± 1.7	0.344
Time to first flatus (d, mean ± SD)	3.1 ± 0.8	3.2 ± 0.7	0.827
Time to resumption of liquids (d, mean ± SD)	3.1 ± 0.9	3.3 ± 1.5	0.209
Time to first liquid meal (d, mean ± SD)	4.2 ± 1.2	4.8 ± 2.8	0.650
Time to first soft meal (d, mean ± SD)	5.9 ± 2.0	6.5 ± 2.8	0.396
Postoperative hospitalization (d, mean ± SD)	8.8 ± 5.0	9.6 ± 3.9	0.042

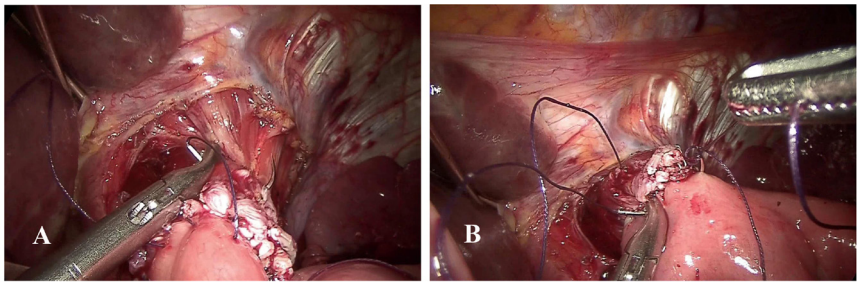

Figure 4. Esophagojejunostomy with suturing of the seromuscular layer all in the anterior wall. A. The seromuscular layer of the "anterior wall" is sutured with horizontal mattress sutures using the traction suture on the right. **B**. The assistant switches to the other traction suture. The assistant pulls outwards again, turning the right wall of the anastomotic stoma into an anterior wall. The seromuscular layer of the "anterior wall" is sutured with single horizontal mattress sutures using the traction suture on the right. Once done, suturing of the seromuscular layer is finished.

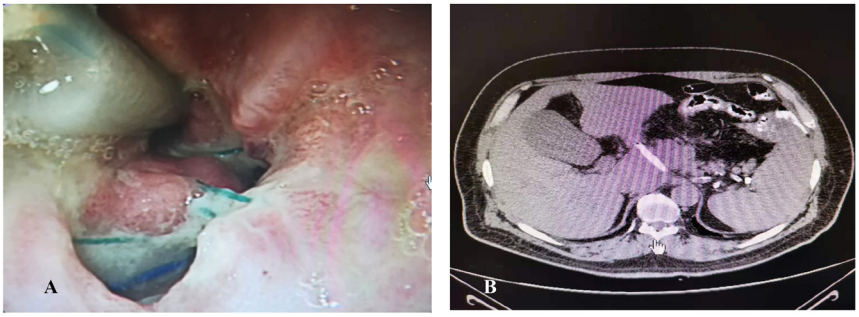

Figure 5. Imaging study of a patient suffering from anastomotic leakage. A. Gastroscopy revealed that the drainage tube crossed the anastomotic stoma. **B**. A CT scan indicated that the anastomotic stoma was draining adequately. There was no fluid accumulation around the anastomotic stoma.

Figure 6. Imaging study of a patient suffering from anastomotic stenosis. A. Anastomotic stenosis was evident during gastroscopy since the gastroscope could not pass. **B**. A balloon expander was used to dilate the anastomotic stoma during gastroscopy. **C**. The anastomotic stoma after balloon dilatation.

dysphagia symptoms 6 months postoperatively, and examinations revealed anastomotic stenosis. This was alleviated using endoscopic dilatation (Figure 6).

The patients' first passage of gas via the anus occurred at 2.6 ± 0.8 days (1-3) postoperatively, first liquid intake occurred 3.1 ± 0.8 (3-6) days postoperatively, and the first intake of semi-liquid food occurred 4.2 ± 1.2 (4-8) days postoperatively. The mean duration of postoperative hospitalization was 8.8 ± 5.0 (9-13) days. Patients who underwent hand-sewn esophagojejunostomy did not differ from those who underwent conventional mechanical esophagojejunostomy in terms of complications during or after surgery. The mean follow-up was 15 (4-33) months (Table 3).

4. Discussion

During most total gastrectomies, digestive tract reconstruction is still performed laparoscope-assisted, but total laparoscopic total gastrectomy has developed rapidly over the past 10 years (*9*). Due to its technical complexity, total laparoscopic esophagojejunostomy has always been a major challenge in TLTG (*10*). Currently there are no standard procedures for intracorporeal esophagojejunostomy.

For a laparoscopic esophagojejunostomy, side-to-end anastomosis can be performed with a circular stapler or side-to-side anastomosis can be performed with an Endo-GIA stapler, followed by suturing of the joint opening or

Table 3. Comparison of complications

Variables	China stitch group (n = 20)	Mechanical suturing group (n = 21)	P value
Intraoperative Complications			
Splenic ischemia	0	0	0.956
Vessel bleeding	0	1	0.943
Liver laceration due to the retractor	0	1	0.943
Postoperative Complications*			
No complications	18	17	0.553
Grade I	0	1	0.943
Grade II	6	6	0.932
Grade IIIa	1	0	0.952
Grade IIIb	0	1	0.943
Complications in detail			
Anastomosis-related complications	2	3	0.758
Leakage	1	1	0.956
Stenosis	1	2	0.913
Bleeding	0	0	0.956
Intra-abdominal infection	3	4	0.843
Pancreatic fistula	0	1	0.943
Lymphatic fistula	0	1	0.943
Pneumonia	3	2	0.812
Wound infection	1	0	0.943
Overall	7	8	0.714

* According to the Clavien-Dindo classification.

delta-shaped anastomosis (*11-14*). Esophagojejunostomy may also be performed using hand-sewn technique. However, this procedure is used much less often than other procedures in clinical practice because suturing the seromuscular layer of the posterior wall is difficult and a high level of suturing skill is required (*7*). The purpose of the current study was to devise and attempt a new hand-sewn technique for esophagojejunostomy. Traction supplied by an assistant is used to turn both the left and right walls of the esophagus into an anterior wall, avoiding the difficulty of suturing a posterior wall. The current authors look forward to the spread of this procedure.

Anastomosis techniques using a circular stapler include a manual technique, a purse-string technique, Hiki's modified stapler anvil technique (*15*), a stapler anvil (OrVil™) inserted trans-orally (*16*), and use of a reverse puncturing device (*17*). The rationale for circular stapler anastomosis is similar to that for open surgery, so it is easily understood by surgeons. The OrVil™ technique or the reverse puncturing device technique is most commonly used in clinical practice. The OrVil™ technique facilitates a intracorporeal circular stapling esophagojejunostomy using a stapler anvil that is inserted trans-orally. This technique has a significant advantage since it avoids the necessity of placing the stapler anvil in the abdominal cavity in the event of a high anastomotic plane. This technique is relatively easy to master. Several advantages of this technique are that purse-string sutures are not needed and that the technique is simpler. A special device is not needed to place the stapler anvil. However, the OrVil™ was designed for insertion of the stapler anvil into the esophagus via the oral cavity; this site is not aseptic, so there is a risk of abdominal infection and oral cavity or esophageal injury (*16,18*). Some statistical data have indicated that the risk of postoperative anastomotic stenosis after use of a circular stapler is about 2.8% (*19*). In addition, expense has also limited the clinical use of this technique.

Side-to-side anastomosis techniques using the Endo-GIA stapler include the overlap method (*11*) and functional end-to-end anastomosis (FEEA) (*20-22*). These anastomosis techniques are less technically complex. They can effectively prevent the occurrence of anastomotic stenosis (*23-26*). However, the closure of the joint opening with the Endo GIA makes the overlap procedure easier but tends to cause stenosis. These techniques cannot completely guarantee that resection margins are negative, which runs counter to the surgical principle of removing the neoplasm. When using such a technique for reconstruction, the neoplasm should be carefully defined pre- and intraoperatively. In addition, both anastomosis techniques require a relatively long esophageal stump and are performed at a relatively low position. Thus, these techniques are limited to a benign esophageal stump with adequate length.

The hand-sewn esophagojejunostomy technique only using small instruments such as a needle holder and grasping forceps had the advantage of avoiding flaws related to use of large instruments. The hand-sewn technique is less expensive than mechanical reconstruction, and it does not require a long esophageal stump, so this technique has obvious advantages. Failed mechanical anastomosis or anastomotic stenosis resulting in an esophageal stump of insufficient length to complete mechanical reconstruction present difficulties in clinical practice.

Hand-sewn esophagojejunostomy might be the only salvage technique that can be performed with a short esophageal stump. However, this technique is technically complex and takes longer for reconstruction than other techniques, so it can sometimes only be performed by an experienced surgeon. Therefore, surgeons need more training and time to overcome the learning curve. The "China stitch" hand-sewn esophagojejunostomy technique reduces the difficulty of manual reconstruction and the time needed to perform anastomosis. It is also amenable to certain unexpected situations that might occur during the use of stapler. This was a retrospective observational study. A new technique has been explored in order to reduce operating time, to reduce the difficulty of procedure, and to enable repeated pathological examination of surgical margins.

It should be noted that this was a retrospective observational study, without patients randomized controlled in the two groups. There was probably selection bias because the patients with cancer in early stages or cancer located distal from the dentate line were tended to underwent this hand-sewn esophagojejunostomy technique when it started to be performed. Randomized controlled trails with larger series are important to evaluate its safety and effects on short-term oncological prognosis compared with mechanical esophagojejunostomy.

5. Conclusion

The "China stitch", a novel hand-sewn esophagojejunostomy technique for total laparoscopic total gastrectomy, is a cost-effective, safe, and effective method for reconstruction.

Acknowledgements

This study was supported by the Beijing Municipal Education Commission general scientific research project.(no. KM202010025008)

References

1. Nakauchi M, Suda K, Kadoya S, Inaba K, Ishida Y, Uyama I. Technical aspects and short- and long-term outcomes of totally laparoscopic total gastrectomy for advanced gastric cancer: A single-institution retrospective study. Surg Endosc. 2016; 30:4632-4639.
2. Liao T, Deng L, Yao X, Ouyang M. Comparison of the safety and efficacy between linear stapler and circular stapler in totally laparoscopic total gastrectomy: Protocol for a systematic review and meta-analysis. BMJ Open. 2019; 9:e028216.
3. Kawamura H, Ohno Y, Ichikawa N, Yoshida T, Homma S, Takahashi M, Taketomi A. Anastomotic complications after laparoscopic total gastrectomy with esophagojejunostomy constructed by circular stapler (OrVil™) versus linear stapler (overlap method). Surg Endosc. 2017; 31:5175-5182.
4. Kawaguchi Y, Shiraishi K, Akaike H, Ichikawa D. Current status of laparoscopic total gastrectomy. Ann Gastroenterol Surg. 2019; 3:14-23.
5. Inokuchi M, Otsuki S, Fujimori Y, Sato Y, Nakagawa M, Kojima K. Systematic review of anastomotic complications of esophagojejunostomy after laparoscopic total gastrectomy. World J Gastroenterol. 2015; 21:9656-9665.
6. Takayama Y, Kaneoka Y, Maeda A, Fukami Y, Takahashi T, Uji M. A novel technique of hand-sewn purse-string suturing by double ligation method (DLM) for intracorporeal circular esophagojejunostomy. J Gastric Cancer. 2019; 19:290-300.
7. Xu X, Huang C, Mou Y, Zhang R, Pan Y, Chen K, Lu C. Intra-corporeal hand-sewn esophagojejunostomy is a safe and feasible procedure for totally laparoscopic total gastrectomy: Short-term outcomes in 100 consecutive patients. Surg Endosc. 2018; 32:2689-2695.
8. He H, Li H, Ye B, Liu F. Single purse-string suture for reinforcement of duodenal stump during laparoscopic radical gastrectomy for gastric cancer. Front Oncol. 2019; 9:1020.
9. Kodera Y, Yoshida K, Kumamaru H, Kakeji Y, Hiki N, Etoh T, Honda M, Miyata H, Yamashita Y, Seto Y, Kitano S, Konno H. Introducing laparoscopic total gastrectomy for gastric cancer in general practice: A retrospective cohort study based on a nationwide registry database in Japan. Gastric Cancer. 2019; 22:202-213.
10. Okabe H, Tsunoda S, Tanaka E, Hisamori S, Kawada H, Sakai Y. Is laparoscopic total gastrectomy a safe operation? A review of various anastomotic techniques and their outcomes. Surgery Today. 2015; 45:549-558.
11. Inaba K, Satoh S, Ishida Y, Taniguchi K, Isogaki J, Kanaya S, Uyama I. Overlap method: Novel intracorporeal esophagojejunostomy after laparoscopic total gastrectomy. J Amer Coll Surgeons. 2010; 211:e25-29.
12. Nagai E, Ohuchida K, Nakata K, Miyasaka Y, Maeyama R, Toma H, Shimizu S, Tanaka M. Feasibility and safety of intracorporeal esophagojejunostomy after laparoscopic total gastrectomy: Inverted T-shaped anastomosis using linear staplers. Surgery. 2013; 153:732-738.
13. Matsuda T, Iwasaki T, Mitsutsuji M, Hirata K, Maekawa Y, Tsugawa D, Sugita Y, Shimada E, Kakeji Y. Surgical outcomes of intracorporeal circular-stapled esophagojejunostomy using modified over-and-over suture technique in laparoscopic total gastrectomy. Surg Endoscopy. 2015; 29:3386-3391.
14. Kanaya S, Kawamura Y, Kawada H, Iwasaki H, Gomi T, Satoh S, Uyama I. The delta-shaped anastomosis in laparoscopic distal gastrectomy: Analysis of the initial 100 consecutive procedures of intracorporeal gastroduodenostomy. Gastric Cancer. 2011; 14:365-371.
15. Hiki N, Fukunaga T, Yamaguchi T, Nunobe S, Tokunaga M, Ohyama S, Seto Y, Muto T. Laparoscopic esophagogastric circular stapled anastomosis: A modified technique to protect the esophagus. Gastric Cancer. 2007; 10:181-186.
16. Jeong O, Park YK. Intracorporeal circular stapling esophagojejunostomy using the transorally inserted anvil (OrVil) after laparoscopic total gastrectomy. Surg Endoscopy. 2009; 23:2624-2630.
17. Omori T, Oyama T, Mizutani S, Tori M, Nakajima K, Akamatsu H, Nakahara M, Nishida T. A simple and safe technique for esophagojejunostomy using the

hemidouble stapling technique in laparoscopy-assisted total gastrectomy. Amer J Surg. 2009; 197:e13-17.
18. Cianchi F, Macrì G, Indennitate G, Mallardi B, Trallori G, Biagini MR, Badii B, Staderini F, Perigli G. Laparoscopic total gastrectomy using the transorally inserted anvil (OrVil™): A preliminary, single institution experience. SpringerPlus. 2014; 3:434.
19. Etoh T, Inomata M, Shiraishi N, Kitano S. Minimally invasive approaches for gastric cancer-Japanese experiences. J Surg Onc. 2013; 107:282-288.
20. Matsui H, Uyama I, Sugioka A, Fujita J, Komori Y, Ochiai M, Hasumi A. Linear stapling forms improved anastomoses during esophagojejunostomy after a total gastrectomy. Amer J Surg. 2002; 184:58-60.
21. Okabe H, Obama K, Tanaka E, Nomura A, Kawamura J, Nagayama S, Itami A, Watanabe G, Kanaya S, Sakai Y. Intracorporeal esophagojejunal anastomosis after laparoscopic total gastrectomy for patients with gastric cancer. Surg Endoscopy. 2009; 23:2167-2171.
22. Kim HS, Kim BS, Lee IS, Lee S, Yook JH, Kim BS. Comparison of totally laparoscopic total gastrectomy and open total gastrectomy for gastric cancer. J Laparoendoscopic & Advanced Surg Techniques Part A. 2013; 23:323-331.
23. Kim EY, Choi HJ, Cho JB, Lee J. Totally laparoscopic total gastrectomy versus laparoscopically assisted total gastrectomy for gastric cancer. Anticancer Res. 2016; 36:1999-2003.
24. Lee IS, Kim TH, Kim KC, Yook JH, Kim BS. Modified techniques and early outcomes of totally laparoscopic total gastrectomy with side-to-side esophagojejunostomy. J Laparoendoscopic & Advanced Surg Techniques Part A. 2012; 22:876-880.
25. Gong CS, Kim BS, Kim HS. Comparison of totally laparoscopic total gastrectomy using an endoscopic linear stapler with laparoscopic-assisted total gastrectomy using a circular stapler in patients with gastric cancer: A single-center experience. World J Gastroenter. 2017; 23:8553-8561.
26. Umemura A, Koeda K, Sasaki A, Fujiwara H, Kimura Y, Iwaya T, Akiyama Y, Wakabayashi G. Totally laparoscopic total gastrectomy for gastric cancer: Literature review and comparison of the procedure of esophagojejunostomy. Asian J Surg. 2015; 38:102-112.

Received December 9, 2019; Revised February 14, 2020; Accepted February 19, 2020.

[§]These authors contributed equally to this work.

*Address correspondence to:
Nengwei Zhang or Aminbuhe, Oncology Surgery Department, Beijing Shijitan Hospital, Capital Medical University (Peking University Ninth School of Clinical Medicine), Beijing, China 100038.
E-mail: zhangnw1@sohu.com or amin734@sohu.com

Released online in J-STAGE as advance publication February 25, 2020.

Brief Report

DOI: 10.5582/bst.2020.01030

Clinical characteristics and therapeutic procedure for four cases with 2019 novel coronavirus pneumonia receiving combined Chinese and Western medicine treatment

Zhenwei Wang[1], Xiaorong Chen[2], Yunfei Lu[2], Feifei Chen[3], Wei Zhang[3,*]

[1] Department of Respiratory Disease, Yueyang Hospital of Integrated Traditional Chinese and Western Medicine, Shanghai University of Traditional Chinese Medicine, Shanghai, China;
[2] Department of Traditional Chinese Medicine, Shanghai Public Health Clinical Center, Shanghai, China;
[3] Department of Respiratory Disease, Shuguang Hospital Affiliated to Shanghai University of Traditional Chinese Medicine, Shanghai, China.

SUMMARY Pneumonia associated with the 2019 novel coronavirus (2019-nCoV) is continuously and rapidly circulating at present. No effective antiviral treatment has been verified thus far. We report here the clinical characteristics and therapeutic procedure for four patients with mild or severe 2019-nCoV pneumonia admitted to Shanghai Public Health Clinical Center. All the patients were given antiviral treatment including lopinavir/ritonavir (Kaletra®), arbidol, and Shufeng Jiedu Capsule (SFJDC, a traditional Chinese medicine) and other necessary support care. After treatment, three patients gained significant improvement in pneumonia associated symptoms, two of whom were confirmed 2019-nCoV negative and discharged, and one of whom was virus negative at the first test. The remaining patient with severe pneumonia had shown signs of improvement by the cutoff date for data collection. Results obtained in the current study may provide clues for treatment of 2019-nCoV pneumonia. The efficacy of antiviral treatment including lopinavir/ritonavir, arbidol, and SFJDC warrants further verification in future study.

Keywords 2019-nCoV, lopinavir, ritonavir, arbidol, Shufeng Jiedu Capsule

1. Introduction

Coronaviruses mainly cause respiratory tract infections and some strains have high infectivity and mortality as well as heavy damage on public health, such as severe acute respiratory syndrome (SARS) and Middle East respiratory syndrome (MERS) (*1*). A pneumonia associated with the 2019 novel coronavirus (2019-nCoV) emerged in Wuhan, China in December, 2019 and has spread rapidly, with 24,324 confirmed cases in mainland China as of February 4, 2020 (*2,3*). The most common clinical presentation is fever, fatigue, and dry cough and some patients present with nasal congestion, runny nose, and diarrhea (*4*). In severe cases, dyspnea usually occurs one week after the disease onset and some patients can rapidly progress to acute respiratory distress syndrome (ARDS), septic shock, refractory metabolic acidosis, and coagulation disorders (*4*). Thus far, there is no approved or verified effective drugs specific to the virus (*5*). We report here that four patients with mild or severe 2019-nCoV pneumonia have been cured or have significant improvement in their respiratory symptoms after treatment with combined lopinavir/ritonavir (Kaletra®), arbidol, and Shufeng Jiedu Capsule (SFJDC, a traditional Chinese medicine) on the base of supportive care.

2. Methods

2.1. Patients

For this retrospective study, four patients were recruited from January 21 to January 24, 2020 at Shanghai Public Health Clinical Center, Shanghai, China, which is a designated hospital for 2019-nCoV pneumonia. All patients were diagnosed as having 2019-nCoV pneumonia according to WHO interim guidance. Informed consent to therapeutic regimen was obtained from each patient prior to treatment.

2.2. Data collection

Epidemiological, demographic, clinical, laboratory, management, and outcome data were collected through

Table 1. Demographics, baseline characteristics, and clinical outcomes of 4 patients admitted to Shanghai Public Health Clinical Center

Items	Case 1	Case 2	Case 3	Case 4
Age	32	19	63	63
Sex	Male	Male	Male	Female
Exposure history	Recent travel to Wuhan	Resident of Wuhan	Close contact with 2019-nCoV patient	Recent travel to Wuhan
Chronic medical illness	Fatty liver	None	None	None
Days from illness onset to diagnosis confirmation	11	6	1	2
Clinical outcome	Discharged	Discharged	Remained in hospital	Remained in hospital

Table 2. Clinical characteristics at presentation and treatment of patients with 2019-nCoV pneumonia

Items	Case 1	Case 2	Case 3	Case 4
Signs and symptoms				
Fever	Yes	Yes	Yes	Yes
Cough		Yes	Yes	Yes
Fatigue	Yes	Yes		
Dizziness	Yes			Yes
Nasal congestion		Yes		
Rhinorrhea		Yes		
Constipation	Yes			Yes
Respiratory rate	22/min	19/min	26/min	22/min
Lung auscultation	Rhonchi (left lower lobe)	No rhonchi	Rhonchi (right lower lobe)	Rhonchi (left lower lobe)
Chest CT findings				
Unilateral pneumonia		Yes	Yes	
Bilateral pneumonia	Yes			Yes
Treatment				
Oxygen therapy	Yes	Yes	Yes	Yes
Mechanical ventilation				Yes
Antibiotic treatment	Yes	Yes	Yes	Yes
Lopinavir/ritonavir/arbidol/SFJDC	Yes	Yes	Yes	Yes
Intravenous immunoglobulin therapy				Yes

a review of medical records. Clinical outcomes were followed up until February 4, 2020. Laboratory confirmation of 2019-CoV was done in Shanghai Municipal Center for Disease Control and Prevention. Throat-swab specimens from the upper respiratory tract that were obtained from all patients at admission were maintained in viral-transport medium. 2019-nCoV was confirmed by real-time RT-PCR using the same protocol described previously (*6*). All patients were given chest computed tomography (CT) or chest radiography.

3. Results and Discussion

3.1. Demographics and baseline characteristics

Four patients with 2019-nCoV are included in this study, two of whom are under the age of 35 and the other two are over the age of 60 (Table 1). All the patients had epidemiologic linkage to areas with community transmission of 2019-nCoV. Among them, two patients (Case 1 and 4) had recent travel history to Wuhan, one patient (case 2) is a student who was ordinarily a resident in Wuhan and went back to Shanghai for winter holiday, and one patient (Case 3) is the husband of a confirmed 2019-nCoV case. It took 11 and 6 days from disease onset to confirmed diagnosis for case 1 and case 2, while 1 and 2 days for case 3 and case 4. Fatty liver was reported in the case 1. No underlying medical conditions were reported in the other three cases.

3.2. Clinical characteristics and laboratory assessment

On admission, the most common symptoms were fever or history of fever, followed by cough, fatigue, dizziness, nasal congestion, and rhinorrhea (Table 2). Diarrhea was not observed in all patients, on the contrary, two of them were reported to have constipation. Physical examination revealed increased respiratory rate in three patients, one of whom had tachypnea (26/min). Lung auscultation revealed rhonchi in left or right lower lobe in three patients. In all patients, there were marked abnormalities on chest radiography; involvement of both lungs was found by chest computerized tomography (CT) in 2 patients at presentation. Ground-glass opacities and consolidation were the most common radiologic

Table 3. Clinical laboratory results of patients with 2019-nCoV pneumonia

Variable	Case 1		Case 2		Case 3		Case 4	
	Before treatment	After treatment	Before treatment	After treatment	Before treatment	After treatment	Before treatment	After treatment
Blood, routine								
Leucocytes ($\times 10^9$ per L; normal range 3.5-9.5)	4.23	4.68	6.48	6.58	4.40	5.31	6.84	10.84
Neutrophils (%; normal range 50-70)	57.2	49.1	57.0	47.6	50.0	55.4	93	94
Lymphocytes (%; normal range 20-40)	30.3	37.1	30.6	39.4	24.5	25.0	6.10	3.2
Blood gas analysis								
pH (normal range 7.35-7.45)	7.33	7.33	7.43	7.33	7.40	7.36	7.44	7.33
PCO_2 (kPa, normal range 4.65-6.0)	5.42	6.05	4.55	5.96	5.45	5.59	4.23	5.52
PO_2 (kPa, normal range 10.6-13.3)	22.00	11.90	16.6	13.4	7.60	12.0	5.45	21.9

findings. On admission, leucocytes were in the normal range in all the patients (Table 3). One patient (case 4) had neutrophils above the normal range, indicating the existence of concurrent bacterial infection. Lymphocytes were below the normal range in one patient (case 4) and within the normal range in other three patients. Blood gas analysis revealed that oxygen pressure was below the normal range in two patients (7.60 kPa in case 3 and 5.45 kPa in case 4) (Table 3). On the basis of the above results, two patients (case 1 and 2) were diagnosed with mild pneumonia and the other two patients (case 3 and 4) with severe pneumonia.

3.3. Treatment and clinical outcomes

All patients received antiviral treatment, including lopinavir/ritonavir (Kaletra®, lopinavir 400 mg/ritonavir 100 mg, q12h, po), arbidol (0.2 g, tid, po), and SFJDC (2.08 g, tid, po). The duration of antiviral treatment was 6-15 days. In addition, all patients were all given antibiotic treatment and started on supplemental oxygen, delivered by nasal cannula after admission to hospital (Table 2).

Patient 1 was admitted to hospital on January 21, 2020 and thereafter received the above treatment. On January 27, routine blood analysis revealed that leucocytes and lymphocytes were increased, indicating recovery and restoration of immune function (Table 3). On January 29, chest CT demonstrated bilateral pneumonia with scattered multiple nodules, which was obviously improved compared with that obtained on January 21 (Figure 1). 2019-nCoV was twice negative in throat-swab specimens from the upper respiratory tract. The patient was free of fever, productive cough, dyspnea, short breath, abdominal pain, and diarrhea, and thus discharged on January 29, 2020.

Patient 2 was admitted to hospital on January 24, 2020 and then received the above mentioned treatment. On January 28, routine blood analysis showed increased count of leucocytes and lymphocytes (Table 3). Blood gas analysis revealed no obvious abnormity. On January 29, chest CT revealed unilateral pneumonia in the left lobe, which was mildly improved compared with the

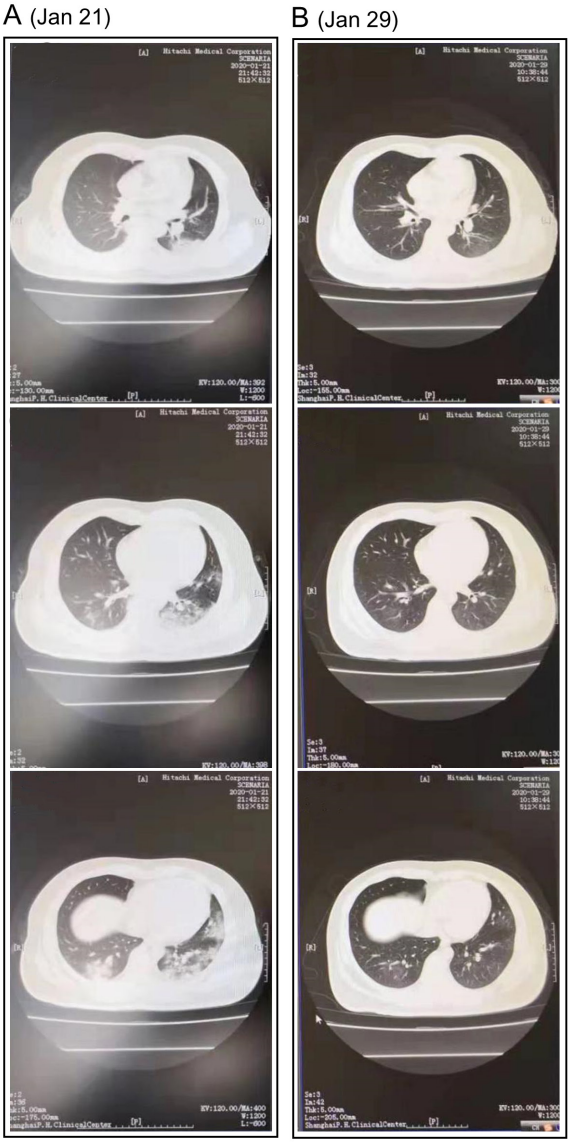

Figure 1. Chest CTs of patient 1 obtained on January 21 (A) and January 29 (B), 2020.

images obtained on January 24 (Figure 2). Results of two continuous 2019-nCoV tests were negative for throat-swab specimens. Symptoms associated with pneumonia had improved and the patient was discharged on January 30, 2020.

Patient 3 was admitted to hospital on January 24, 2020 and thereafter received the above mentioned treatment. The fever disappeared after one day of treatment. On January 29, chest CT showed progressed pneumonia in the right lobe (Figure 3). The treatment was continuous and the pneumonia appearance improved on February 1 as reflected by the CT image (Figure 3). On February 3, blood gas analysis demonstrated obviously increased oxygen pressure compared with that at admission. The patient had mild cough with white phlegm, and was free of fever, dyspnea, short breath, abdominal pain, and diarrhea. 2019-nCoV test result was negative for the first time on February 4, 2020. The patient remained in hospital for the second virus test.

Patient 4 was admitted to hospital on January 22, 2020. In addition to the above mentioned treatments, the patient was also given human seroalbumin and γ-immunoglobulin. On January 31, the patient was given an intubated ventilator-assisted breathing therapy because of refractory low blood oxygen pressure. Routine blood analysis on February 1 demonstrated the percentages of neutrophils and lymphocytes were 94% and 3.2%, respectively, which were comparable with those at admission (Table 3). Chest radiograph on this

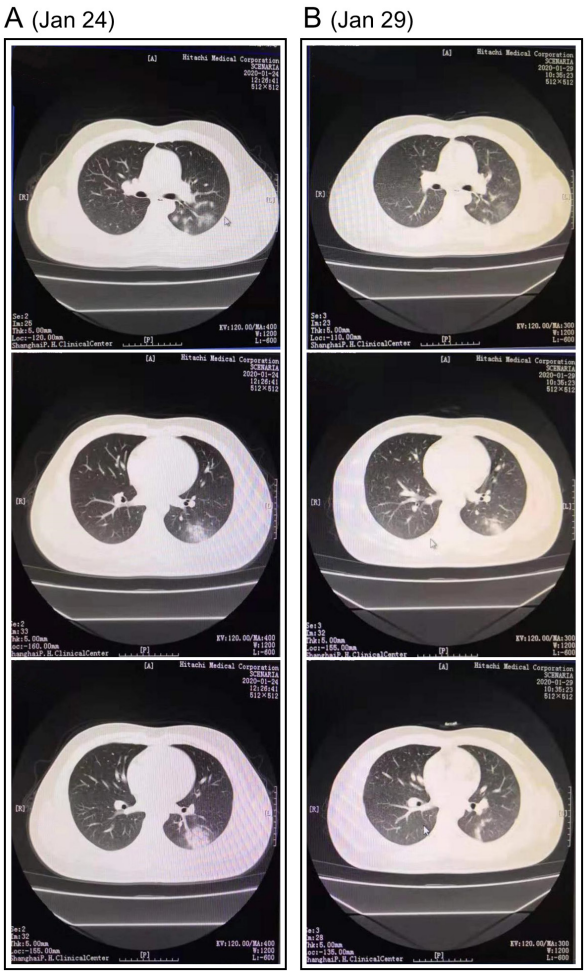

Figure 2. Chest CTs of patient 2 obtained on January 24 (A) and January 29 (B), 2020.

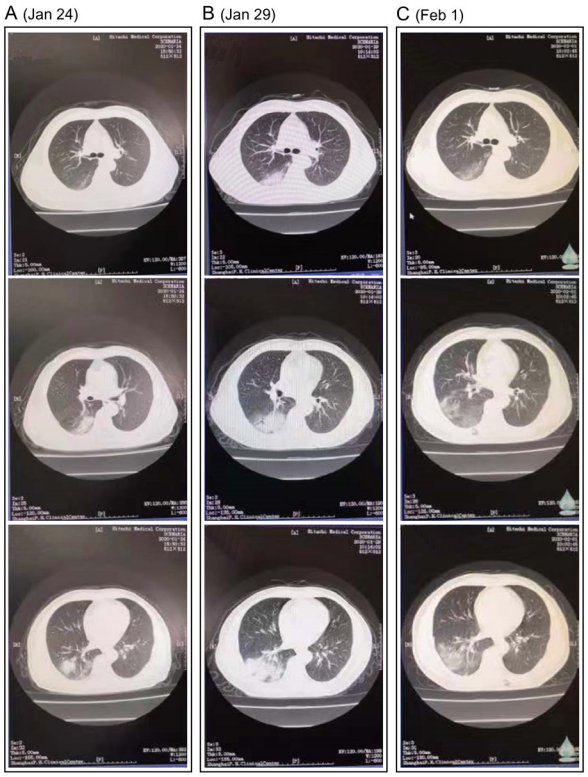

Figure 3. Chest CTs of patient 3 obtained on January 24 (A) and January 29 (B), and February 1 (C), 2020.

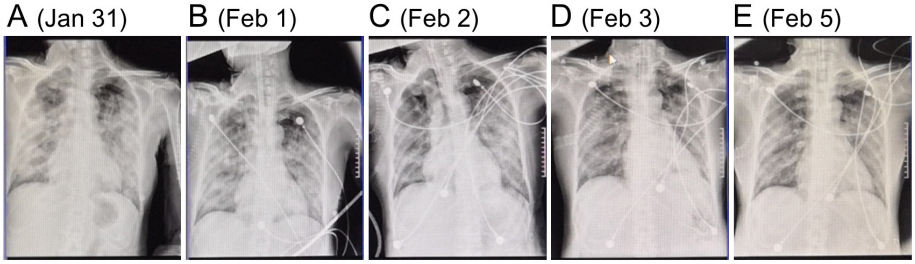

Figure 4. Posteroanterior chest radiographs of patient 4 obtained on January 31 (A), February 1 (B), February 2 (C), February 3 (D), and February 5 (E), 2020.

day demonstrated bilateral pneumonia, which improved compared to the image obtained on January 31 (Figure 4). Chest radiograph on February 2 revealed further mild improvement. On February 3, bilateral pneumonia remained but the appearances of left lobe improved and right lobe mildly worsened. On February 5, the appearance of pneumonia improved compared with the last image (Figure 4). The patient was still using ventilators at data cutoff.

We report here the clinical characteristics and therapeutic procedure for four patients with 2019-CoV pneumonia receiving comprehensive therapy. The antivirus treatment regimen includes lopinavir/ritonavir (Kaletra®), arbidol, and SFJDC. By February 4, 2020, two patients were confirmed 2019-nCoV negative and one patient was virus-negative at the first test. Lopinavir/ritonavir (Kaletra®) is a human immunodeficiency virus (HIV) medicine used in combination with other medicines to treat adults and children over 14 days of age who are infected with HIV-1 (*7*). It was revealed that lopinavir/ritonavir among SARS-CoV patients was associated with substantial clinical benefit (fewer adverse clinical outcomes) (*8*). The combination of lopinavir and ritonavir is currently a recommended antivirus regimen in the latest version of Diagnosis and Treatment of Pneumonia Caused by 2019-nCoV (version 5) issued by National Health Commission of the People's Republic of China (*4*). Arbidol is an antiviral treatment for influenza infection used in Russia and China (*9*). It was claimed that arbidol was effective against 2019-nCoV at a concentration range of 10-30 μM *in vitro* (*10*). A randomized multicenter controlled clinical trial of arbidol in patients with 2019-nCoV (ChiCTR2000029573) has been initiated in China (*11*). SFJDC is a traditional Chinese medicine for treatment of influenza in China. This drug is also recommended for treating 2019-nCoV infection in the latest version of Diagnosis and Treatment of Pneumonia Caused by 2019-nCoV (version 5) (*4*).

In conclusion, two mild and two severe 2019-nCoV pneumonia patients were given combined Chinese and Western medicine treatment, three of whom gained significant improvement in pneumonia associated symptoms. The remaining patient with severe pneumonia has shown signs of improvement by the cutoff date for data collection. The efficacy of antiviral treatment including lopinavir/ritonavir, arbidol, and SFJDC warrants further verification in future study.

Acknowledgements

The study is supported by Shanghai Municipal Key Clinical Specialty (shslczdzk05101) and Shanghai Key Clinical Laboratory of Internal Medicine of Traditional Chinese Medicine (14DZ2273200).

References

1. Gralinski LE, Menachery VD. Return of the Coronavirus: 2019-nCoV. Viruses. 2020; 12. doi: 10.3390/v12020135.
2. Zhu N, Zhang D, Wang W, *et al*. A novel coronavirus from patients with pneumonia in China, 2019. N Engl J Med. 2020. doi: 10.1056/NEJMoa2001017.
3. Notification of 2019-nCoV infection. National Health Commission of the People's Republic of China. *http://www.nhc.gov.cn/xcs/yqtb/202002/17a03704a99646ffad6807bc806f37a4.shtml* (accessed February 5, 2019). (in Chinese)
4. Diagnosis and Treatment of Pneumonia Caused by 2019-nCoV (version 5). *http://www.nhc.gov.cn/yzygj/s7653p/202002/3b09b894ac9b4204a79db5b8912d4440.shtml* (accessed February 5, 2020). (in Chinese)
5. Lu H. Drug treatment options for the 2019-new coronavirus (2019-nCoV). Biosci Trends. 2020. doi: 10.5582/bst.2020.01020.
6. Huang C, Wang Y, Li X, *et al*. Clinical features of patients infected with 2019 novel coronavirus in Wuhan, China. Lancet. 2020. doi: 10.1016/S0140-6736(20)30183-5.
7. Su B, Wang Y, Zhou R, Jiang T, Zhang H, Li Z, Liu A, Shao Y, Hua W, Zhang T, Wu H, He S, Dai L, Sun L. Efficacy and tolerability of lopinavir/ritonavir- and efavirenz-based initial antiretroviral therapy in HIV-1-infected patients in a tertiary care hospital in Beijing, China. Front Pharmacol. 2019; 10:1472.
8. Chu CM, Cheng VC, Hung IF, Wong MM, Chan KH, Chan KS, Kao RY, Poon LL, Wong CL, Guan Y, Peiris JS, Yuen KY, Group HUSS. Role of lopinavir/ritonavir in the treatment of SARS: initial virological and clinical findings. Thorax. 2004; 59:252-256.
9. Wang Y, Ding Y, Yang C, Li R, Du Q, Hao Y, Li Z, Jiang H, Zhao J, Chen Q, Yang Z, He Z. Inhibition of the infectivity and inflammatory response of influenza virus by arbidol hydrochloride in vitro and *in vivo* (mice and ferret). Biomed Pharmacother. 2017; 91:393-401.
10. News. *http://www.sd.chinanews.com/2/2020/0205/70145.html* (accessed February 5, 2020). (in Chinese)
11. Chinese Clinical Trial Registry. *http://www.chictr.org.cn/showproj.aspx?proj=49065* (accessed February 5, 2019).

Received February 2, 2020; Revised February 5, 2020, Accepted February 6, 2020.

**Address correspondence to:*
Wei Zhang, Department of Respiratory Disease, Shuguang Hospital Affiliated to Shanghai University of Traditional Chinese Medicine, Shanghai, China.
E-mail: zhangw1190@sina.com

Released online in J-STAGE as advance publication February 9, 2020.

Communication

DOI: 10.5582/bst.2020.01020

Drug treatment options for the 2019-new coronavirus (2019-nCoV)

Hongzhou Lu[1,2,3,*]

[1] Scientific Research Center, Shanghai Public Health Clinical Center, Fudan University, Shanghai, China;
[2] Department of Infectious Diseases, Shanghai Public Health Clinical Center, Fudan University, Shanghai, China;
[3] Department of Infectious Disease, Huashan Hospital Affiliated to Fudan University, Shanghai, China.

SUMMARY As of January 22, 2020, a total of 571 cases of the 2019-new coronavirus (2019-nCoV) have been reported in 25 provinces (districts and cities) in China. At present, there is no vaccine or antiviral treatment for human and animal coronavirus, so that identifying the drug treatment options as soon as possible is critical for the response to the 2019-nCoV outbreak. Three general methods, which include existing broad-spectrum antiviral drugs using standard assays, screening of a chemical library containing many existing compounds or databases, and the redevelopment of new specific drugs based on the genome and biophysical understanding of individual coronaviruses, are used to discover the potential antiviral treatment of human pathogen coronavirus. Lopinavir /Ritonavir, Nucleoside analogues, Neuraminidase inhibitors, Remdesivir, peptide (EK1), arbidol, RNA synthesis inhibitors (such as TDF, 3TC), anti-inflammatory drugs (such as hormones and other molecules), Chinese traditional medicine, such ShuFengJieDu Capsules and Lianhuaqingwen Capsule, could be the drug treatment options for 2019-nCoV. However, the efficacy and safety of these drugs for 2019-nCoV still need to be further confirmed by clinical experiments.

Keywords 2019-nCoV, Coronaviruses, pneumonia

As of January 22, 2020, a total of 571 cases of the 2019-new coronavirus (2019-nCoV) have been reported in 25 provinces (districts and cities) in China (*1*). Among them, 95 cases were serious and 17 cases died (all from Hubei Province). WHO Collaborating Centre for Infectious Disease Modelling estimated a total of 4,000 cases of 2019-nCoV in Wuhan City (uncertainty range: 1,000-9,700) had onset of symptoms by 18th January 2020 (the last reported onset date of any case) (*2*). Identifying the drug treatment options as soon as possible is critical for the response to the 2019-nCoV outbreak (*3*).

At present, there is no vaccine or antiviral treatment for human and animal coronavirus (COV). Because of its key role in the virus cell receptor interaction, the surface structure of spike glycoprotein(s) is particularly important for the development of antivirals. Treatment of such severe influenza still presents multiple challenges. There are several general methods that could be used to discover a potential antiviral treatment for the human pathogen coronavirus.

The first one is to test the existing broad-spectrum antiviral drugs by using standard assays, which have been used to treat other viral infections (*4*). These methods can measure the effects of these drugs on the cytopathy, viral production and plaque formation of living cells and/or pseudocoronaviruses. Examples of drugs identified using this method include interferon I (IFN- alpha, beta, kappa, lamda, epsilon, *etc*.) and interferon II (interferon gamma, *etc*.). These drugs have obvious advantages, known pharmacokinetic and pharmacodynamic properties, side effects and drug regimens. However, they have no specific anti coronavirus effect and may be related to serious adverse reactions.

The second method involves the screening of a chemical library containing many existing compounds or databases, including information about transcription characteristics in different cell lines (*5*). This method can quickly and high-throughput screen many easily obtained compounds, and then further evaluate them by antiviral assay. Various drugs have been identified in these drug reuse programs, including many drugs with important physiological and/or immunological effects, such as affecting neurotransmitter regulation, estrogen receptor, kinase signal transduction, lipid or sterol metabolism, protein processing and DNA synthesis or repair.

The third approach involves the redevelopment of

new specific drugs based on the genome and biophysical understanding of individual coronaviruses (*6*). Examples include siRNA molecules or inhibitors targeting specific viral enzymes involved in the viral replication cycle, mAb targeting host receptor, inhibitor of host cell protease, inhibitor of host cell endocytosis virus, human derived or humanized mAb targeting S1 RBD and antiviral peptide targeting S2. Although most of these drugs have anti coronavirus activity in vitro and/or in vivo, their pharmacokinetic and pharmacodynamic properties, as well as side effect characteristics, have yet to be evaluated in animal and human trials. In addition, development of these drugs can allow drugs to become clinically useful treatment options, but it usually takes several years to provide reliable treatment for patients. The main drawback of this approach is that although many of the identified drugs show anti-coronavirus activity in vitro, most of them are not clinically useful because they are associated with immunosuppression or have a value of half the EC50 of anti-coronavirus, which is significantly higher than the peak serum concentration (Cmax) that can be achieved at the treatment dose.

In general, these three drug discovery methods are usually used together during the emerging coronavirus outbreak, and can be roughly divided into virus based and host based treatment selection candidate drug compounds.

For the current new coronavirus, according to the guidelines (*7*), IFN- alpha (5 million U bid inh) and lopinavir/ritonavir(400 mg/100 mg *bid po*) are recommended as antiviral therapy. IFN- alpha is a broad spectrum antiviral drug, which can be used to treat HBV. Lopinavir is one kind of protease inhibitor used to treat HIV infection, with ritonavir as a booster. Lopinavir and/or lopinavir litonavir have anti coronavirus activity in vitro. In Severe Acute Respiratory Syndrome (SARS) treatment, Hong Kong scholars found that compared with ribavirin alone, patients treated with lopinavir/ritonavir and ribavirin had lower risk of acute respiratory distress syndrome (ARDS) or death (*8*).

In addition, Nucleoside analogs may have multiple mechanisms of action, including lethal mutagenesis, specific or non specific chain termination, and inhibition of nucleotide biosynthesis (*9*). Fabiravir and ribavirin are representatives of nucleoside analogs, which combined with fabiravir and oseltamivir in the treatment of severe influenza is better than oseltamivir alone (*10*).

Besides, Remdesivir may be the best potential drug for the treatment of 2019-nCoV. Animal experiments showed that compared with the control group, Remdesivir can effectively reduce the virus titer of mice infected with Middle East Respiratory Syndrome (Mers)-CoV, improve the lung tissue damage, and its effect is better than that of the treatment group treated with Lopinavir/Ritonavir combined with interferon-β (*11*). The drug has completed the phase III clinical trial for treatment of Ebola virus infection, and the pharmacokinetics and safety for the human body have relatively complete data (*12*). However, the efficacy and safety of Remdesivir in patients with 2019-nCoV infection still need to be further confirmed by clinical research.

Neuraminidase inhibitors (NAIs) such as oral oseltamivir, inhaled zanamivir, and intravenous peramivir are recommended as antiviral treatment in influenza (*13*). Oral oseltamivir has been widely used for 2019-nCoV or suspected cases in China hospitals. The mainstay for patients is intiation of antiviral medication as soon as possible after illness onset. It has shown that neuraminidase inhibitors are effective as empirical treatment in MERS-CoV infection (*14*), however, there is no exact evidence that oseltamivir is effective in the treatment of 2019-nCoV.

At present, some other types of drugs have been found to be effective in vitro, such as fusion peptide (EK1) (*15*), arbidol (*16*), RNA synthesis inhibitors (such as TDF, 3TC) anti-inflammatory drugs (such as hormones and other molecules), *etc*. In addition, Chinese medicine, such as ShuFengJieDu Capsules and Lianhuaqingwen Capsules, has also played a role in the prevention and treatment of new respiratory infectious diseases such as influenza A (H1N1) (*17,18*). However, the efficacy and safety of these drugs in 2019-nCoV need to be further confirmed by clinical experiments.

In general, there are no specific antiviral drugs or vaccines for 2019-nCoV. All of the drug options come from experience treating SARS, MERS or some other new influenza virus previously. Active symptomatic support remains key to treatment. These drugs above would be helpful and the efficacy needs to be further confirmed.

Acknowledgement

This research was funded by the 13th Five-Year National Science and Technology Major Project from Ministry of Science and Technology of the People's Republic of China (Grant No.: 2017ZX09304027).

References

1. National Health Commission of the People's Republic of China. Pneumonia epidemic situation of new coronavirus infection on January 23, 2020. *http://www.nhc.gov.cn/yjb/s3578/202001/5d19a4f6d3154b9fae328918ed2e3c8a.shtml* (accessed January 23, 2020).
2. Natsuko Imai. Report 2: Estimating the potential total number of novel Coronavirus cases in Wuhan City, China. *http://www.imperial.ac.uk/mrc-global-infectious-disease-analysis/news--wuhan-coronavirus/* (accessed January 23, 2020).
3. Lu H, Stratton CW, Tang YW. Outbreak of Pneumonia of Unknown Etiology in Wuhan China: the Mystery and the Miracle. J Med Virol. 2020. doi: 10.1002/jmv.25678.
4. Kim Y, Liu H, Galasiti Kankanamalage AC, Weerasekara S, Hua DH, Groutas WC, Chang KO, Pedersen NC.

Reversal of the Progression of Fatal Coronavirus Infection in Cats by a Broad-Spectrum Coronavirus Protease Inhibitor. PLoS Pathog. 2016; 12:e1005531.
5. Channappanavar R, Fett C, Mack M, Ten Eyck PP, Meyerholz DK, Perlman S. Sex-Based Differences in Susceptibility to Severe Acute Respiratory Syndrome Coronavirus Infection. J Immunol. 2017; 198:4046-4053.
6. Zumla A, Chan JF, Azhar EI, Hui DS, Yuen KY. Coronaviruses - drug discovery and therapeutic options. Nat Rev Drug Discov. 2016; 15:327-47.
7. National Health Commission of the People's Republic of China. Notice on printing and distributing the diagnosis and treatment plan of pneumonia with new coronavirus infection (trial version 3). *http://www.nhc.gov.cn/yzygj/s7653p/202001/f492c9153ea9437bb587ce2ffcbee1fa.shtml* (accessed January 23, 2020).
8. Chu CM, Cheng VC, Hung IF, Wong MM, Chan KH, Chan KS, Kao RY, Poon LL, Wong CL, Guan Y, Peiris JS, Yuen KY; HKU/UCH SARS Study Group.. Role of lopinavir/ritonavir in the treatment of SARS: initial virological and clinical findings.Thorax. 2004; 59:252-256.
9. Arabi YM, Alothman A, Balkhy HH, *et al*. Treatment of Middle East Respiratory Syndrome with a combination of lopinavir-ritonavir and interferon-β1b (MIRACLE trial): study protocol for a randomized controlled trial. Trials. 2018;19:81.
10. Wang Y, Fan G, Salam A, Horby P, Hayden FG, Chen C, Pan J, Zheng J, Lu B, Guo L, Wang C, Cao B; CAP-China Network. Comparative effectiveness of combined favipiravir and oseltamivir therapy versus oseltamivir monotherapy in critically ill patients with influenza virus infection. J Infect Dis. 2019; pii: jiz656.
11. Sheahan TP, Sims AC, Leist SR, *et al*. Comparative therapeutic efficacy of remdesivir and combination lopinavir, ritonavir, and interferon beta against MERS-CoV. Nat Commun. 2020 ; 11:222.
12. Agostini ML, Andres EL, Sims AC, *et al*. Coronavirus Susceptibility to the Antiviral Remdesivir (GS-5734) Is Mediated by the Viral Polymerase and the Proofreading Exoribonuclease. mBio. 2018; 9: pii: e00221-18.
13. Chow EJ, Doyle JD, Uyeki TM. Influenza virus-related critical illness: prevention, diagnosis, treatment. Crit Care. 2019 ; 23:214.
14. Bleibtreu A, Jaureguiberry S, Houhou N, Boutolleau D, Guillot H, Vallois D, Lucet JC, Robert J, Mourvillier B, Delemazure J, Jaspard M, Lescure FX, Rioux C, Caumes E, Yazdanapanah Y. Clinical management of respiratory syndrome in patients hospitalized for suspected Middle East respiratory syndrome coronavirus infection in the Paris area from 2013 to 2016. BMC Infect Dis. 2018; 18:331.
15. Xia S, Yan L, Xu W, Agrawal AS, Algaissi A, Tseng CK, Wang Q, Du L, Tan W, Wilson IA, Jiang S, Yang B, Lu L. A pan-coronavirus fusion inhibitor targeting the HR1 domain of human coronavirus spike. Sci Adv. 2019; 5:eaav4580.
16. Coleman CM, Sisk JM, Mingo RM, Nelson EA, White JM2, Frieman MB. Abelson Kinase Inhibitors Are Potent Inhibitors of Severe Acute Respiratory Syndrome Coronavirus and Middle East Respiratory Syndrome Coronavirus Fusion. J Virol. 2016; 90:8924-8933.
17. Ji S, Bai Q, Wu X, Zhang DW, Wang S, Shen JL, Fei GH. Unique synergistic antiviral effects of Shufeng Jiedu Capsule and oseltamivir in influenza A viral-induced acute exacerbation of chronic obstructive pulmonary disease. Biomed Pharmacother. 2020;121:109652.
18. Ding Y, Zeng L, Li R, Chen Q, Zhou B, Chen Q, Cheng PL, Yutao W, Zheng J, Yang Z, Zhang F. The Chinese prescription lianhuaqingwen capsule exerts anti-influenza activity through the inhibition of viral propagation and impacts immune function. BMC Complement Altern Med. 2017; 17:130.

Received January 23, 2020; Accepted January 27, 2020.

**Address correspondence to:*
Hongzhou Lu, Shanghai Public Health Clinical Center, Fudan University, No.2901, Caolang Road, Jinshan District, Shanghai 201508, China.
E-mail: luhongzhou@fudan.edu.cn

Released online in J-STAGE as advance publication January 28, 2020.

Letter

DOI: 10.5582/bst.2020.01047

Breakthrough: Chloroquine phosphate has shown apparent efficacy in treatment of COVID-19 associated pneumonia in clinical studies

Jianjun Gao[1,*], Zhenxue Tian[2], Xu Yang[2]

[1] Department of Pharmacology, School of Pharmacy, Qingdao University, Qingdao, China;
[2] Department of Pharmacy, Qingdao Municipal Hospital, Qingdao, China.

SUMMARY The coronavirus disease 2019 (COVID-19) virus is spreading rapidly, and scientists are endeavoring to discover drugs for its efficacious treatment in China. Chloroquine phosphate, an old drug for treatment of malaria, is shown to have apparent efficacy and acceptable safety against COVID-19 associated pneumonia in multicenter clinical trials conducted in China. The drug is recommended to be included in the next version of the Guidelines for the Prevention, Diagnosis, and Treatment of Pneumonia Caused by COVID-19 issued by the National Health Commission of the People's Republic of China for treatment of COVID-19 infection in larger populations in the future.

Keywords COVID-19, SARS-CoV-2, 2019-nCoV, pneumonia, chloroquine

The coronavirus disease 2019 (COVID-19) virus, emerged in December 2019, has spread rapidly, with cases now confirmed in multiple countries. As of February 16, 2020, the virus has caused 70,548 infections and 1,770 deaths in mainland China and 413 infections in Japan (*1*). A great deal of effort has been made to find effective drugs against the virus in China (*2*). On February 17, 2020, the State Council of China held a news briefing indicating that chloroquine phosphate, an old drug for treatment of malaria, had demonstrated marked efficacy and acceptable safety in treating COVID-19 associated pneumonia in multicenter clinical trials conducted in China (*3*).

In the early *in vitro* studies, chloroquine was found to block COVID-19 infection at low-micromolar concentration, with a half-maximal effective concentration (EC_{50}) of 1.13 μM and a half-cytotoxic concentration (CC_{50}) greater than 100 μM (*4*). A number of subsequent clinical trials (ChiCTR2000029939, ChiCTR2000029935, ChiCTR2000029899, ChiCTR2000029898, ChiCTR2000029868, ChiCTR2000029837, ChiCTR2000029826, ChiCTR2000029803, ChiCTR2000029762, ChiCTR2000029761, ChiCTR2000029760, ChiCTR2000029740, ChiCTR2000029609, ChiCTR2000029559, and ChiCTR2000029542) have been quickly conducted in China to test the efficacy and safety of chloroquine or hydroxychloroquine in the treatment of COVID-19 associated pneumonia in more than 10 hospitals in Wuhan, Jingzhou, Guangzhou, Beijing, Shanghai, Chongqing, and Ningbo (*5*). Thus far, results from more than 100 patients have demonstrated that chloroquine phosphate is superior to the control treatment in inhibiting the exacerbation of pneumonia, improving lung imaging findings, promoting a virus-negative conversion, and shortening the disease course according to the news briefing. Severe adverse reactions to chloroquine phosphate were not noted in the aforementioned patients. Given these findings, a conference was held on February 15, 2020; participants including experts from government and regulatory authorities and organizers of clinical trials reached an agreement that chloroquine phosphate has potent activity against COVID-19. The drug is recommended for inclusion in the next version of the Guidelines for the Prevention, Diagnosis, and Treatment of Pneumonia Caused by COVID-19 issued by the National Health Commission of the People's Republic of China.

Chloroquine is used to prevent and treat malaria and is efficacious as an anti-inflammatory agent for the treatment of rheumatoid arthritis and lupus erythematosus. Studies revealed that it also has potential broad-spectrum antiviral activities by increasing endosomal pH required for virus/cell fusion, as well as interfering with the glycosylation of cellular receptors of SARS-CoV (*6,7*). The anti-viral and anti-inflammatory activities of chloroquine may account for its potent efficacy in treating patients with COVID-19 pneumonia.

Chloroquine is a cheap and safe drug that has been used for more than 70 years. In light of the urgent clinical demand, chloroquine phosphate is recommended to treat COVID-19 associated pneumonia in larger populations in the future.

References

1. Notification of 2019-nCoV infection. National Health Commission of the People's Republic of China. *http://www.nhc.gov.cn/xcs/yqfkdt/202002/18546da875d74445bb537ab014e7a1c6.shtml* (accessed February 17, 2020). (in Chinese)
2. Lu H. Drug treatment options for the 2019-new coronavirus (2019-nCoV). Biosci Trends. 2020.
3. Audio transcript of the news briefing held by the State Council of China on February 17, 2020. The National Health Commission of the People's Republic of China. *http://www.nhc.gov.cn/xcs/yqfkdt/202002/f12a62d10c2a48c6895cedf2faea6e1f.shtml* (accessed February 18, 2020). (in Chinese)
4. Wang M, Cao R, Zhang L, Yang X, Liu J, Xu M, Shi Z, Hu Z, Zhong W, Xiao G. Remdesivir and chloroquine effectively inhibit the recently emerged novel coronavirus (2019-nCoV) *in vitro*. Cell Res. 2020.
5. Chinese Clinical Trial Registry. *http://www.chictr.org.cn/searchproj.aspx?title=%E6%B0%AF%E5%96%B9&officialname=&subjectid=&secondaryid=&applier=&studyleader=&ethicalcommitteesanction=&sponsor=&studyailment=&studyailmentcode=&studytype=0&studystage=0&studydesign=0&minstudyexecutetime=&maxstudyexecutetime=&recruitmentstatus=0&gender=0&agreetosign=&secsponsor=&regno=&regstatus=0&country=&province=&city=&institution=&institutionlevel=&measure=&intercode=&sourceofspends=&createyear=0&isuploadrf=&whetherpublic=&btngo=btn&verifycode=&page=1* (accessed February 18, 2019).
6. Savarino A, Boelaert JR, Cassone A, Majori G, Cauda R. Effects of chloroquine on viral infections: an old drug against today's diseases? Lancet Infect Dis. 2003; 3:722-727.
7. Yan Y, Zou Z, Sun Y, Li X, Xu KF, Wei Y, Jin N, Jiang C. Anti-malaria drug chloroquine is highly effective in treating avian influenza A H5N1 virus infection in an animal model. Cell Res. 2013; 23:300-302.

Received February 18, 2020; Accepted February 18, 2020.

**Address correspondence to:*
Jianjun Gao, Department of Pharmacology, School of Pharmacy, Qingdao University, Qingdao, Shandong, China.
E-mail: gaojj@qdu.edu.cn

Released online in J-STAGE as advance publication February 19, 2020.

BST
BioScience Trends

Guide for Authors

1. Scope of Articles

BioScience Trends is an international peer-reviewed journal. BioScience Trends devotes to publishing the latest and most exciting advances in scientific research. Articles cover fields of life science such as biochemistry, molecular biology, clinical research, public health, medical care system, and social science in order to encourage cooperation and exchange among scientists and clinical researchers.

2. Submission Types

Original Articles should be well-documented, novel, and significant to the field as a whole. An Original Article should be arranged into the following sections: Title page, Abstract, Introduction, Materials and Methods, Results, Discussion, Acknowledgments, and References. Original articles should not exceed 5,000 words in length (excluding references) and should be limited to a maximum of 50 references. Articles may contain a maximum of 10 figures and/or tables.

Brief Reports definitively documenting either experimental results or informative clinical observations will be considered for publication in this category. Brief Reports are not intended for publication of incomplete or preliminary findings. Brief Reports should not exceed 3,000 words in length (excluding references) and should be limited to a maximum of 4 figures and/or tables and 30 references. A Brief Report contains the same sections as an Original Article, but the Results and Discussion sections should be combined.

Reviews should present a full and up-to-date account of recent developments within an area of research. Normally, reviews should not exceed 8,000 words in length (excluding references) and should be limited to a maximum of 100 references. Mini reviews are also accepted.

Policy Forum articles discuss research and policy issues in areas related to life science such as public health, the medical care system, and social science and may address governmental issues at district, national, and international levels of discourse. Policy Forum articles should not exceed 2,000 words in length (excluding references).

Case Reports should be detailed reports of the symptoms, signs, diagnosis, treatment, and follow-up of an individual patient. Case reports may contain a demographic profile of the patient but usually describe an unusual or novel occurrence. Unreported or unusual side effects or adverse interactions involving medications will also be considered. Case Reports should not exceed 3,000 words in length (excluding references).

News articles should report the latest events in health sciences and medical research from around the world. News should not exceed 500 words in length.

Letters should present considered opinions in response to articles published in BioScience Trends in the last 6 months or issues of general interest. Letters should not exceed 800 words in length and may contain a maximum of 10 references.

3. Editorial Policies

Ethics: BioScience Trends requires that authors of reports of investigations in humans or animals indicate that those studies were formally approved by a relevant ethics committee or review board.

Conflict of Interest: All authors are required to disclose any actual or potential conflict of interest including financial interests or relationships with other people or organizations that might raise questions of bias in the work reported. If no conflict of interest exists for each author, please state "There is no conflict of interest to disclose".

Submission Declaration: When a manuscript is considered for submission to BioScience Trends, the authors should confirm that 1) no part of this manuscript is currently under consideration for publication elsewhere; 2) this manuscript does not contain the same information in whole or in part as manuscripts that have been published, accepted, or are under review elsewhere, except in the form of an abstract, a letter to the editor, or part of a published lecture or academic thesis; 3) authorization for publication has been obtained from the authors' employer or institution; and 4) all contributing authors have agreed to submit this manuscript.

Cover Letter: The manuscript must be accompanied by a cover letter signed by the corresponding author on behalf of all authors. The letter should indicate the basic findings of the work and their significance. The letter should also include a statement affirming that all authors concur with the submission and that the material submitted for publication has not been published previously or is not under consideration for publication elsewhere. The cover letter should be submitted in PDF format. For example of Cover Letter, please visit http://www.biosciencetrends.com/downcentre.php (Download Centre).

Copyright: A signed JOURNAL PUBLISHING AGREEMENT (JPA) form must be provided by post, fax, or as a scanned file before acceptance of the article. Only forms with a hand-written signature are accepted. This copyright will ensure the widest possible dissemination of information. A form facilitating transfer of copyright can be downloaded by clicking the appropriate link and can be returned to the e-mail address or fax number noted on the form (Please visit Download Centre). Please note that your manuscript will not proceed to the next step in publication until the JPA Form is received. In addition, if excerpts from other copyrighted works are included, the author(s) must obtain written permission from the copyright owners and credit the source(s) in the article.

Suggested Reviewers: A list of up to 3 reviewers who are qualified to assess the scientific merit of the study is welcomed. Reviewer information including names, affiliations, addresses, and e-mail should be provided at the same time the manuscript is submitted online. Please do not suggest reviewers with known conflicts of interest, including participants or anyone with a stake in the proposed research; anyone from the same institution; former students, advisors, or research collaborators (within the last three years); or close personal contacts. Please note that the Editor-in-Chief may accept one or more of the proposed reviewers or may request a review by other qualified persons.

Language Editing: Manuscripts prepared by authors whose native language is not English should have their work proofread by a native English speaker before submission. If not, this might delay the publication of your manuscript in BioScience Trends.

The Editing Support Organization can provide English proofreading, Japanese-English translation, and Chinese-English translation services to authors who want to publish in BioScience Trends and need assistance before submitting a manuscript. Authors can visit this organization directly at http://www.iacmhr.com/iac-eso/support.php?lang=en. IAC-ESO was established to facilitate manuscript preparation by researchers whose native language is not English and to help edit works intended for international academic journals.

4. Manuscript Preparation

Manuscripts should be written in clear, grammatically correct English and submitted as a Microsoft Word file in a single-column format. Manuscripts must be paginated and typed in 12-point Times New Roman font with 24-point line spacing. Please do not embed figures in the text. Abbreviations should be used as little as possible and should be explained at first mention unless the term is a well-known abbreviation (*e.g.* DNA). Single words should not be abbreviated.

Title Page: The title page must include 1) the title of the paper (Please note the title should be short, informative, and contain the major key words); 2) full name(s) and affiliation(s) of the author(s), 3) abbreviated names of the author(s), 4) full name, mailing address, telephone/fax numbers, and e-mail address of the corresponding author; and 5) conflicts of interest (if you have an actual or potential conflict of interest to disclose, it must be included as a footnote on the title page of the manuscript; if no conflict of

interest exists for each author, please state "There is no conflict of interest to disclose"). Please visit Download Centre and refer to the title page of the manuscript sample.

Abstract: The abstract should briefly state the purpose of the study, methods, main findings, and conclusions. For article types including Original Article, Brief Report, Review, Policy Forum, and Case Report, a one-paragraph abstract consisting of no more than 250 words must be included in the manuscript. For News and Letters, a brief summary of main content in 150 words or fewer should be included in the manuscript. Abbreviations must be kept to a minimum and non-standard abbreviations explained in brackets at first mention. References should be avoided in the abstract. Key words or phrases that do not occur in the title should be included in the Abstract page.

Introduction: The introduction should be a concise statement of the basis for the study and its scientific context.

Materials and Methods: The description should be brief but with sufficient detail to enable others to reproduce the experiments. Procedures that have been published previously should not be described in detail but appropriate references should simply be cited. Only new and significant modifications of previously published procedures require complete description. Names of products and manufacturers with their locations (city and state/country) should be given and sources of animals and cell lines should always be indicated. All clinical investigations must have been conducted in accordance with Declaration of Helsinki principles. All human and animal studies must have been approved by the appropriate institutional review board(s) and a specific declaration of approval must be made within this section.

Results: The description of the experimental results should be succinct but in sufficient detail to allow the experiments to be analyzed and interpreted by an independent reader. If necessary, subheadings may be used for an orderly presentation. All figures and tables must be referred to in the text.

Discussion: The data should be interpreted concisely without repeating material already presented in the Results section. Speculation is permissible, but it must be well-founded, and discussion of the wider implications of the findings is encouraged. Conclusions derived from the study should be included in this section.

Acknowledgments: All funding sources should be credited in the Acknowledgments section. In addition, people who contributed to the work but who do not meet the criteria for authors should be listed along with their contributions.

References: References should be numbered in the order in which they appear in the text. Citing of unpublished results, personal communications, conference abstracts, and theses in the reference list is not recommended but these sources may be mentioned in the text. In the reference list, cite the names of all authors when there are fifteen or fewer authors; if there are sixteen or more authors, list the first three followed by *et al.* Names of journals should be abbreviated in the style used in PubMed. Authors are responsible for the accuracy of the references. Examples are given below:

Example 1 (Sample journal reference):
Inagaki Y, Tang W, Zhang L, Du GH, Xu WF, Kokudo N. Novel aminopeptidase N (APN/CD13) inhibitor 24F can suppress invasion of hepatocellular carcinoma cells as well as angiogenesis. Biosci Trends. 2010; 4:56-60.

Example 2 (Sample journal reference with more than 15 authors):
Darby S, Hill D, Auvinen A, *et al.* Radon in homes and risk of lung cancer: Collaborative analysis of individual data from 13 European case-control studies. BMJ. 2005; 330:223.

Example 3 (Sample book reference):
Shalev AY. Post-traumatic stress disorder: diagnosis, history and life course. In: Post-traumatic Stress Disorder, Diagnosis, Management and Treatment (Nutt DJ, Davidson JR, Zohar J, eds.). Martin Dunitz, London, UK, 2000; pp. 1-15.

Example 4 (Sample web page reference):
Ministry of Health, Labour and Welfare of Japan. Dietary reference intakes for Japanese. *http://www.mhlw.go.jp/houdou/2004/11/h1122-2a.html* (accessed June 14, 2010).

Tables: All tables should be prepared in Microsoft Word or Excel and should be arranged at the end of the manuscript after the References section. Please note that tables should not in image format. All tables should have a concise title and should be numbered consecutively with Arabic numerals. If necessary, additional information should be given below the table.

Figure Legend: The figure legend should be typed on a separate page of the main manuscript and should include a short title and explanation. The legend should be concise but comprehensive and should be understood without referring to the text. Symbols used in figures must be explained.

Figure Preparation: All figures should be clear and cited in numerical order in the text. Figures must fit a one- or two-column format on the journal page: 8.3 cm (3.3 in.) wide for a single column, 17.3 cm (6.8 in.) wide for a double column; maximum height: 24.0 cm (9.5 in.). Please make sure that the symbols and numbers appeared in the figures should be clear. Please make sure that artwork files are in an acceptable format (TIFF or JPEG) at minimum resolution (600 dpi for illustrations, graphs, and annotated artwork, and 300 dpi for micrographs and photographs). Please provide all figures as separate files. Please note that low-resolution images are one of the leading causes of article resubmission and schedule delays. All color figures will be reproduced in full color in the online edition of the journal at no cost to authors.

Units and Symbols: Units and symbols conforming to the International System of Units (SI) should be used for physicochemical quantities. Solidus notation (*e.g.* mg/kg, mg/mL, mol/mm^2/min) should be used. Please refer to the SI Guide www.bipm.org/en/si/ for standard units.

Supplemental data: Supplemental data might be useful for supporting and enhancing your scientific research and BioScience Trends accepts the submission of these materials which will be only published online alongside the electronic version of your article. Supplemental files (figures, tables, and other text materials) should be prepared according to the above guidelines, numbered in Arabic numerals (*e.g.*, Figure S1, Figure S2, and Table S1, Table S2) and referred to in the text. All figures and tables should have titles and legends. All figure legends, tables and supplemental text materials should be placed at the end of the paper. Please note all of these supplemental data should be provided at the time of initial submission and note that the editors reserve the right to limit the size and length of Supplemental Data.

5. Submission Checklist

The Submission Checklist will be useful during the final checking of a manuscript prior to sending it to BioScience Trends for review. Please visit Download Centre and download the Submission Checklist file.

6. Online Submission

Manuscripts should be submitted to BioScience Trends online at http://www.biosciencetrends.com. The manuscript file should be smaller than 5 MB in size. If for any reason you are unable to submit a file online, please contact the Editorial Office by e-mail at office@biosciencetrends.com.

7. Accepted Manuscripts

Proofs: Galley proofs in PDF format will be sent to the corresponding author via e-mail. Corrections must be returned to the editor (proof-editing@biosciencetrends.com) within 3 working days.

Offprints: Authors will be provided with electronic offprints of their article. Paper offprints can be ordered at prices quoted on the order form that accompanies the proofs.

Page Charge: Page charges will be levied on all manuscripts accepted for publication in BioScience Trends ($140 per page for black white pages; $340 per page for color pages). Under exceptional circumstances, the author(s) may apply to the editorial office for a waiver of the publication charges at the time of submission.

(*Revised February 2013*)

Editorial and Head Office:
Pearl City Koishikawa 603
2-4-5 Kasuga, Bunkyo-ku
Tokyo 112-0003 Japan
Tel: +81-3-5840-8764
Fax: +81-3-5840-8765
E-mail: office@biosciencetrends.com